Experimental investigation of the complex liquid liquid equilibrium in the system pure/technical grade nonionic surfactant + water + oil.

vorgelegt von

Dipl.-Ing.

Philipp Schrader

aus Göttingen

von der Fakultät III – Prozesswissenschaften

der technischen Universität Berlin

zur Erlangung des akademischen Grades

Doktor der Ingenieurwissenschaften

-Dr.-Ing.-

genehmigte Dissertation

Promotionsausschuss:

Vorsitzender: Prof. Dr.-Ing. Eckhard Flöter

Gutachterin: Prof. Dr. rer. nat. habil. Sabine Enders

Gutachter: Prof. Bernhard Wolf

Tag der wissenschaftlichen Aussprache: 13.12.2013

Berlin 2014

D 83

Danksagung:

Die vorliegende Arbeit entstand im Rahmen des Sonderforschungsbereichs Transregio 63 „InPrompt“ während meiner Tätigkeit als wissenschaftlicher Mitarbeiter von Januar 2010 bis Oktober 2013 am Fachgebiet für Thermodynamik und thermische Verfahrenstechnik an der TU Berlin. Ich möchte der Deutschen Forschungsgemeinschaft (DFG) für die geleistete finanzielle Unterstützung danken.

Des Weiteren möchte ich meiner Doktormutter Prof. Dr. rer. nat. habil. Sabine Enders für die Überlassung des interessanten und spannenden Themas danken. Während meiner Arbeit an der Dissertation bot sie mir stets die Möglichkeit zur freien wissenschaftlichen Arbeit. Darüber hinaus hatte ich die Gelegenheit die Forschungsergebnisse im nationalen und internationalen Rahmen vorzustellen. Auch für die wissenschaftlichen Anregungen und Diskussionen möchte ich mich bedanken. Zudem bedanke ich mich bei allen die zum Gelingen dieser Arbeit beigetragen haben. Dazu gehören natürlich alle Doktorand_innen sowie Mitarbeiter_innen des Instituts. Außerdem tragen zum Gelingen der Arbeit einen großen Teil all jene bei, die mich ertragen und begleiten, interessiert oder desinteressiert. Allen sei diese Arbeit gleichermaßen gewidmet.

Prof. Dr. habil. Bernhard Wolf möchte ich für die freundliche Übernahme des Koreferats danken. Prof. Dr.-Ing. Eckhard Flöter danke ich für die Übernahme des Prüfungsvorsitzes.

Abstract:

Surfactant containing systems are in the focus of interest since many years. Until today the general phase- and aggregation behavior for the systems containing nonionic surfactant + water + alkane is well described in literature. One of the most important characteristic of these systems is the occurrence of a three phase liquid liquid equilibrium (LLE) with the microemulsion as the middle phase. The microemulsion incorporates large amount of water and hydrocarbon and therefore it can be used e.g. to solubilize water soluble catalyst in non-aqueous environment. For application of these systems the phase- and aggregation behavior has to be known in detail. However, due to the specific microstructure the thermodynamic modeling with classical thermodynamic according to Gibbs is not feasible. Therefore techniques were developed within this work for an efficient and fast detection of tie lines within the binary subsystems as well as in the ternary system. Beside the measurement of the binary system pure surfactant $C_{12}E_8$ + water as well as technical grade surfactant Genapol X080® + water, new data for the binary system water and pure 1-dodcene as well as water + technical grade 1-dodecene was measured. For the first time the solubility of water in pure and technical 1-dodecene was determined within a large temperature range. Furthermore, the solubility of pure and technical grade 1-dodecene in water could be determined successfully. The phase prism was measured across a wide temperature range for a system containing pure substances and a system containing technical grade substances in order to investigate the influence of impurities and the surfactant degree of ethoxylation on the LLE. The differences between a system containing pure substances and a system containing technical grade substances are enormous. Phase change temperatures differ up to 40°C and also the number of coexisting phases is increasing. A four phase liquid equilibrium in a system containing technical grade surfactants is reported for the first time, where the microemulsion splits into two phases. Exemplary for the hydroformylation reaction the influence of formed product as well as the catalyst influence was investigated on the LLE resulting that the catalyst influence on the LLE is negligible contrary to the product influence. The formed aldehyde lowers the Winsor III temperature significantly and therefore the reaction temperature has to be adopted.

Kurzzusammenfassung:

Aufgrund verschiedenster Anwendungsmöglichkeiten sind tensidhaltige Systeme immer mehr Gegenstand universitärer aber auch industrieller Forschung. Das Phasenverhalten von Systemen des Typs nichtionisches Tensid + Wasser + Alkan ist in der Literatur sehr gut beschrieben. Ein wichtiges Merkmal dieser Systeme ist das Auftreten eines Dreiphasen flüssig-flüssig Gleichgewichtes, wobei die Mittelphase Mikroemulsion genannt wird. Die Mikroemulsion, die zu großen Teilen aus Wasser und Kohlenwasserstoffen besteht, kann verwendet werden, um z.B. hydrophile Katalysatorsysteme in einer hydrophoben Umgebung zu lösen. Aus anwendungstechnischer Sicht ist es erforderlich, dass Phasen- und Aggregationsverhalten genauestens zu kennen. Aufgrund der speziellen Mikrostruktur der Mikroemulsion ist es nicht möglich mit der Gibbs'schen Thermodynamik dieses Verhalten vorherzusagen, der Anwender ist daher ausschließlich auf experimentelle Daten angewiesen. Innerhalb dieser Arbeit wurden Methoden entwickelt, die eine schnelle, sichere und reproduzierbare Konodenmessung in den binären Randsystemen, aber auch im ternären System zulassen. Es sind die flüssig-flüssig Gleichgewichte in den binären Systemen Wasser + $C_{12}E_8$, sowie Wasser + Genapol X080® bestimmt worden. Darüber hinaus wurden erstmalig die binären Systeme Wasser + 1-Dodecen und Wasser + technisches 1-Dodecen über einen großen Temperaturbereich vermessen. Um den Einfluss der Verwendung technischer Stoffe auf das Phasengleichgewicht zu bestimmen, wurde das Phasenprisma für das System $C_{12}E_8$ + Wasser + 1-Dodecen, sowie das Phasenprisma für das System Genapol X080® + Wasser + 1-Dodecen untersucht. Dabei stellte sich heraus, dass nicht nur die Phasenwechseltemperaturen um bis zu 40°C voneinander abweichen, sondern auch die Anzahl der koexistierenden Phasen ansteigt. Es wurde erstmalig ein Aufspalten der Mikroemulsion in zwei Phasen beobachtet. Um solche Systeme als Reaktionssyssteme z.B. in der Hydroformylierung anwenden zu können, wurde der Einfluss von Aldehyd und Katalysator auf das flüssig-flüssig Gleichgewicht bestimmt. Es zeigte sich, dass der Einfluss des Katalysators vernachlässigbar ist im Gegensatz zum Aldehydeinfluss. Im Sinne einer optimalen Reaktionsführung ist daher die Temperatur mit steigendem Aldehydanteil entsprechend anzupassen.

Contents

Contents iii

List of tables vi

List of figures viii

1. Introduction 1

2. Surfactants 4

2.1 Type of surfactants 5

2.1.1 Nonionic surfactants 6

2.1.2 Ionic surfactants 11

2.1.3 Zwitterionic surfactants 14

2.2 Phase- and aggregation behavior 15

2.2.1 Surfactant + water 16

2.2.1.1 Phase diagrams 16

2.2.1.2 Micelles and CMC 20

2.2.2 Surfactant + water + oil 30

2.2.2.1 Phase prism 31

2.2.2.2 Kahlweit's fish 34

2.2.3 Surfactant + water + oil +salt 35

2.3 Synthesis of surfactants 38

2.4 Technical grade surfactants and purification techniques 39

3. Applying surfactants for chemical reactions: Hydroformylation of alkenes 43

3.1 Hydroformylation reaction 44

3.2 Catalysts for hydroformylation 45

3.3 Industrial hydroformylation 48

3.3.1 Industrial hydroformylation of short chain alkenes 49

3.3.2 Industrial hydroformylation of long chain alkenes 50

3.4 Hydroformylation in microemulsions 51

3.5 Other approaches for hydroformylation 54

4. Experimental methods 57

4.1 Materials 57

4.2 Sampling 57

4.3 Detection of surfactant 58

4.4 Detection of 1-dodecene 60

4.5 Detection of water 62

4.6 Measurement of Kahlweit's fish 63

4.7 Detection of surfactant decomposition 64

4.8 Measurement error 64

5. Results and discussion 66

5.1 Kahlweit's fish 66

5.1.1 Influence of the ethoxylate chain length 68

5.1.2 Influence of technical grade substances 71

5.1.3 Influence of the aldehyde 72

5.1.4 Influence of the Rh - SulfoXantPhos catalyst 75

5.2 Cloud point curve measurements 76

5.2.1 $C_{12}E_8$ + water 77

5.2.2 $C_{12}E_8$ + 1-dodecene 80

5.2.3 Genapol X 080® + water 80

5.2.4 Genapol X080® + technical 1-dodecene 83

5.3 Tie line and solubility measurements 83

5.3.1 1-Dodecene + water 83

5.3.2 Technical + 1-dodecene + water 85

5.3.3 $C_{12}E_8$ + 1-dodecene + water 87

5.3.4 Genapol X080® + technical 1-dodecene + water 95

5.3.5 Four phase LLE in the system Genapol X080® + 1-dodecene + water 106

5.4 Comparison of pure and technical grade surfactant and 1-dodecene 108

5.5 Calculation of the binary phase and aggregation behavior: The Nagarajan and Ruckenstein model 110

6. Summary and Outlook 112

7. Literature 114

List of tables

Table 1: HLB classification of different surfactants. 5

Table 2: Experimental determined phase transition temperatures for system A gauged with the optical method. T_1: phase transition from Winsor I to Winsor III; T_2: Phase transition from Winsor III to Winsor II; T_3: Phase transition from Winsor I to Winsor IV; T_4: Phase transition from Winsor IV to Winsor II at given γ and fixed α=0.5. 67

Table 3: Phase change data for the system water + $C_{12}E_4$ + pure 1-dodecene; T_1: phase transition from Winsor I to Winsor III; T_2: Phase transition from Winsor III to Winsor II; T_3: Phase transition from Winsor I to Winsor IV; T_4: Phase transition from Winsor IV to Winsor II at given γ and fixed α=0.5. 69

Table 4: Phase change data for the system water + $C_{12}E_6$ + 1-dodecene; T_1: phase transition from Winsor I to Winsor III; T_2: Phase transition from Winsor III to Winsor II; T_3: Phase transition from Winsor I to Winsor IV; T_4: Phase transition from Winsor IV to Winsor II at given γ and fixed α=0.5. 70

Table 5: Phase change temperatures for system B; T_1: phase transition from Winsor I to Winsor III; T_2: Phase transition from Winsor III to Winsor II at given γ and fixed α=0.5. 72

Table 6: Phase change temperatures for system A, β=0.25; T_1: phase transition from Winsor I to Winsor III; T_2: Phase transition from Winsor III to Winsor II; T_3: Phase transition from Winsor I to Winsor IV; T_4: Phase transition from Winsor IV to Winsor II at given γ and fixed α=0.5. 74

Table 7: Phase change temperatures for system A, β=0.5; T_1: phase transition from Winsor I to Winsor III; T_2: Phase transition from Winsor III to Winsor II; T_3: Phase transition from Winsor I to Winsor IV; T_4: Phase transition from Winsor IV to Winsor II at given γ and fixed α=0.5. 75

Table 8: Phase change temperatures for system A with α=0.5 and β=0.5 containig $w_{Rh\text{ - }SulfoXantPhos}=2*10^{-5}$. T_1 phase transition from Winsor I to Winsor III; T_2: Phase transition from Winsor III to Winsor II at given γ. 76

Table 9: Experimental cloud point temperatures without peroxide formation related to the $C_{12}E_8$ + water binary subsystem. 78

Table 10: Experimental cloud point temperatures with peroxide formation related to the $C_{12}E_8$ + water binary subsystem. 78

Table 11: Demixing temperatures for the system Genapol X080® + water. 81

Table 12: LLE data for the 1-dodecene rich side in the 1-dodecene + water binary subsystem in dependency of temperature. 84

Table 13: Water solubility in technical grade 1-dodecene. 86

Table 14: LLE data for system A at temperatures 30°C, 40°C, 50°C and 60°C. Superscript I denotes the oil rich phase and superscript II denotes the aqueous phase. 89

Table 15: LLE data for system A at temperatures 70°C and 80°C. Superscript I denotes the oil rich phase, superscript II denotes the microemulsion phase and superscript III denotes the aqueous phase. 92

Table 16: LLE data for system A at 90°C. Superscript I denotes the oil rich phase and superscript II denotes the aqueous phase. 93

Table 17: Measured LLE data for system B in the Winsor I phase region. Superscript I denotes the oil rich phase and superscript II denotes the aqueous phase. 99

Table 18: Phase composition for system B in the Winsor IV region at 70°C and 80°C. 101

Table 19: LLE data for system B at 90°C. Superscript I denotes the oil rich phase, superscript II denotes the microemulsion phase and superscript III denotes the aqueous phase. 102

Table 20: Phase compositions for the binary systems attached to the three phase region at temperatures 85°C and 90°C. 104

List of figures

Figure 1: Chemical structure of an alkylpolyoxethylenether surfactant C_iE_j. 6

Figure 2: General structure of an alkyl phenyl polyethoxylate. 7

Figure 3: General structure of an alkylpolygylcoside surfactant C_xG_y. 8

Figure 4: General structure of a saccharose fatty acid ester. 9

Figure 5: General scheme of a fatty amine ethoxylate. 10

Figure 6: Structure of a gemini surfactant molecule with two hydrophobic tails and two hydrophilic head groups connect by a spacer molecule. 10

Figure 7: Chemical structure of a Na – soap. 11

Figure 8: Structure of sodium dodecyl sulfate (SDS). 12

Figure 9: Linear (left) and branched (right) sodium alkyl benzene sulfonat. 13

Figure 10: Structure of like cetyl trimethyl ammonium bromide (CTAB), a general structure of a fatty amine salt and a fatty diamine salt. 14

Figure 11: Examples for zwitterionic surfactants: 1) betaine with n=1; 2) taurine with n=2; 3) homoglycine with n=2 and 4) sulfobetaine with n=2. 15

Figure 12: General phase diagram of a nonionic surfactant C_iE_j + water system. L: Micellar solution; 1.) M + L: Monodisperse surfactant solution in equilibrium with micellar solution; 2.) L_1 + L_2: Micellar solution L_1 in equilibrium with micellar solution L_2; L; H, C, La: Lyotropic mesophases. 17

Figure 13: Selected structures of liquid crystalline mesophases. 18

Figure 14: Different micelle shapes in dependency of surfactant concentration in aqueous solution according to Nagarajan and Ruckenstein (95). 21

Figure 15: Influence of the carbon chain length on the CMC for the nonionic surfactant C_iE_8 at 25°C (solid squares, (127)) as well as influence of the ethoxylate chain length on the CMC for the nonionic surfactant $C_{12}E_j$ at 25°C (open squares, (74)). 27

Figure 16: CMC of $C_{14}E_8$ (squares), $C_{10}E_8$ (stars), $C_{10}E_4$ (triangles) taken from (128) and $C_{12}E_4$ (open squares), $C_{12}E_6$ (open circles), $C_{12}E_8$ (circles) taken from (129) in dependency of temperature. 27

Figure 17: CMC of Na – soaps in dependency of carbon chain length at 20°C from (74). 28

Figure 18: Water solubility of alkanes (solid squares) and water solubility of alkenes (open squares) at 25°C from (146). 32

Figure 19: Schematic phase prism and projection of the critical line for a system composed of nonionic surfactant + water + oil. The critical line is projected on the binary water + surfactant system for four different systems: 1) no Winsor III phase, 2) system with a tricritical point T_{triCr}, 3) system with a small Winsor III phase temperature range, 4) system with a distinct Winsor III phase temperature range. In system 3) and 4) the endpoint of the critical line beginning in the Winsor I system is marked by C and the origin of the critical line passing through the Winsor II system is marked by D. 33

Figure 20: Three different cross sections through the phase prism Section A at different surfactant mass fractions γ and Section B and C at two different constant surfactant mass fractions γ_1 and γ_2. 34

Figure 21: Schematic phase behavior at constant temperature for the system water + salt + oil. 36

Figure 22: Schematic phase behavior at constant temperature for the system surfactant + salt + oil. 37

Figure 23: Schematic phase behavior at constant temperature below the LCST within the binary subsystem surfactant + water for the system surfactant + lyotropic salt + oil. 37

Figure 24: Schematic influence of salt addition to a quaternary system composed of surfactant + water + oil + hydrotropic salt (solid line) and surfactant + water + oil + lyotropic salt (dashed line) in dependency of temperature. 38

Figure 25: General reaction scheme of an ethoxylation reaction. 39

Figure 26: General scheme of the hydroformylation reaction. 44

Figure 27: Chemical formula of the TPP (left side) and TPPTS ligand (right side). 46

Figure 28: Phosphine ligands for hydroformylation: 1. BIPHEPHOS ligand, 2. XantPhos ligand and 3. SulfoXantPhos ligand. 47

Figure 29: General flow chart of the Ruhrchemie hydroformylation process. 50

Figure 30: Novel concept for a continuous hydroformylation of long chain alkenes. 53

Figure 31: Calibration curve for the surfactant $C_{12}E_8$. 59

Figure 32: Calibration curve of surfactant Genapol X080®. 59

Figure 33: Calibration curve for pure 1-dodcene. 60

Figure 34: Calibration curve for technical 1-dodecene. 61

Figure 35: Gas stripping apparatus for 1-dodecene enrichment. 62

Figure 36: Calibration curve for volumetric Karl Fischer water detection. 63

Figure 37: Kahlweit's fish for system A at α equal to 0.5. 67

Figure 38: Kahlweit's fish at constant oil-water ratio α=0.5 for $C_{12}E_8$ (solid squares and solid line), $C_{12}E_6$ (open squares and dashed line) and $C_{12}E_4$ (open circles and dotted line) at different surfactant mass fraction γ in dependency of temperature. 69

Figure 39: Kahlweit's fish for system A (open squares and dashed line) compared to system B (solid squares and solid lines) at constant α=0.5. 71

Figure 40: Influence of tridecanal to system A (squares and solid line: $\beta_{tridecanal}$=0; triangles and dotted line: $\beta_{tridecanal}$=0.25; circles and dashed line $\beta_{tridecanal}$=0.50). 73

Figure 41: Influence of the Rh – SulfoXantPhos catalyst on the LLE of system A with α=0.5 and β=0.5. Black squares and line system A without Rh – SulfoXantPhos catalyst; open squares system A with Rh – SulfoXantPhos catalyst, $w_{Rh-SulfoXantPhos}=2*10^{-5}$. 76

Figure 42: Experimental cloud point temperatures for the system $C_{12}E_8$ + water (squares: samples with peroxide formation; circles system without peroxide formation). 77

Figure 43: LLE data for the system $C_{12}E_8$ + water (open circles: (91); stars: (265); open triangles: (90); open pentagons: (266); solid squares: this work). 79

Figure 44: Cloud point curve for the system $C_{12}E_8$ +water (solid squares) and Genapol X080® + water (open squares). 81

Figure 45: Cloud point curve for the system Genapol X080® + water (squares: (268) and circle: (267)). 82

Figure 46: Experimental temperature dependent water solubility in pure 1-dodecene. 83

Figure 47: Solubility of several alkanes (open squares: (146)) and alkenes (open circles: (146), star: this work) in dependency of chain length at room temperature (25°C). 85

Figure 48: Water solubility in pure 1-dodecene (squares) and water solubility in technical 1-dodecene. 86

Figure 49: Tie lines for system A at 30°C. 87

Figure 50: Tie lines for system A at 40°C. 88

Figure 51: Tie lines for system A at 50°C. 88

Figure 52: Tie lines for system A at 60°C. 89

Figure 53: LLE for system A at 70°C (triangles and solid line) and 80°C (squares and dotted line). 92

Figure 54: Tie lines for system A at 90°C. 93

Figure 55: $C_{12}E_8$ weight fraction in the aqueous phase at a constant feed (w_{C12E8}≈0.04) in dependency of temperature. 94

Figure 56: w_{C12E8} in the oil rich phase at a constant feed (w_{C12E8}≈0.04) in dependency of temperature. 95

Figure 57: Tie lines for system A [squares and solid line] and system B [open triangles and dashed line] at 30°C. 96

Figure 58 Tie lines for system A [squares and solid line] and system B [open triangles and dashed line] at 40°C 96

Figure 59: Tie lines for system A [squares and solid line] and system B [open triangles and dashed line] at 50°C. 97

Figure 60: Tie lines for system A [squares and solid line] and system B [open triangles and dashed line] at 60°C. 97

Figure 61: Tie lines for system A [solid triangles and black line] and system B [open triangles and dashed line] as well as one phase compositions for system B [open circles] at 70°C. 98

Figure 62: Tie lines for system A [solid triangles and black line] and system B [open triangles and dashed line] as well as one one phase composition for system B [open circles] at 80°C. 98

Figure 63: Tie lines for system A [solid squares and black line] and system B [open triangles and dashed line] at 90°C. 102

Figure 64: Tie lines [solid squares and black line] attached to the three phase LLE [dashed line and open triangles] at 85°C. 103

Figure 65: Tie lines [solid squares and black line] attached to the three phase LLE [dashed line and open triangles] at 90°C. Open circles specify single phase compositions. 103

Figure 66: $w_{Genapol\ X080}$ in the aqueous phase at a constant feed ($w_{Genapol\ X080}$ ≈0.04) in dependency of temperature. 104

Figure 67: $w_{Genapol\ X080}$ in the oil rich phase at a constant feed ($w_{Genapol\ X080}$ ≈0.04) in dependency of temperature. 105

Figure 68: Single tie line (solid line), phase compositions within the coexisting phases (open squares) and feed weight fraction (solid square) at 30°C for system B. 106

Figure 69: Four phase liquid liquid equilibrium in system B at 90°C. 107

Figure 70: Chromatogramm of Genapol X080® (dashed line, $w_{Genapol\ X080®}$=0.00054) and $C_{12}E_8$ (solid line, w_{C12E8}=0.00058) dissolved in 1-propanol. 108

Figure 71: FTIR spectrum for fresh Genapol X080® (dashed line) and Genapol X080® heated for 48h at 90°C (solid line). 109

Figure 72: Chromatogram of technical 1-dodecene (dashed line, $w_{1\text{-dodecene, technical}}$=0.00058) and pure 1-dodecene (solid line, $w_{1\text{-dodecene, pure}}$=0.00051). 110

Figure 73: Calculated LLE for the system $C_{12}E_8$ and water (dotted line modeled cloud point curve from (270), squares this work). Triangles experimental CMC data from (129), dashed line predicted CMC from (270). 111

1. Introduction

A world without surfactants would be a world with many miscibility gaps. Independent of structure surfactants are omnipresent in life. Not only in the human body and metabolism amphiphilic substances are absolutely necessary, one can find them also in everyday life. The most common application of surfactants is certainly the application as detergent or dish liquid. Beside this, one other span of application is food and food processing. Whether milk, mayonnaise, dressings and sauces or ice-cream, without emulsifying agents the appearance of these products would be at least two phase. The taste or mouthfeel would be likewise much different from the usual. Also in cosmetics surfactants are essential parts of shampoos, crèmes, liquid soaps or shower gels. In addition to this part of surfactant application which is present for everybody everyday there is another not less important part of surfactant application. For more than 130 years surfactants are into the focus of interest in academic as well as in industrial research. Based on their unique features, namely that they are soluble in polar solvents like water and simultaneously soluble in non-polar solvents like hydrocarbons a wide field of application is opened. Especially nonionic surfactants exhibit a broad manifoldness since they can be tailor made for almost any application. In field of chemical engineering surfactant containing systems can be used for introducing water soluble catalyst in organic synthesis (1). Often one has to force the challenge that there is on the one hand a catalyst-ligand system with excellent turn over frequency (TOF) and selectivity but on the other hand the catalyst-ligand system is mainly water soluble. If hydrocarbons with a small carbon number as feedstock are used this problem is less crucial, given that the water solubility of short chain hydrocarbons is limited but still high enough to establish an economical process (2). However, for any process with long chain hydrocarbons the problem becomes pestering. Here surfactants come in. If a nonionic surfactant is added to a system containing water and e.g. long chain alkane/alkene at small surfactant concentrations above the critical micelle concentration (CMC) oil can be solubilized inside

micelles within the aqueous phase. If surfactant concentration and temperature are increasing a microemulsion can be formed. Within this microemulsion large amounts of water and oil are incorporated due to the specific microstructure. This allows a contact of educt and catalyst and therefore high reaction rates and the advantages of homogeneous catalysis (high reaction rates or conversion, no transport limitation) can be combined with the advantages of heterogeneous catalysis (excellent catalyst recycling). The catalyst recycling can be in some cases the bottleneck of the process. If an extreme high price catalyst is applied, for example Rh catalyst in the field of hydroformylation this is one important issue. Having in mind Rh is temporary more expensive than gold and therefore a nearly complete catalyst recycling is necessary (3). To operate this process a clear knowledge about the phase and aggregation behavior is not only preferable it is absolutely fundamental. However, just the knowledge about the phase behavior is not adequate since for example the catalyst loss has to be estimated. For estimating this loss the amount of e.g. water in the oil rich phase has to be known as the catalyst is mainly water soluble. Also for reaction it is necessary to know at first at which temperatures a microemulsion is formed and secondly the amount of water and oil dissolved in the microemulsion in dependency of temperature must be known, too. This data can be used to find an optimal reaction temperature, where the amount of water and oil is maximal in the middle phase. The utilization of surfactant containing systems in e.g. a miniplant with highly purified surfactants, as they are normally used for obtaining data on chemical media, is not practical due to the enormous high price. For any application in a technical or miniplant scale technical grade surfactants have to be applied. However, a technical grade surfactant is not comparable with a pure substance; it is rather a multi component mixture including inter alia surfactant molecules with different ethoxylate and/or alkyl chain length. Therefore, it is necessary to work on the following tasks:

1. For a first overview about the phase behavior in the ternary system octaethylene glycol dodecyl ether $C_{12}E_8$ + water + pure 1-dodecene the Kahlweit's fish should be measured.

2. For tie line measurement it is necessary to establish the analytics of thermal instable polar and apolar components simultaneously as well as the fast and reproducible measurement of trace components.

3. The complex phase behavior including tie lines of the ternary system $C_{12}E_8$ + water + pure 1-dodecene has to be studied across a wide temperature range.

4. The influence of surfactants on the ternary LLE with a different degree of ethoxylation has to be studied.

5. Additional it is further necessary to investigate the catalyst influence and the product influence on the LLE.

6. The phase prism has to be studied again with a system containing technical grade surfactant + water + technical grade 1-dodecene in order to obtain the influence of the surfactant quality on the LLE.

2. Surfactants

All surfactants have, beside of any further classification, which will be introduced later, one thing in common: They consist of parts either hydrophilic or hydrophobic and thus they are called "amphiphilic". This causes the fact that they are miscible or partly miscible with polar solvents like water and non-polar solvents like hydrocarbons. One other common feature is the adsorption at interfaces [Liquid/Gas, Liquid/Liquid, Liquid/Solid] which leads to another denotation: Surface active agents. The first amphiphilic substances produced by mankind were soaps. The process of soap production was described more than two thousand years ago by Pliny according to Preston (4) and Pliny suggested soap as an additive for hair dyeing (4). Since these old days a various number of surfactants have been discovered and hence the number of applications has been increased as well. Nowadays surfactants are used beside the classical utilization for cleaning and washing in nearly every field of life, the annual production was in 2008 about $12x10^9$kg/a (5). They are widely used in food technology as emulsifying agents in ice cream, milk products as well as in functional food in order to solubilize non-polar compounds in the often aqueous environment (6), (7) and (8); having in mind that water is one of the major food components. In photo industry surfactants are important to produce the photosensitive layer within the film, the film emulsion (9). Since the introduction of digital photography this field is growing less, given that the application of photographic film is pushed back. Also in processing technology they are used as floating agents (10), as well as extraction media for cloud point extraction of phenolic or aromatic compounds out of e.g. water (11). In analytics they are used for micellar liquid chromatography since the 1990s (12). In the last years they came more in the focus of interest as a reaction media for e.g. chemical industry. Catalysts in micelles can be locked in hydrophilic phases and so new high performing catalysts can be applied for several chemical reactions like Suzuki couplings (13) or Diels – Alder reactions (14). Aside this micellar approach microemulsions are discussed for reactions in the last years intensively by Schomäcker and

coworkers (15), (16), (17) and (18); in a laboratory scale and also as a recent development in a miniplant scale (19).

2.1 Type of surfactants

It is obvious that for this tremendous class of amphiphilic substances a classification is necessary. Their structure incorporates in all cases a hydrophobic tail and a hydrophilic head group. The tail group consists of hydrocarbons (linear-, branched-, ring structures or a combination). The head group consists of polar or charged groups; one surfactant molecule can enclose more than one head or tail group. It is common to classify surfactants based on the charge of the polar part in nonionic, ionic and zwitterionic surfactants. Another classification system is the hydrophil-lipophil balance (HLB) introduced by Griffin in 1949 (20). The molecule is divided into two parts: a hydrophilic part and a hydrophobic part. On the basis of the molecular weight (M_l= lipophilic part's molecular weight; M_g= molecular weight of the molecule) of each part the HLB can be calculated.

$$HLB = 20\left(1 - \frac{M_l}{M_g}\right) \quad \textbf{(1)}$$

The HLB is arbitrary standardized between zero and twenty. This HLB figure can be used in some cases as a benchmark to classify the surfactant molecules for possible applications. Dörfler (21) suggests the following applications for surfactants given in Table 1.

Table 1: HLB classification of different surfactants.

Surfactant HLB	Application
$1{,}5 \leq HLB \leq 3$	Anti-foaming agent
$3 \leq HLB \leq 8$	Water in oil emulsifying agent
$7 \leq HLB \leq 9$	Wetting agent
$9 \leq HLB \leq 18$	Oil in water emulsifying agent

Due to the calculation of the HLB, it is possible that surfactants with a large difference in the molecular weight show nearly the same HLB. But according to experimental results of Kahlweit and Strey (22) the solubilisation capacity is increasing with increasing the molecular weight. Therefore e.g. C_6E_3 (HLB=12.7) and $C_{12}E_6$ (HLB=12.4) are both oil in water emulsifier and according to the HLB concept nearly similar, but the emulsifying capacity of $C_{12}E_6$ is more than four times increased compared to C_6E_3 (22).

2.1.1 Nonionic surfactants

Nonionic surfactants as the name implies do not include disassociating functional groups. Theoretical a virtually indefinite number of molecules are imaginable. Nevertheless, only a limited number of structures play a role in application and research. One important group are the alkylpolyoxyethylenethers surfactants abbreviated C_iE_j with the in Figure 1 represented structure, where i specifies the carbon atom number in the hydrophobic tail and j the ethoxylate unit number within the surfactant molecule.

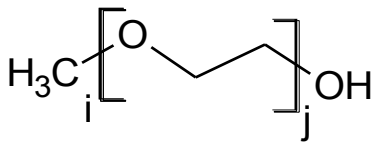

Figure 1: Chemical structure of an alkylpolyoxethylenether surfactant C_iE_j.

Since their discovery in the early 1930's (23) the application was at first discussed sparely for applications in laundry detergents (24). But not only twenty years later these surfactants were produced and established in industrial applications like emulsion polymerization (23), oil recovery (25), fertilizer production (26) and household applications (27). Alkyl polyoxyethylene surfactants are not sensitive to hard water, like ionic surfactants and soaps. But contrary to soaps and ionic surfactants the water solubility is decreasing with increasing temperature. Alkyl polyoxyethylene surfactants are produced from ethoxylation of appropriate primary alcohols. Details of production

will be discussed in 2.3. This group shows a better biodegradability than alkyl phenol polyethoxylates containing surfactants (28) but there are some concerns about the degradation rate, which is important in waste water treatment plants (29) and (30). The degradation rate in waste water treatment is decreasing with increasing the degree of ethoxylation (30). Furthermore, the toxicity is increased with increasing the carbon chain length and decreasing the degree of ethoxylation as well (29). Some not distantly related amphiphilic substances are the alkyl phenyl polyethoxylates. In Figure 2 a general structure is depicted.

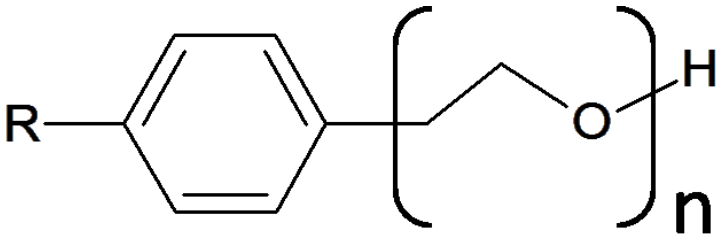

Figure 2: General structure of an alkyl phenyl polyethoxylate.

These compounds as shown in Figure 2 were introduced in the late 1930's as they feature an increased washing power hitherto not reached by any synthetic detergent at all (31). Alkyl phenyl polyethoxylates are still produced until now in considerable amounts. In 2008 more than $5x10^6$kg were produced (28). They were widely used in household products like dishwashing detergents, washing agents and other household detergents (32). During the last thirty years they came under criticism due to environmental reasons. If the widely used Nonyl phenyl ethoxylated surfactants are disintegrated in sewage treatment plants; 4-nonyl phenol can remain and accumulate in the food chain. The toxicity of 4-nonyl phenol is similar to heavy metals (33). Other degradation products can act like endocrine disruptors, which mean that they interact with the secretion, transport, binding, action and elimination of natural hormones in the body, which are responsible for the maintenance of homeostasis, reproduction and development (34). Based on these facts the common use of these surfactants were strongly restricted in Europe since 2003 (35). One other major group of nonionic surfactants are the group of alkypolyglycosides; the general chemical structure is denoted in Figure 3

abbreviated C_xG_y here x is specifying the number of carbon atoms in the tail and y the number of glucose units.

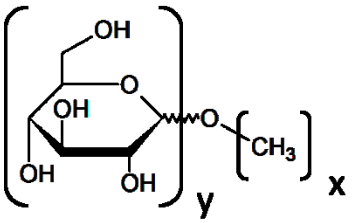

Figure 3: General structure of an alkylpolygylcoside surfactant C_xG_y.

These surfactants came in the focus of interest during the last twenty years, given that they can be produced from renewable sources like sugar, starch and plant oils (36). The alkylpolyglycosides possess a good biodegrability and therefore they are often claimed as “green surfactants” (37) or also “novel surfactants” (38). The phase and aggregation behavior in aqueous solution and multicomponent mixtures is part of several studies (39), (40), (41), (42), (43) and (44). In contrast to alkyl polyethers C_iE_j the solubility of alkyl polyglycosides C_xG_y in hydrocarbons is limited (43). Because of their low toxicity and dermatological safety they are utilized in a broad field of applications like cosmetics, laundry detergents, pharmaceuticals and also agro-chemicals (37), (41), (45) and (46). However, aside the risen interest in these molecules the last two decades, they have been known since 120 years (47). The first application of the alkyglycosides was proposed more than forty years later in 1934 as an emulsifying agent and as a cleaning agent (48). Though, the synthesis in a technical scale of the alkyglycosides was not known at this time. In 1941 the first technical practicable synthesis catalyzed by nitric, sulphuric, hydrochloric and phosphoric acid was patented and introduced into industry (49). During the next decades a lot of application areas were discussed, but they remain in niches like plasticizers plant or animal based adhesives (49) or emulsifying agents for penicillin (50). The commercially prosperity begun in the 1980’s shortly after the first plants for long chain alkyl polyglycosides were established (45). Beside of glucose other sugars like fructose, saccharose, etc. can be used as the polar head group. Furthermore, numerous niche surfactants exist alongside the three mentioned bulk nonionic surfactants. Some are suitable for food applications,

like the sugar fatty acid esters, produced via estrification of sugar with fatty acids. They are decomposed into sugar and fatty acid e.g. in the human body. Typically, these surfactants are based only on renewable sources in almost any case saccharose is used as a feedstock given that the availability in a high purity for a low price is excellent (51). Figure 4 depicts a general structure of a saccharose fatty acid ester.

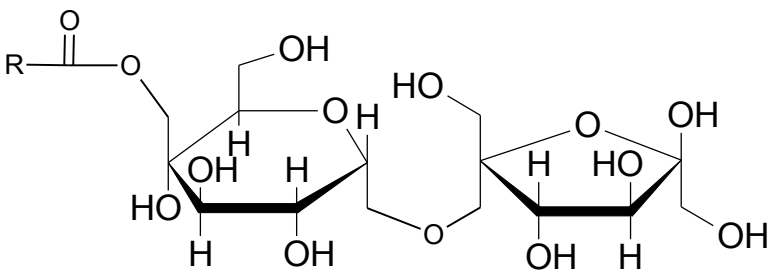

Figure 4: General structure of a saccharose fatty acid ester.

Since the fabrication in a chemical way is complex, the production process is changing over to enzymatic catalysis offering a perfect stereoselectivity, regioselectivity and marginal contamination with unwanted byproducts and often hazardous solvents. The moderate conditions of enzymatic catalysis also avoid sugar caramelization (51). On the other hand the chemical production avoids problems with the needed solubilisation of the feedstock. However, then often complicated and complex purifications steps are necessary due to the fact that in chemical processes hazardous solvents like dimethylformamide (DMF) or dimethyl sulfoxide (DMSO) are necessary to dissolve the reaction products (52). Understandably for application in food any content of DMF or DMSO is unacceptable. Surfactants based on alicyclic compounds e.g. sterols like cholesterol, campesterol and stigmasterol are successfully applied in personal care products like cosmetic and pharmaceutics (53) and (54). Of course their application is limited hence the high price of the feedstock. Typically these surfactants consist of ethoxylated sterols but also combination of glycosides and sterols are discussed in literature (53). For replacing the linear benzyl ethoxylates, beside linear alcohol ethoxylates and other surfactants, the fatty amine ethoxylates came in the focus of interest the last years. In Figure 5 the general scheme is depicted.

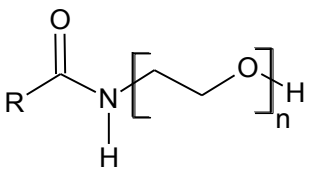

Figure 5: General scheme of a fatty amine ethoxylate.

The amine bond leads to a good biodegrability (55). In contrast to the above mentioned saccharose fatty acid esters or ethoxylated sterols the synthetic route to obtain fatty amine ethoxylates is simple and in wide parts similar to the well-known ethoxylation of long chain alcohols (56). The latest introduced surfactants are probably the group of the gemini surfactants. The term was introduced by Menger and Littau (57) in 1991. In most of the cases they are ionic surfactants, but also nonionic gemini surfactants exist (58). Regardless whether they are ionic or nonionic, the structure in principle is of similar type. The head groups of two surfactant molecules are connected either via an atomic bond or a so called space molecule. The spacer molecule is providing in this case the linkage between the two surfactant molecules. Figure 6 demonstrates the general structure of an arbitrary gemini molecule with an optional spacer molecule. For the case it is a ionic gemini surfactant, instead of a nonionic head group, a ionic head group is embedded in the structure.

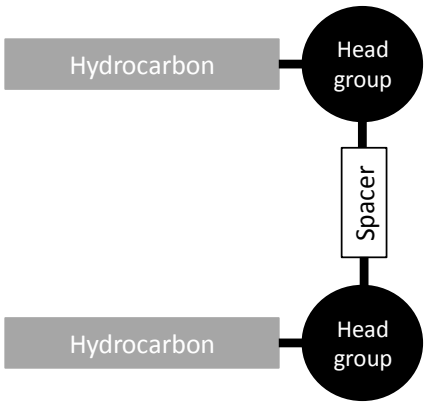

Figure 6: Structure of a gemini surfactant molecule with two hydrophobic tails and two hydrophilic head groups connect by a spacer molecule.

Various authors (59), (60), (61), (62) and (63) discuss sugar based gemini surfactants. But some gemini surfactants are also prepared of alkyl polyoxyethylene ethers C_iE_j (58) and (64). In literature

the nomenclature, Gem_nE_m is used, where n indicates the alkyl chain length and m the number of ethoxylate units. For these dimeric surfactants, it is reported that the critical micelle concentration (CMC) is about two orders of magnitude lower than for the monomeric surfactant molecule C_iE_j (58). Furthermore, they are more efficient in reducing the surface tension and the cloud – point temperature is about 40°C lower than in the aqueous solution of the monomeric counterpart (64).

2.1.2 Ionic surfactants

Ionic surfactants are distinguished by dissociation in aqueous media. In dependency of their structure they can dissociate in anionic or cationic surfactants. Ionic surfactants have been produced commercially almost a decade (they were the first commercially produced surfactants) The breakthrough of ionic surfactants begun in world war two when alkyl lauryl sulfonates replaced fatty acid soaps as a result of material shortage (65). Today more than 60% of the surfactants produced worldwide are anionic surfactants (66). The counter ions are typically sodium and potassium (commonly applied for water soluble surfactants) or calcium and magnesium (applied for oil soluble surfactants) (66). Ion groups building the ionic head are manifold, like carboxylate, sulfate, sulfonate and phosphate groups. However, only the most widely used anionic surfactants are introduced in the next paragraph. One of the well-known anionic surfactant e.g. for daily applications is soap. In chemical terms soaps are the sodium or potassium salts of fatty acids. Figure 7 depicts the general structure of sodium soap.

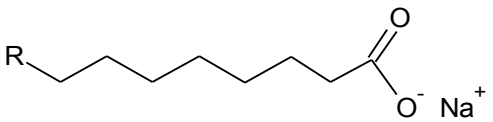

Figure 7: Chemical structure of a Na – soap.

Soaps will be obtained with help of the soapification process, meaning the reaction of fatty acids (mostly from herbal or animal sources) with NaOH or KOH. In almost every detergent or other applications in industry they are replaced by other synthetic surfactants, because they are forming

with calcium or magnesium ions from hard water in water non soluble lime soaps. These lime soaps induce e.g. laundry bloom. Nevertheless they are a few applications until today in which other soaps are still in use until now. Aluminum based soaps are widely used as a thickener in paint, cosmetics, food and pharmaceutics hence they are nontoxic (67). The mechanism of thickening in the apolar enviroment is still under discussion. Most of the authors quote a network forming with help of hydrogen bonding between hydroxyl groups of two aluminum based soaps (68), (69) and (70). Also the aggregation of reversed micelles to a gel network in the apolar environment is suggested by Wang and Rackaitis (67). In water the formation of gels with soap containing systems is not reported. At low concentrations the soap is dissolved in water and no aggregation occurs. When the concentration of soap reaches the CMC micelles are formed. Monoesters of sulfuric acid represent another important group of anionic surfactants. Typically they contain eight to 16 carbon atoms and were produced by esterification of linear or branched long chain alcohols (66). The esterification of 1-dodecanol and following neutralization with e.g. NaOH leads to sodium dodecyl sulfate (SDS) a widely spread surfactant. In Figure 8 the chemical structure of SDS is depicted.

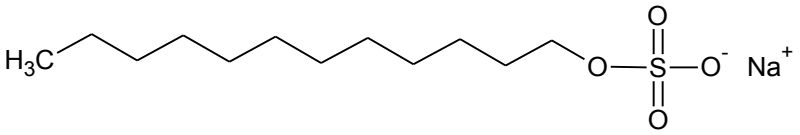

Figure 8: Structure of sodium dodecyl sulfate (SDS).

The phase and aggregation behavior of SDS and water is subject of several publications (71), (72) and (73). Above 25°C SDS is completely miscible with water until approximately 40 wt. % SDS, there is no LCST demixing behavior like it is often reported for the system nonionic surfactant + water. At higher concentrations several liquid crystalline phases are formed. At about 40 wt. % the hexagonal phase is evolving. When the concentration increases the two dimensional monoclinic, the rhombohedral, the cubic phase, the tetragonal and the lamellar phase formed (71). At room temperature (25°C) the CMC of SDS is about 8.3 mMol per liter with increasing the temperature the CMC is increasing, at 70°C the CMC is about 11.4 mMol per liter (74). The other important group of anionic surfactants is

the group of sulfonates. They are produced by sulfonation of alkylbenzenes and are part of nearly all formulations of household detergents like washing powder, cleaning agents and so on. Secondary, they are used widely for industrial applications (66). Until the 1950's branched alkylbenzenes were commonly used as a feedstock for the synthesis of branched alkyl benzene sulfonates. With emergence of environmental concerns they were replaced by linear alkyl benzene sulfonates (LAB) (65) and commonly used until today. Figure 9 depicts a general schema of a LAB and a branched alkyl benzene sulfonate.

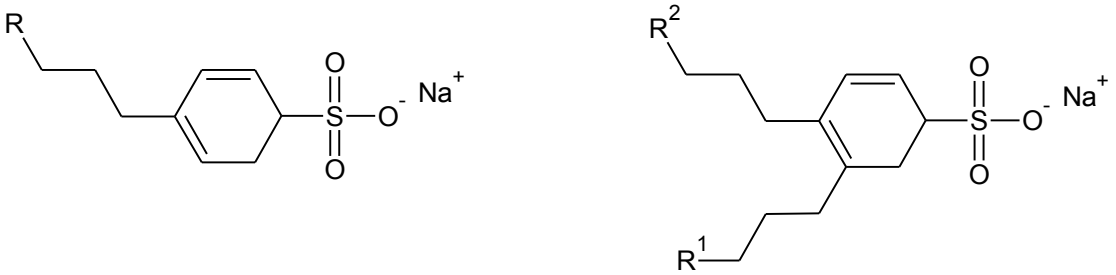

Figure 9: Linear (left) and branched (right) sodium alkyl benzene sulfonat.

Alongside anionic gemini surfactants came into the focus of interest the last years. Anionic gemini surfactants obey the general structure depicted in Figure 6, only the not charged head group is replaced by an anionic head group e.g. sulfate, carboxylate, sulfonate, phosphate and amide groups (75). The other group within the ionic surfactants is the group of cationic surfactants. The majority of cationic surfactants are amine or quaternary ammonium based (66). The drawback of amine based surfactants is their pH sensitiveness. The protonated state only exists at low pH values. If the pH value is increasing the protonated state is disappearing due to the acid base balance (66). Figure 10 shows the structure of ternary ammonium surfactants like fatty amine salts or fatty diamine salts and quaternary ammonium surfactants like cetyl trimethyl ammonium bromide (CTAB). Quaternary ammonium surfactants like CTAB are weak pH sensitive and used in applications like disinfectants due to their bactericidal characteristics (76). The phase and aggregation behavior is comparable with other ionic surfactants. Above the CMC, which is specified with 0.92 mMol/L (77), micelles are formed and at high concentrations liquid crystalline phases like hexagonal phases are existent (78).

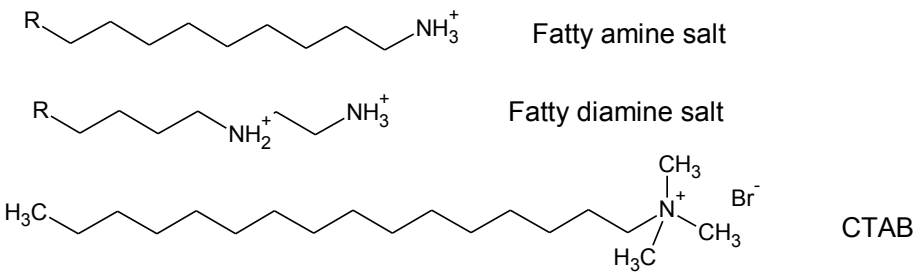

Figure 10: Structure of like cetyl trimethyl ammonium bromide (CTAB), a general structure of a fatty amine salt and a fatty diamine salt.

Typically ionic surfactants show no liquid liquid phase split in micellar solutions with a LCST in aqueous environment. To the knowledge of the author only the phase split of dodecyltributylammonium bromide is reported in the literature (79). The dodecyltributylammonium bromide + water systems split into two isotropic phases above the critical point at approximately 48°C and 46 wt. % surfactant (79). In contrast to nonionic surfactant's phase split the critical concentration is very high.

2.1.3 Zwitterionic surfactants

Zwitterionic surfactants include two oppositional charged groups. In many cases the source of the positive charge is ammonium. The source of negative charge is varied more often, but carboxylate is beside sulfate a commonly used source for the negative charge. They possess singular dermatological properties and do not interact with hard water (80). Therefore, zwitterionics are suitable for personal care products like shampoo and shower gel (66). Outwards they are formal uncharged technically one has to consider them as nonionic surfactants. However, some characteristics meet with ionic surfactants others meet with nonionic surfactants. The melting points are unusually high compared to other nonionic surfactants with a similar structure. The detection of melting point is usually impossible due to thermal decomposition (81). Krafft points are featured from zwitterionics, they show a characteristic common with nonionics (82). But in contrast to salts, which ionic surfactants are, zwitterionic surfactants undergo no ion exchange and they do not enhance conductivity.

Therefore, it is clear that they should not be mixed up with salts (81). Within the zwitterionic surfactants one can distinguish between amphoteric, acidic and basic surfactants. In Figure 11 four different zwitterionic surfactants are shown.

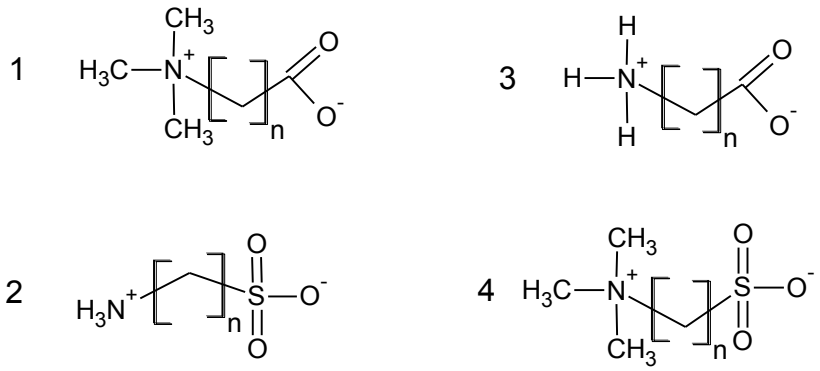

Figure 11: Examples for zwitterionic surfactants: 1) betaine with n=1; 2) taurine with n=2; 3) homoglycine with n=2 and 4) sulfobetaine with n=2.

2.2 Phase- and aggregation behavior

For understanding the surfactant's characteristics the knowledge about the chemical structure is important but not the unique important issue. The phase- and aggregation behavior is in the same manner important. Surfactants are distinguished by a large phase- and aggregation behavior diversity. In aqueous solutions surfactants show a fascinating and challenging behavior. At low concentrations they are dissolved in a monomeric state in the solvent. When a specific concentration is reached surfactant molecule self-assembly is beginning and micelles are formed. This concentration is the well-known critical micelle concentration CMC but it is not a fixed concentration, it is rather a concentration range when self-assembly sets in. In this range the trend of several properties like surface tension, density and osmotic pressure is changing. The CMC is a major key-figure of every different surfactant. With raising concentration liquid crystalline phases with high viscosity are formed. The surfactant molecules within the solution now have a long range order. A typical class of surfactants with a distinctive phase- and aggregation behavior is the class of the nonionic alkyl polyglycol ethers C_iE_j.

2.2.1 Surfactant + water

2.2.1.1 Phase diagrams

In literature the general phase- and aggregation behavior for systems of the type nonionic surfactant C_iE_j + alkane + water is well described. One of the first, who described the phase- and aggregation behavior, were Shinoda et al. (83). Also other groups attended the research of C_iE_j + water phase diagrams (22), (74), (84), (85), (86), (87), (88) and (89). The influence of ethoxylate chain length on the phase and aggregation behavior was investigated in several studies at constant carbon chain length (74), (90), (91), (92) and (93). The carbon chain length was equal twelve carbon atoms like the surfactant octaethylene glycol mono dodecyl ether used in this study. Figure 12 depict two general C_iE_j nonionic surfactant + water phase behaviors. At low surfactant concentrations the surfactant molecules are dissolved molecular disperse within the solution. When surfactant concentration is increasing aggregates are formed above the CMC. With increasing the surfactant concentration the aggregation number is increasing as well as the micelle shape is transforming from more spherical aggregates to cylindrical forms.

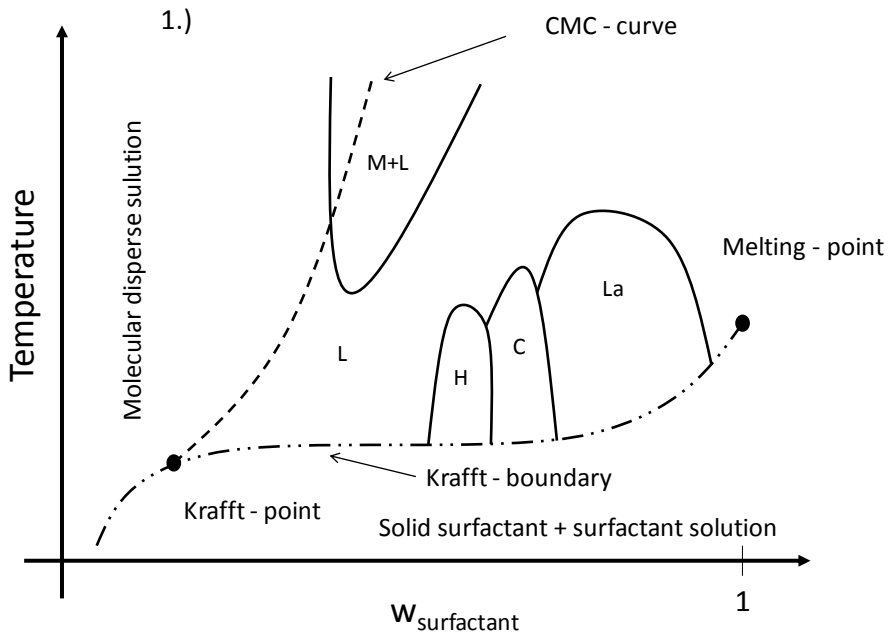

2.)

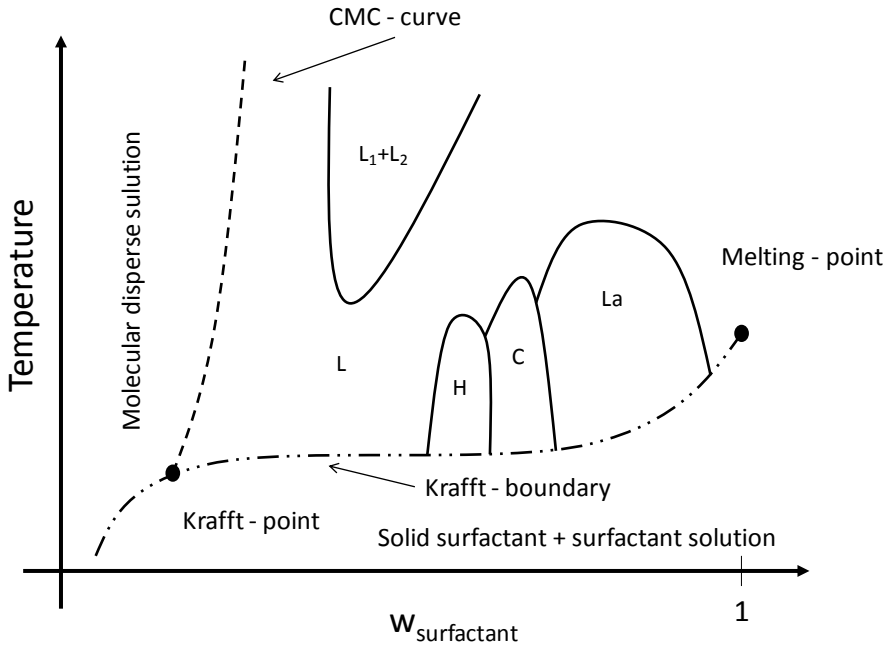

Figure 12: General phase diagram of a nonionic surfactant C_iE_j + water system. L: Micellar solution; 1.) M + L: Monodisperse surfactant solution in equilibrium with micellar solution; 2.) L_1 + L_2: Micellar solution L_1 in equilibrium with micellar solution L_2; L; H, C, La: Lyotropic mesophases.

If the nonionic surfactant concentration in the aqueous solution is in the range below approximately $w_{surfactant} \approx 0.2$ to $w_{surfactant} \approx 0.3$ the solution exists typically as single isotropic phase (94). If the temperature is increasing phase separation can occur and the solution splits into two phases. This is caused by the cleavage of hydrogen bonds with increasing temperature. As it is depicted in Figure 12 1.) and Figure 12 2.) the solution splits into two phases. Two cases are possible: 1.) In equilibrium one phase contains monomeric dissolved surfactant molecules and the other micelles (96) or 2.) both containing micelles (94) and (95). This miscibility gap exhibits the shape of a close loop miscibility gap, but at ambient pressure the upper critical solution temperature (UCST) is above the boiling point. The lower critical solution temperature (LCST) is in general below the boiling point (84), (86) and (96). The LCST is increasing with increasing j when i remain constant. Likewise the LCST is increasing with increasing i at constant j (90). It is typical that the LCST observed in systems composed of nonionic surfactants and water is located at diluted solutions. In nearly any case the concentration of the critical point is below approximately $w_{surfactant} \approx 0.05$ (94). At highly large concentrations lyotropic mesophases are formed as a result of micellar superstructures due to

hydrogen bonds. As a simplification in Figure 12 only the most common liquid crystalline phases are denoted such as the hexagonal phase H or the lamellar phase L. Within this phase the axes of the rod like micelles are orientated hexagonal. One can distinguish between regular hexagonal phases and inverse hexagonal phases. Subsequent the cubic phase C is formed composed of spherical aggregates. Cubic phases are highly viscous and formation of cubic phase can last up to several weeks in extreme cases. The formation of inverse cubic phases is depending on surfactant possible, too (21). Finally, lamellar phases are formed consisting of layers of surfactant and water molecules. Within these layers the surfactant molecules are ordered. In dependency of this order it is differentiated between L_α, L_β and L_β'. Viscosity is generally lower than in cubic phases (21). In Figure 13 the structure of liquid crystalline phases is depicted.

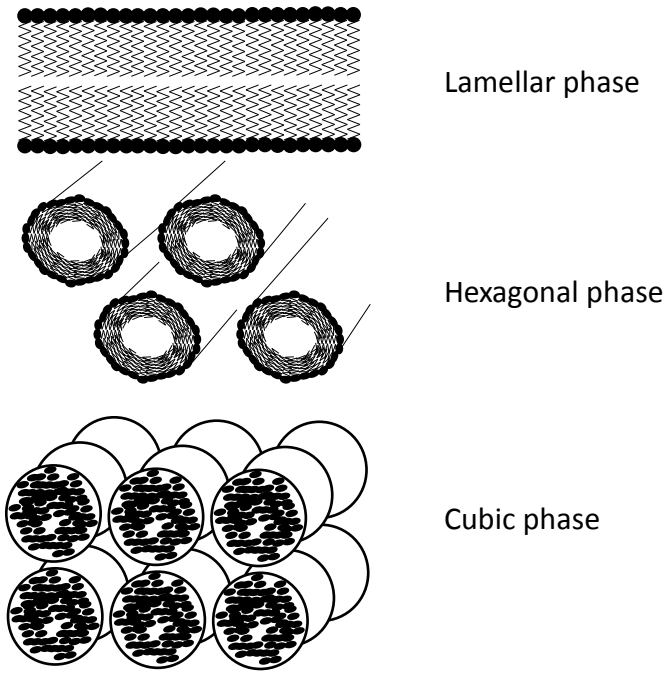

Figure 13: Selected structures of liquid crystalline mesophases.

At high surfactant concentrations and low temperatures (below the melting point of the surfactant) the surfactant acts as a solid and is not complete dissolved in the solution. With increasing temperature suddenly the whole amount of surfactant is dissolved in the aqueous solution. Sometimes this aspect is compared to a melting point (21) and predominantly it is called “Krafft-

boundary" (21). The intersection between Krafft-boundary and CMC-curve is named Krafft-point in honor of F. Krafft (Figure 12). The influence of the j number is crucial for the LLE. The system C_iE_j + water shows with increasing j the occurrence of several liquid crystalline mesophases. At a constant i, e.g. i=12, for $C_{12}E_3$ only the L_α phase arises, during further growth of j the normal cubic bicontinous, the hexagonal and the cubic phase occurs for j exceeding seven (90). Furthermore, the "critical temperature", that means the temperature the liquid crystalline vanishes is arising likewise (90). In particular occurrence of the cubic phase can be interpreted with the excluded volume effect due to the increased ethoxylate chain length (97). At low temperatures and high surfactant mass fractions the ethoxylate chain is profoundly hydrated and multifold H – bonds are existing. Therefore the free water is reduced and the spherical shaped micelles are ordered to a cubic liquid crystalline phase. At high temperature the H – bonds are broken and then the micelles are existent without any order. On basic illustration for these phenomena is the packing parameter ρ, with decreasing the ethoxylate chain length the packing parameter ρ becomes bigger. The packing parameter can be calculated according to Israelachvili et al. (98) by using **Eq. (2).**

$$\rho = \frac{v}{a_0 l_c} \qquad \textbf{(2)}$$

Thereby a_0 stands for the optimal surface occupied by one surfactant molecule at the oil-water interface. The surface a is equal a_0 if the free energy for one surfactant molecule inside the micelle is minimized. l_c represents the so called critical carbon chain length, l_c which is similarly to the length of one fully extended carbon chain. v means the volume of the hydrocarbon micelle core. If $\rho \leq \frac{1}{3}$ the surfactant molecules are arranged with a high curvature and spherical micelles are favored. These spherical micelles can be ordered at high surfactant mass fractions to the cubic liquid crystalline phase. For $\frac{1}{3} \leq \rho \leq 1$ the surfactant molecules are arranged cone shaped and lamellar or hexagonal liquid crystalline phases are favored. Finally, if $\rho \geq 1$ cylindrical micelles are formed, ordered already in a structure leading to a bilayer structure (99). The surfactant's melting point is

increasing with increasing the ethoxylate chain and it is also increasing with growing carbon atom number (97).

2.2.1.2 Micelles and CMC

The conception of micelle formation was postulated by Nägeli in 1879 in order to explain characteristics of starch or casein solutions (100). Later it was adopted to clarify gelation of silica and agar-agar. It was believed that micelles formed from monomeric molecules adhere at each other and form the gel (101). The concept of micelle formation from monomeric molecules was then transferred to soaps by Laing and McBain (102). Davies and Bury (103) introduced the idea of a "critical concentration for micelles" or CMC in 1930. Above this concentration micelles will be formed, below not. Accepted and established was the formation of soap micelles in aqueous soap solutions more than five years later (104) but the exact structure was still unclear. Schulman and Hoar later discovered the molecular structure of a micelle (105). Not only for basic research the CMC is an important characteristic quantity of every surfactant also for industrial research and application the knowledge of CMC is crucial. For example in detergent industry the CMC, beside the HLB – number **Eq. (1)**, was widely used for decades to detect and to gauge the washing power of different surfactants (106) and (107). The micelle formation in general is proceeding as the following. At surfactant concentrations below the CMC the surfactants are dissolved molecular disperse and they adsorb primarily at the oil/water or water/air interface. At a certain concentration the interface is occupied by surfactant molecules, the surfactant molecules show self-assembly and micelles are formed in the bulk phase. Here mainly two different forces are responsible for that phenomenon: On the one hand there is a hydrocarbon chain in an aqueous environment this leads to a strong force to transfer this hydrocarbon chain in an apolar surrounding. On the other hand an opposite force is generated hence there is the polar part of the surfactant in the polar solvent (86). This effect summarized as hydrophobic effect is responsible for the micelle formation (108). The surfactant self-

assembly yields to a variety of molecular formation. Different micelles can be formed as depicted in Figure 14.

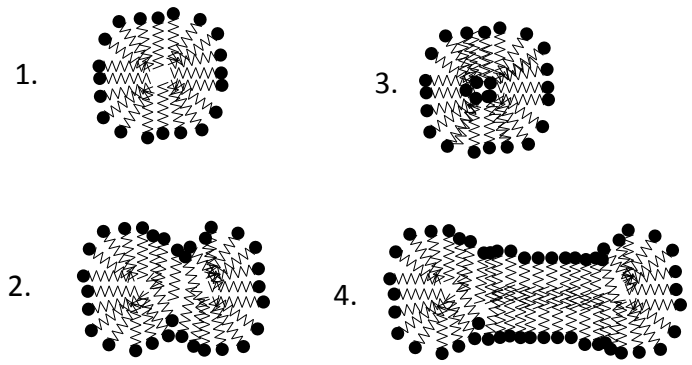

Figure 14: Different micelle shapes in dependency of surfactant concentration in aqueous solution according to Nagarajan and Ruckenstein (95).

The micelle formation in aqueous media is conjunct with a sharp transition of different physical properties. In opposite to that the physical properties of non-aqueous surfactant solutions do not undergo a sharp transition at a certain surfactant concentration. Therefore Ruckenstein (109) concluded that there is no CMC in non-aqueous or "dry" surfactant solutions with e.g. hydrocarbons. According to Kahlweit et al. (110) the formation of micelles in non-aqueous solvents is likewise controversial. Of course in literature CMC data especially for non-aqueous surfactant solutions prepared with ionic surfactants like SDS and CTAB as well as nonionic surfactants can be found according to Ramadan et al. (111), Evans et al. (112), Rico and Lattes (113) and Garibri et al. (114). Ramadan et al. (111) reported the micelle formation in hydrazine by fluorescence measurement. However, the used hydrazine contained water in a not negligible range: $w_{water} = 0.005$. Evans et al. (112) determined the CMC of tetradecylpyridinium bromide and hexadecylpyridinium bromide in ethylammonium nitrate prepared in the following way: Nitric acid was given in a cooled aqueous solution of ethylamine containing $w_{water} = 0.25$. The ethylammonium nitrate was dried in a rotary evaporator at 60°C under vacuum and then dried again in a lyophilizer. It was assumed that at the

end of this procedure the ethylammonium nitrate is dry, but the authors did not check with help of e.g. Karl-Fischer water detection. Rico and Lattes (113) measured the micelle formation of ionic surfactants in formamide. The formamide was used as delivered without drying; the given purity was 99.5%. Garibri et al. (114) measured the CMC of the ionic surfactants cetyltrimethylammonium bromide and cetylpyridinium bromide in ethylene glycol. Unfortunately, no data about the purity or the water content of the used ethylene glycol is given within the paper. The phase and aggregation behavior in aqueous media can be calculated with different approaches from statistical thermodynamics or equilibrium constants for micellisation. By neglecting the aggregation behavior Rudolph at al. (115) used a combination of the well-known Peng-Robinson equation of state (EOS) and the UNIQUAC g^E-model for describing the LLE containing water + C_4E_1, water + $C_6E_{j=3-4}$ and $C_7E_{j=3-5}$. Alongside Garcia-Lisbona et al. (116) used the statistical associating fluid theory with a hard sphere term (SAFT-HS) to calculate the cloud point curves for different aqueous alkyl polyoxyethylene surfactants. Browarzik and Browarzik (117) used a model to calculate the aggregation behavior as well as the phase behavior based on the mass-action law and continuous thermodynamics. They described the LLE for water + $C_6E_{j=2-4}$, water + $C_7E_{j=3-5}$, water + $C_8E_{j=3-6}$ and water + $C_{12}E_{j=4-6}$. The basis work to develop a model for the free energy change of micellization was done by Tanford (118). This basic approach was later pursued any further by Nagarajan and Ruckenstein (95), (119) and (120) as well as Puvvada and Blankschtein (94) and (121). Nagarajan and Ruckenstein (95) developed a model that allows the prediction of CMC, micelles size distribution and micelle form of nonionic, ionic and zwitterionic surfactants without any experimental data kept by examination of surfactants solutions except the area of the polar head group. The latter model was applicated by Enders and Häntzschel (122) in order to model the LLE of n – alkyl glucopyranosides + water. The model is briefly summarized in the following section:

The Gibbs energy of a surfactant containing solution can be calculated with help of three different contributions (Gibbs energy of micellisation G_0, Gibbs energy of mixing G_{mix} and an excess contribution G_E) according to **Eq. (3)**:

$$\frac{G_{sol}}{kT} = \frac{G_0}{kT} + \frac{G_{mix}}{kT} + \frac{G_E}{kT} \quad \textbf{(3)}$$

where k denotes the Boltzmann constant and T the thermodynamic temperature. According to Enders and Häntzschel (122), Blankschtein et al. (123) and Nagarajan (124) the Gibbs energy of mixing can be calculated by using **Eq. (4).**

$$G_{mix} = G - G_W - \sum_{g=1}^{\infty} G_g = kT \cdot \left[N_W \ln(X_w) + \sum_{g=1}^{\infty} N_g \ln(X_g) \right] \quad \textbf{(4)}$$

N_g denotes the number of aggregates with aggregation number g, X_g the mole fraction of the latter, N_W the number of water molecules and X_W the water mole fraction. An analytical expression for G_E **Eq. (5)** was proposed by Blankschtein et al. (123) and reads**:**

$$G_E = kT \cdot \left[-\frac{1}{2} \cdot C(T) \cdot \gamma \cdot \frac{N_S \cdot X_S}{1 + (\gamma - 1) \cdot X_S} \right] \quad \textbf{(5)}$$

with

$$C(T) = C_1 + \frac{C_2}{T} \quad \textbf{(6)}$$

N_S denotes the number of surfactant molecules and X_S the surfactant mole fraction. C_1, C_2 and γ are adjustable parameters. For parameter adjustment LLE data can be used. The LLE can be calculated with help of this g^E model. It is obvious that $G_E \neq 0$ for $X_S = 1$, this is the result of the following assumption: Within the pure surfactant micelles are existing, these micelles interact and therefore they differ from the non-aggregated pure surfactant. This has the consequence that $G_E \neq 0$ for micelles given that the reference state is the non-aggregated pure surfactant. The Gibbs energy of micellisation G_0 can be calculated using **Eq. (7)** according to Enders and Häntzschel (122).

$$G_0 = N_W \mu_{0W} + \sum_{g=1}^{\infty} N_g \mu_{0g} \quad \textbf{(7)}$$

G_0 can be obtained by knowing the standard potential of water μ_{0w} and the standard potential of aggregates μ_{0g} with aggregate number g. The chemical standard potential $\Delta\mu_{0g}$ for one surfactant molecule is defined by

$$\Delta\mu_{0g} = \frac{\mu_{0g}}{g} - \mu_{01} = (\mu_{0g})_{tr} + (\mu_{0g})_{def} + (\mu_{0g})_{ster} + (\mu_{0g})_{int} \quad \textbf{(8)}$$

according to Nagarajan and Ruckenstein (95) it is depending on temperature and aggregate shape. The "transfer term" $(\mu_{0g})_{tr}$ is representing the change in the free energy when the hydrophobic part of the surfactant is transferred from aqueous solution inside the micelle. Inside the micelle the hydrocarbon chain is treated as a liquid hydrocarbon. With help of solubility data of different hydrocarbons in water it is possible to estimate the transfer process of a methylene and a methyl group of the hydrocarbon tail from aqueous surrounding to the micelle interior. It is obvious that the liquid state inside the micelle cannot be the same liquid state that is on hand in liquid hydrocarbon since a small section of the hydrocarbon chain remains in contact with water at the micelle surface. In their preliminary papers (119) and (120) an empirical model was used to determine this contribution but later Nagarajan and Ruckenstein (95) used a lattice model to calculate the "deformation term" $(\mu_{0g})_{def}$. $(\mu_{0g})_{def}$ takes the deformation of the hydrophobic hydrocarbon chain inside the micelle into account. When a surfactant aggregate is formed an interface between the hydrophobic part of the micelle and the enclosed aqueous phase is generated. The change in the free energy associated with this phenomenon is represented by the term $(\mu_{0g})_{int}$. The contribution $(\mu_{0g})_{ster}$ is considering steric interactions between the surfactant's polar head groups. At the surface of the micelle the polar head groups are closing ranks and steric interactions as e.g. repulsion must be attended. For the case that the surfactant molecule contains a zwitterionic head group as shown in Figure 11 permanent dipole interactions can be considered in $(\mu_{0g})_{dipole}$. With help of this model it is also possible to consider ionic surfactants with the contribution $(\mu_{0g})_{ionic}$. The detailed calculation is described by Nagarajan and Ruckenstein (95). The first derivative of **Eq. (4)** and **Eq. (7)** with respect to N_W and N_g and holding pressure, temperature and N_g or rather $N_{g\neq g}$ and N_W

constant leads to the athermal chemical potential of water μ_W and to the athermal chemical potential of aggregates with aggregation number g, μ_g according to Blankschtein et al. (123). The chemical potentials μ_W and μ_g are given in **Eq. (9)** and **Eq. (10)**:

$$\left(\frac{\partial \frac{G_0 + G_{mix}}{kT}}{\partial N_W}\right)_{N_{g,T,P}} = \frac{\mu_W^{id}}{kT} = \frac{\mu_{0W}}{kT} + \ln(X_W) + 1 - X_W - \sum_{g=1}^{\infty} X_g \quad \textbf{(9)}$$

$$\left(\frac{\partial \frac{G_0 + G_{mix}}{kT}}{\partial N_g}\right)_{N_{g\neq g',N_W,T,P}} = \frac{\mu_g^{id}}{kT} = \frac{\mu_{0g}}{kT} + \ln(X_{Wg}) + 1 - g\left(X_W + \sum_{g=1}^{\infty} X_g\right) \quad \textbf{(10)}$$

The excess contribution is according to Blankschtein et al. (123) given in the following way:

$$\left(\frac{\partial \frac{G_E}{kT}}{\partial N_W}\right)_{N_{g,T,P}} = \frac{\mu_W^E}{kT} = \frac{1}{2} C\gamma \frac{X_S^2}{[1 + (\gamma - 1)X_S]^2} \quad \textbf{(11)}$$

$$\left(\frac{\partial \frac{G_E}{kT}}{\partial N_g}\right)_{N_{g\neq g',N_W,T,P}} = \frac{\mu_g^E}{kT} = \frac{1}{2} Cg\left\{\frac{(1 - X_S)^2}{[1 + (\gamma - 1)X_S]^2} - 1\right\} \quad \textbf{(12)}$$

Using the principle of the multiple chemical equilibrium (125) or Mukerjee constraint (126)

$$\mu_g = g \cdot \mu_1 \quad \textbf{(13)}$$

allows the calculation of size distribution function

$$X_g = X_g(g) \quad \textbf{(14)}$$

According Enders and Häntzschel (122) the size distribution function reads:

$$X_g = X_1^g \cdot e^{\left(-\frac{g \cdot \Delta\mu_{0g}}{kT}\right)} \cdot e^{(g-1)} \quad \textbf{(15)}$$

In literature several numerical methods for determination of the CMC can be found (95) and (122). According to Nagarajan and Ruckenstein (95) the CMC can be found at X_S, given that the number of

surfactant molecules dissolved in the solution is equal to the number of surfactant molecules inside the aggregates. This leads to the following equation:

$$X_1 = \sum_{g=2}^{\infty} gX_g \; with \; X_1 = \frac{1}{2} X_S \qquad \textbf{(16)}$$

Beside this, with help of the number-average aggregation numbers or the mass-average aggregation numbers of the aggregates the CMC can also be calculated. With increasing surfactant concentration these two numbers are escalating (122). This CMC can be identified as inflection point of the functions $g_n = g_n(X_1)$ and $g_w = g_w(X_1)$. The calculation of the two coexisting phases can be done with help of **Eq. (17)** and **Eq. (18)** the equality of the chemical potentials for the compounds in each coexisting phase according to:

$$\mu_W^I(X_S^I) = \mu_W^{II}(X_S^{II}) \qquad \textbf{(17)}$$

$$\mu_1^I(X_S^I) = \mu_1^{II}(X_S^{II}) \qquad \textbf{(18)}$$

The carbon atom number and the number of ethoxylate units influence the CMC significant. If the carbon atom number is fixed, e.g. $C_{i=12}E_j$ with j running from four to twelve the CMC is increasing as depicted in Figure 15. If the number of carbon atoms in the hydrophibic tail is varying and the number of ethoxylate units j is fixed the CMC is increasing with decreasing carbon atoms in the surfactant tail. Figure 15 shows likewise the influence of the carbon atom number on the CMC at constant temperature. Temperature also has influence on CMC

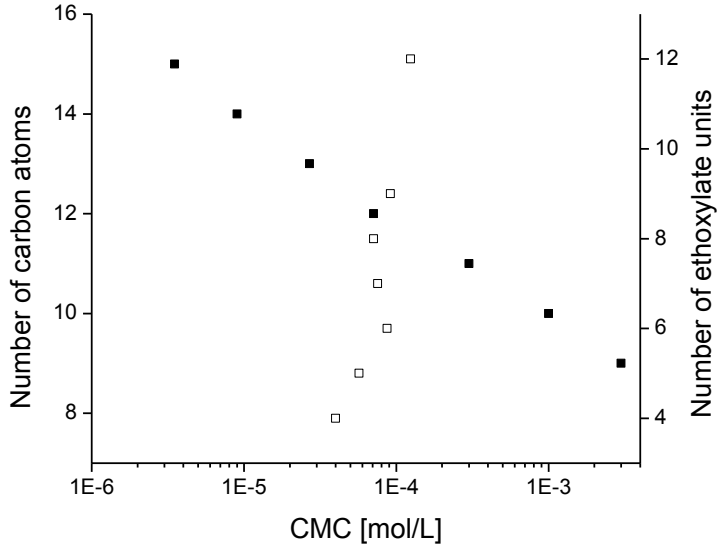

Figure 15: Influence of the carbon chain length on the CMC for the nonionic surfactant C_iE_8 at 25°C (solid squares, (127)) as well as influence of the ethoxylate chain length on the CMC for the nonionic surfactant $C_{12}E_j$ at 25°C (open squares, (74)).

Above 50°C the CMC is increasing again. This is the case, independently for i and j values. . For surfactants of the type C_iE_j the CMC is decreasing with temperature in the range between 10°C and 50°C as it is depicted in Figure 16.

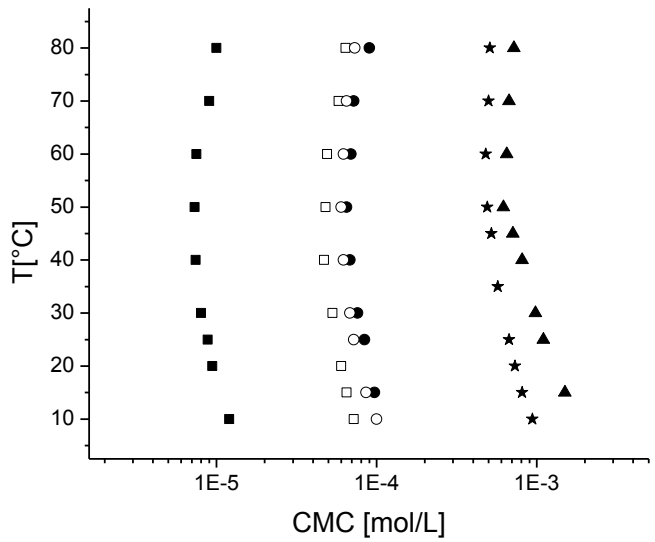

Figure 16: CMC of $C_{14}E_8$ (squares), $C_{10}E_8$ (stars), $C_{10}E_4$ (triangles) taken from (128) and $C_{12}E_4$ (open squares), $C_{12}E_6$ (open circles), $C_{12}E_8$ (circles) taken from (129) in dependency of temperature.

The similar behavior can be observed with ionic surfactants like soaps as Figure 17 depicts. The CMC depends not unsurprisingly strongly on the length of the carbon chain. With increasing the carbon chain length the CMC is decreasing. Also the CMC of soaps depends strongly on temperature: When the temperature is increasing, the CMC is decreasing dramatically (130). At high surfactant concentrations at first hexagonal and then lamellar liquid crystalline phases are formed (131) and beside that also pure soaps can form liquid crystalline phases (132).

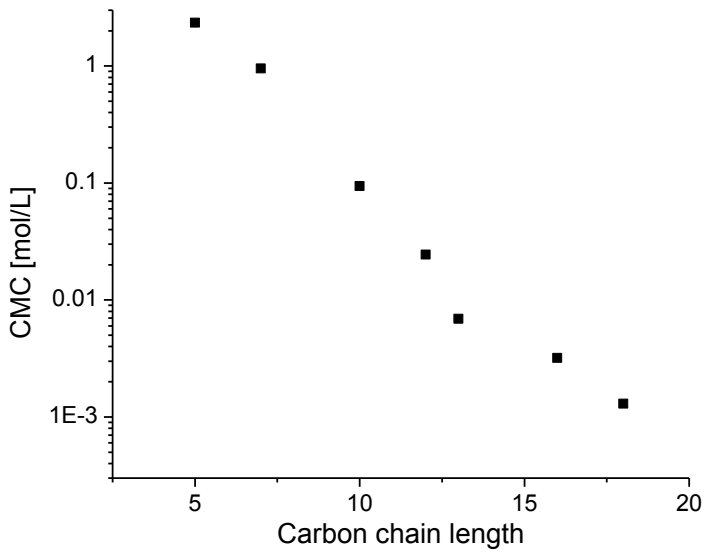

Figure 17: CMC of Na – soaps in dependency of carbon chain length at 20°C from (74).

Furthermore, the formation of liquid crystalline phases in non-aqueous soap systems is reported (133). The CMC, which is more a concentration range than an exact concentration can be measured due to the fact that several variables are changing in the range of CMC. However, the concentration data depends strongly on the measurement device accuracy. A few common methods for CMC detection according to Mukerjee and Mysels (74) are mentioned below:

1. Measuring the surface tension: When surfactant molecules are dissolved in water they adsorb primarily at the surface. Hence the surface tension is reduced when the amount of surfactant is increased. At a specific concentration the surface is fully covered with amphiphiles and the surfactant starts to aggregate within in the bulk phase and micelles are

formed. Henceforward the surface tension remains practically constant. If $\lg c_{surfactant}$ is plotted against the surface tension, the CMC is in evidence as a break of slope in curve progression. Often a minimum in curve progression is observed and indicated as CMC but this minimum appears as a result of e.g. impurities being solubilized in the micelles above CMC.

2. Light scatter measurements: The slope of intensity as well the turbidity of scattered light plotted against the concentration is shifted. At first the slope is moderate decreasing and with aggregate formation this slope is decreasing more abrupt.
3. Measuring the refractive index: Likewise it is possible to detect a change in slope if the solution's refractive index is plotted against surfactant concentration.
4. Measuring the UV/vis spectra: It is well known that the absorption spectrum of several surfactants is changing whether they molecules are present in a micellar form or not.
5. Calorimetric measurements by isothermal titration calorimetry (ITC) or differential scanning calorimetry (DSC): In case of ITC the CMC can be detected as followed: If a micellar solution is diluted with water one can consider two possible reactions. At first the micelles are decomposed into monomers and the heat of dilution and the heat of demicellisation can be recognized. With every injection the surfactant concentration in the aqueous solution is increasing and aggregates are formed at the CMC. Henceforward the micellar solution is diluted without any demicellisation. Thus the heat of dilution is detected. The heat flux, represented by the peak area, is plotted against the number of injections. At CMC the curve exhibits an inflection point based on the change in heat flux. In case of DSC a solution with fixed concentration is heated, the heat flux is compared with a reference. At the temperature micelles are formed the heat flux compared to the reference heat flux is changing and the CMC can be detected in the DSC scan. With this method the temperature influence on CMC can be detected.

6. Measuring bulk properties like density or velocity of sound: At CMC the density as well as the speed of sound is changing.
7. Measuring the absorption spectra of dye: Some dyes added to a surfactant solution exhibit a change in the UV/vis – spectrum when they are solubilized in micelles. The CMC can be determined by preparing solutions in the range of the CMC with the same concentration of dye. The absorption at a specific wavelength is recorded and at the CMC a change in the absorption spectrum is recognized. Orange OT also known as 1-o-tolyl-azo-2-naphtanol is widely used for this application. This method has the disadvantage that the added dye can influence the CMC although only in a slight manner given that the CMC now is detected in a ternary system containing water, surfactant and dye.

2.2.2 Surfactant + water + oil

The system surfactant + water + oil shows a complex phase behavior depending on temperature including three and two phase equilibria. Despite to the binary system water + nonionic surfactant the calculation of the phase behavior in the ternary system water + nonionic surfactant + oil is until today not satisfactory. The most important problem arise in the modeling of the phase behavior of these ternary systems is the bicontinuous structure of the middle phase microemulsion. This structure does not allow the application of classical thermodynamics according to Gibbs (134). The thermodynamic cornerstone of systematic investigation of these systems was put by Winsor in 1948 (135). He was one of the first who suggested a classification for the phase behavior of surfactant containing systems. If a surfactant is put to a mixture of water and oil, at low temperatures the nonionic surfactant is mostly dissolved in the water rich phase. Above the CMC oil is solubilized in micelles. This behavior is also called Winsor I phase behavior, sometimes it is abbreviated with 2 bottom phase meaning the surfactant is located in the bottom phase of the two phase system. When temperature is increasing two different possibilities are feasible: The surfactant solubility is

decreasing in the aqueous phase and the surfactant is crossing to the oil rich phase. In this case no microemulsion is formed. Second, the solubility in the aqueous phase is decreasing, but the solubility of surfactant in the oil rich phase does not increase in the same manner, thus a third phase is formed, the microemulsion. This behavior is called Winsor III phase behavior. At high temperatures the surfactant solubility has changed again: The surfactant is located in the oil rich phase and water can be solubilized in inverse micelles. This behavior is called Winsor II phase behavior or analogue to the two bottom phase now the phase is called two top phase, meaning that the surfactant is now mostly located in the top phase of the two phase system. For the case that the surfactant concentration is high a one phase system is existent. This phase behavior is called Winsor IV phase behavior.

2.2.2.1 Phase prism

The general complex phase behavior of the ternary system surfactant C_iE_j + water + alkane is well described in literature (22), (84), (86), (136), (137), (138), (139), (140), (141), (142), (143), (144) and (145). The first authors who started to investigate the phase and aggregation behavior of nonionic surfactants from the type C_iE_j were Kahlweit, Strey and coworkers (22), (84) and (86). Coming from the binary subsystem water + nonionic surfactant, which is depicted in Figure 12, for the complex phase behavior in the ternary system the subsystems surfactant + oil and water + oil are important as well. The system nonionic surfactant + oil show a UCST demixing behavior, though the upper critical temperature is usually below the melting point and therefore it is practically not detectable. The critical temperature T_c is rising above the melting point in case of hydrophilic surfactants and long chain alkanes. T_C in the system C_6E_5 + alkane is rising from 18°C to 55°C if the alkane chain length is increasing from ten to 16 (22). With increasing the hydrocarbon chain length the water solubility of alkane or alkene is decreasing dramatically as depicted in Figure 18. Hence the system water + alkane as well as the system water + alkene shows broad miscibility gap. The phase prism is emerging from

the Gibbs triangle lying at the bottom using the temperature or sometimes also the pressure as a vertical axis.

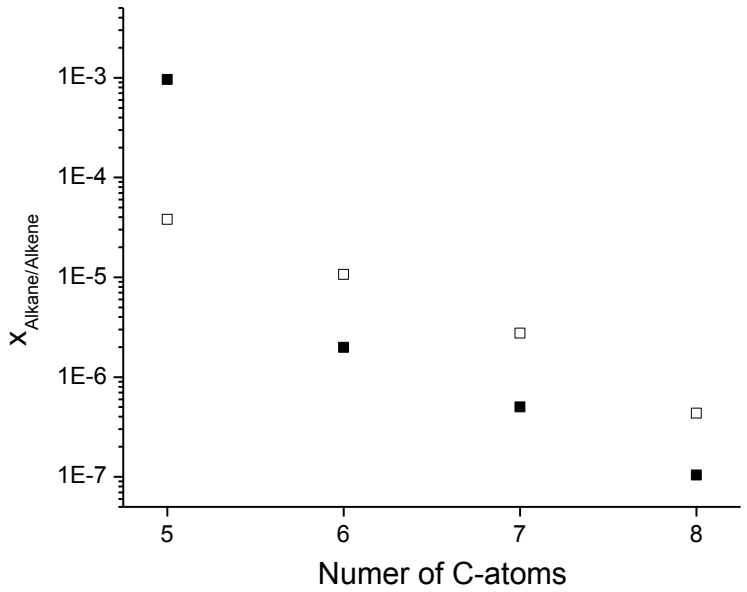

Figure 18: Water solubility of alkanes (solid squares) and water solubility of alkenes (open squares) at 25°C from (146).

As the system water + nonionic surfactant C_iE_j + oil is at moderate pressures practical not changing its demixing behavior with temperature, therefore the axis of choices is T. The schematic phase prism is shown in Figure 19. With help of the binary subsystems and the Gibbs's triangle for each temperature the phase prism can be constructed thus the single triangles are stacked. At low temperatures tie lines are expanded to the nonionic surfactant + water binary subsystem and therefore the critical point is located in the direction of the nonionic surfactant + oil subsystem, given that the solubility of surfactant in water is greater than in the latter system. When temperature is increasing the surfactant can exchange constantly from the aqueous phase to the oil rich phase as it is depicted in Figure 19, system 1. The more the oil's hydrophobicity is increasing or the surfactant's hydrophility is raised the surfactant is piled out the aqueous phase, but not completely miscible with the oil rich phase and henceforward the Winsor III system is evolving as it is shown in Figure 19, system 2 with the tricritical point. Adding a lyotropic salt results the same effect (86).

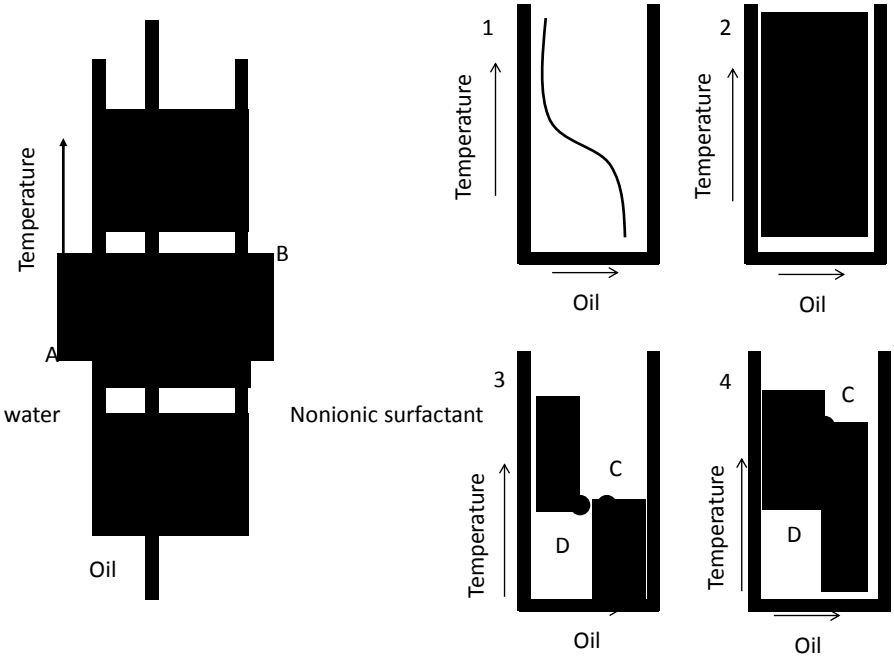

Figure 19: Schematic phase prism and projection of the critical line for a system composed of nonionic surfactant + water + oil. The critical line is projected on the binary water + surfactant system for four different systems: 1) no Winsor III phase, 2) system with a tricritical point T_{triCr}, 3) system with a small Winsor III phase temperature range, 4) system with a distinct Winsor III phase temperature range. In system 3) and 4) the endpoint of the critical line beginning in the Winsor I system is marked by C and the origin of the critical line passing through the Winsor II system is marked by D.

Having in mind that to find a tricritical point in a ternary system is coincidence, there the temperature, pressure and composition is fixed according to the phase rule (22) and (147). At the tricritical point the three existing phases become identical according to (148). If the oil's hydrophobicity is further raised and i and j are fixed or the surfactant's hydrophility is further raised, the Winsor III system temperature range is increased as well, Figure 19 system 3 and 4. The critical line in this system is split into two lines one ending at the temperature the three phase area is disappearing and one starting at the temperature the three phase are is appearing. At higher temperatures the surfactant solubility in the oil rich phase is increasing, resulting that the top of the triangle is moving towards the surfactant + oil binary subsystem. At very high temperatures the surfactant has changed its solubility again and the Winsor II phase behavior is occurring. The tie lines are now expanded towards the surfactant + oil binary subsystem and inverse micelles are formed.

2.2.2.2 Kahlweit's fish

To give a quick overview about the phase and aggregation behavior in the ternary system nonionic surfactant C_iE_j + water + oil the measurement of a complete phase prism is time consuming. Therefore Kahlweit and Strey (22) suggested several sections through the phase prism as depicted in Figure 20 in order to obtain a quick overview about the phase behavior. Section A is the most common section to give a first overview about the temperature dependent phase behavior. One obtain section A when the phase prism is cut at constant oil – water ratio $\alpha = \frac{m_{oil}}{w_{water}}$, e.g. $\alpha = 0.5$ towards the surfactant corner.

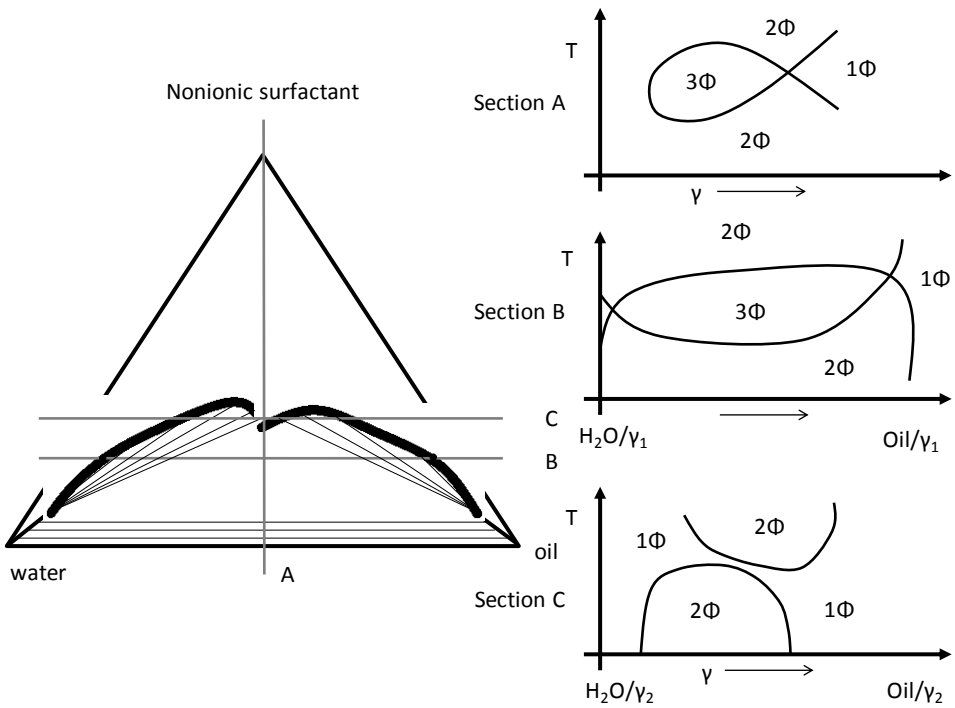

Figure 20: Three different cross sections through the phase prism Section A at different surfactant mass fractions γ and Section B and C at two different constant surfactant mass fractions γ_1 and γ_2.

In general also other oil – water ratios are possible. In dependency of temperature and $\gamma = w_{surfactant}$ the system exhibit two-phase, three-phase and one phase areas. If these areas are plotted in a $T - \gamma$ diagram one can find two-phase areas, a three-phase area represents the "fish body" and a one-phase area represents the "fish tail". In honor of M. Kahlweit, this diagram is called

the “Kahlweit’s fish”. Section B in Figure 20 represents a cut through the two phase area at a constant surfactant mass fraction evolving a three phase LLE. Section C in Figure 20 represents a cut through the two phase area at a constant surfactant concentration above the three phase LLE. In literature one can find several measured “Kalhlweit`s fish” diagrams mainly for the system nonionic surfactant + water + alkane (22), (84), (149), (150), (151) and (152). For systems containing alkenes the data basis is very limited. Notably Haumann et al. (15) published data for ternary systems of the type water + nonionic surfactant +alkene containing different Marlipal®-type surfactants. The phase behavior was detected optically at fixed composition containing $w_{1-\mathrm{dodecene}}: 0.79$, $w_{\mathrm{surfactant}}: 0.13$ respectively $w_{\mathrm{surfactant}}: 0.08$ and in the studied temperature range from 80 to 120°C no three phase equilibrium was reported. Müller et al. (153) and Rost et al. (19) reported a fish diagram for a system containing Marlophen NP9® + technical grade 1-dodecene + water at $\alpha = 0.5$ and Miyagawa et al. (154) reported a fish diagram for a system containing different Lutensol®-type surfactants + technical grade 1-octene or technical grade 1-dodecen at $\alpha = 0.8$. However, until today no fish diagram for a system containing pure surfactant + water + alkene compared with a fish diagram technical grade surfactant + water + alkene is available in literature to the authors knowledge. Furthermore, until today no phase prism for systems containing pure as well as technical grade surfactants + water + alkene were available in literature.

2.2.3 Surfactant + water + oil +salt

The addition of salt to the ternary system surfactant + water + oil has influence on the formation of the three phase body. The influence depends on type of salt it can be either lyotropic or hydrotropic. A lyotropic salt causes the salting out effect for substances with a high molecular weight. The general influence of salt for surfactant containing systems has been studied by Kahlweit and Strey (22), Kahlweit et al. (110) and Lang and Widom (155). Based on the three ternary subsystems the phase behavior in the quaternary system becomes visible. Let us start with the ternary subsystem water +

lyotropic salt + oil. The Gibbs's triangle is plotted in Figure 21. The binary systems water + oil and exhibit a broad miscibility gap and the solubility of salt within the oil is marginal. Starting from the binary system water + oil with addition of salt the system remains in a two phase state. Since the salt solubility in the aqueous phase is higher than the solubility in the oil rich phase tie lines are expanding towards the water + salt binary subsystem. With further salt addition beside the two liquid phases a third solid salt phase evolves.

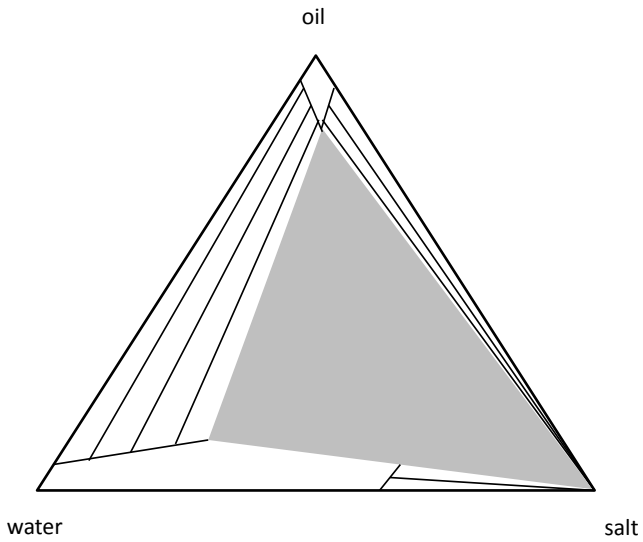

Figure 21: Schematic phase behavior at constant temperature for the system water + salt + oil.

With increasing the salt concentration the oil + surfactant + salt ternary subsystem remains in a three phase state across the whole salt concentration range as depicted in Figure 22 having in mind that both liquid phases are saturated with salt. The binary system surfactant + oil is above the surfactant's melting point complete miscible. Salt addition causes the formation of a solid salt phase beside the liquid phase. In almost all cases the solubility of salt is slightly higher in the surfactant rich phase (22) and therefore the two phase boundary is decreasing towards the oil + salt subsystem.

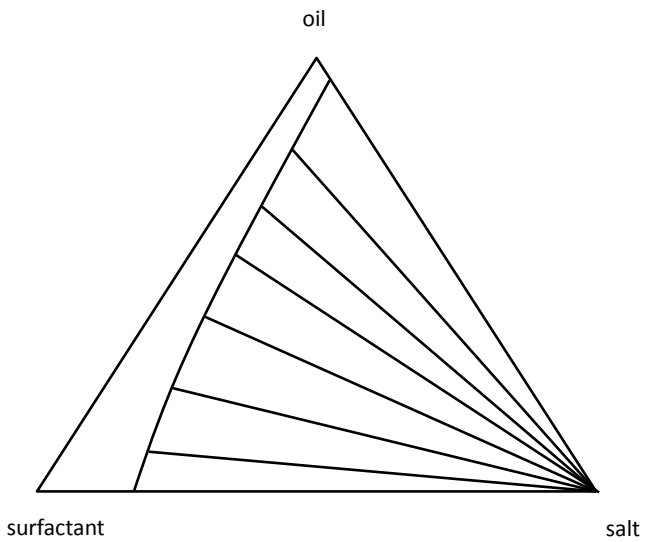

Figure 22: Schematic phase behavior at constant temperature for the system surfactant + salt + oil.

The ternary subsystem surfactant + salt + oil is hardly influenced by temperature. The ternary subsystem water + lyotropic salt + surfactant is the most important one to explain the behavior in the quaternary system. The schematic overview for this system at a constant temperature below the LCST in the binary surfactant + water system is shown in Figure 23.

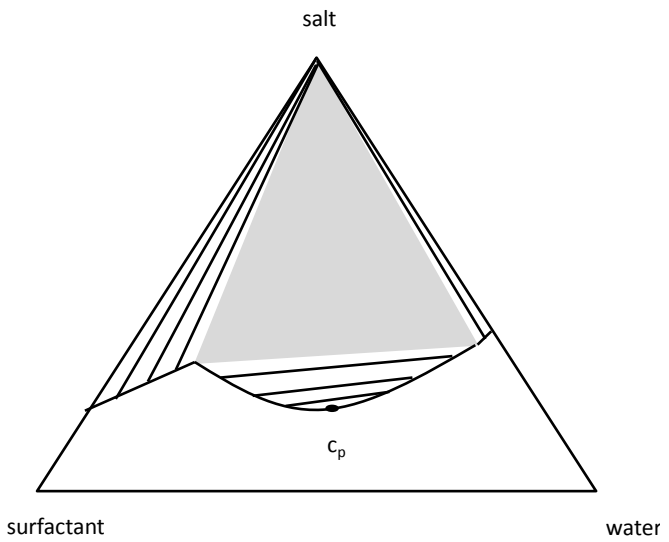

Figure 23: Schematic phase behavior at constant temperature below the LCST within the binary subsystem surfactant + water for the system surfactant + lyotropic salt + oil.

If the system temperature is below the LCST for the binary miscibility gap water + surfactant a homogeneous solution exists in the binary subsystem. By addition of a lyotropic salt at a certain salt mass fraction the salting out effect sets in and a two phase system is evolving. Further addition of salt causes the formation of a third solid phase beside the two liquid phases. In the quaternary system water + surfactant + oil + lyotropic salt the addition of salt leads through the salting out effect to a three phase equilibrium at constant temperature. By further addition of salt the three phase LLE is disappearing due to the coalescence of surfactant and oil rich phase. The effect of lyotropic and hydrotropic salt addition is pointed out in Figure 24.

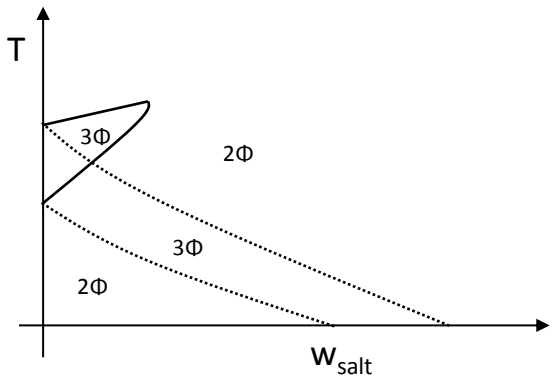

Figure 24: Schematic influence of salt addition to a quaternary system composed of surfactant + water + oil + hydrotropic salt (solid line) and surfactant + water + oil + lyotropic salt (dashed line) in dependency of temperature.

Figure 24 illustrates the addition of salt to the ternary system at a fixed composition of surfactant + water + oil. For the case that a lyotropic salt is added, with increasing salt concentration a three phase body across a wide temperature and salt concentration range is formed due to the salting out effect. If a hydrotropic salt is added to the same system the three phase body is disappearing at high salt concentrations due to the salting in effect.

2.3 Synthesis of surfactants

In general there are many varieties to produce surface active agents, like enzymatic (156), microbiological (157) and (158) and classical chemical synthesis (159) and (160). Of course each

synthesis causes its own byproducts. The C_iE_j type surfactants are often commercially produced by ethylene oxide condensation with long chain alcohols as depicted in Figure 25 according to Corkill et al. (161).

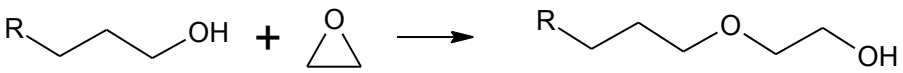

Figure 25: General reaction scheme of an ethoxylation reaction.

It is common to produce the nonionic detergents of the alkyl polyoxyethylene glycol monoether type batchwise in reactors using the Pressindustria alkoxylation process (160) operating between 120°C and 180°C and pressures between five and seven bar (159). This reaction leads not to a fixed number of ethoxylation units rather to a Poisson distribution of the ethoxylate units (162). The range of ethoxylation can be influenced by using different catalysts. If barium is applied as a catalyst, one can obtain a narrow range Poisson distribution (163). For the case that potassium hydroxide is used catalyzing the ethoxylation one receives a broad degree of ethoxylation with a large amount of non-converted educt. In this case the educt is fatty alcohol (164) and (165). If the fatty alcohol itself shows a chain length distribution, of course different alcohols can be found in the product. Degradation products such as peroxides, short chain aldehydes and other alcohols can be found in technical grade surfactants; summarized the byproducts can by hydrophilic, lipophilic or amphiphilic nature (166). All these information support the opinion that any technical grade surfactant is rather a true multicomponent system than an approximate pure substance.

2.4 Technical grade surfactants and purification techniques

Surfactant mixtures or technical grade surfactants are containing a lot of hydrophilic or hydrophobic byproducts as well as surfactant molecules with different carbon or ethoxylate chain length resulting from the surfactant synthesis described in 2.3., Figure 25. Furthermore, they can contain also residues from the catalyst applied for synthesis. To obtain thermodynamic data, pure substances are

preferred e.g. to discuss the carbon chain length or the ethoxylate chain length influence as it is represented in chapter 2.1 and 2.2. For measurement these surfactants have to be highly purified through complex and complicated processes. Due to thermal instability and an extreme low vapor pressure distillation or rectification is supremely ineffective or even infeasible (167) in case of $C_{12}E_j$ vacuum distillation is realizable until j=3, all surfactants with j≥3 decompose due to thermal instability (168). In literature only a few articles concern about surfactant purification. From the beginning of the 1960's chromatographic methods are known as one possible purification step (161) and (169). In addition to that gel permeation chromatography (GPC) can be utilized for surfactant purification (170). Nevertheless, until today the most common technique to obtain pure surfactant with fixed i and j is the preparative high performance liquid chromatography (HPLC) (171). After synthesis three purification steps follow according to Lang and Morgan (96). Primarily the bulk impurities, like not converted glycol and salt are extracted; within a second step not converted olefins and decyl bromide were removed and the final stage is the preparative HPLC purification. However, chromatographic methods are time and cost expensive. More cost effective procedures are possible but one has to accept a potential slight purification effect and an increased surfactant loss. The surfactant can be purified by using a special extraction technique according to Schubert et al. (166), Stubenrauch et al. (171) and Fujimatsu et al. (172). Therefore the complex temperature dependent phase behavior and aggregation behavior is used. The surfactant changes its solubility in the aqueous and in the oil rich phase within a relative small temperature interval. For most of the surfactant impurities this is not the case. They are in the relevant temperature interval either water soluble or oil soluble. If the surfactant is added to a water/oil mixture and the excess phases were replaced by fresh water respectively oil it is possible to remove the more hydrophilic and the more hydrophobic impurities without a significant surfactant loss. At the last separation step the surfactant remains in the oil rich phase and the solvent, e.g. hexane can be evaporated (166). This technique also known as the three phase extraction technique was improved by Stubenrauch et al. (171) in order to remove also impurities that show approximately the same surface activity than the

surfactant. Therefore the surfactant concentration in the ternary mixture water + nonionic surfactant + oil is in the region were evolve of a Winsor III system just meets the requirements. One can assume now that impurities show an exceeded or similar surface activity are preferential located in the tiny middle phase preconditioned the total amount of impurity is small. This is called the "inverse three phase extraction technique" (171). The middle phase can be discarded and the surfactant can be received within the oil phase. On other purification technique according to Lunkenheimer et al. (167) uses a different approach to remove more surfactant active trace impurities: An aqueous surfactant solution is filled in a glass tube featuring a small diameter. If the vessel is placed in a horizontal position there is a large surface. In an upright position the surface is narrowed to the tube's diameter meaning that the trace impurity concentration on this small surface is increased. Now a small amount of liquid (≈50µL) is removed directly from the surface and simultaneously the total amount of trace impurity is reduced. Beside this solid material can be used for adsorbing impurities from ionic surfactant solutions (173) and also crystallization is appropriate for ionic surfactant purification (174). But one has to consider that surfactant purified with help of the mentioned procedures is only available in an mg scale. However, for any economic large scale technical application technical grade surfactant has to be used. This results directly of the exorbitant price of pure surfactants, e.g. the surfactant $C_{12}E_8$ exhibits a three phase area in the for hydroformylation of long chain alkenes relevant temperature range (17), but it is not feasible for labor or technical scale processes given that the price is about $180\frac{€}{g}$ (price mark, July 2013). Here technical grade surfactants can be an option to avoid the latter problems. Therefore one has to consider that technical surfactants are by no means pure substances and it isn't possible to neglect the impurities. Technical grade surfactants are a mixture composed of several C_iE_j, and only the major component $C_{i=a}E_{j=b}$ is given in the data sheet. Moreover very little information is specified for commercially available surfactants. Usually the cloud point at $w_{surfactant} = 0.01$ is given as quality characteristic. To estimate the surfactant quality with help of cloud point is practicable for a rough approximation but not for determining the exact amount of impurities or homologous distribution having in mind that the cloud point curve

progression isn't defined by knowing one cloud point. For the technical grade surfactant Genapol X 080® with the major component $C_{12}E_8$ even the cloud point is not indicated in the certificate of analysis (175). It is well known that yet small impurities have an enormous impact on the data because they are surface active as well. This means even at a negligibly small bulk concentration the concentration of impurities at the interface is in a large scale. This leads to the consequence that surface chemical investigations are not satisfactory (167). In general non surface active impurities might be negligible if the surface tension is measured but they may influence the cloud point curve and vice versa.

3. Applying surfactants for chemical reactions: Hydroformylation of alkenes

Since more than 40 years ago the idea of catalysis in micellar solutions appeared (176) and spread until today through the increased focus on "green chemistry". This means in most instances applying water as solvent in industrial organic chemistry and therefore the development of new approaches for processes, catalysis and reactions. Implementing the solvent water e.g. as catalyst solvent is beneficial in many ways. Often toxic and hardly volatile organic solvents (meaning that the removal of these solvents exhibiting a low vapor pressure is energy intensive) can be replaced by the environmental friendly, economically advantageous and completely safe to use alternative water. Many a time a nearly complete catalyst recycling with help of a simple phase separation step in organic product phase and aqueous catalyst phase is feasible. This is the base for large scale as well as for fine chemical production processes (177). Therefore, from the beginning of the 1970's research focus on the development of novel water soluble ligands for catalysis (152). The bottleneck in many cases applying water as solvent is the marginal solubility in hydrocarbons e.g. alkenes, representing the educts. To correct this disadvantage the addition of a surfactant can be helpful (1) and (178). The general idea is to perform the reaction at high temperatures in the Winsor III (152) or in the Winsor II region (179) and separate respectively recycle the catalyst at low temperatures within the aqueous phase. Until today several reactions, like Suzuki-coupling reactions (152) or Heck reactions (180) to combine two aromatic rings as well as polymerization to obtain almost monodisperse latexes [the polydispesrsity index $\frac{M_W}{M_N}$ with M_W mass-average molar mass and M_N number-average molar mass ranges between 1.05 and 1.08] (181) and oxidation of e.g. high toxic sulfides (182) and cyclohexane (1) are performed with addition of surfactants.

3.1 Hydroformylation reaction

The Rh- or Co- catalyzed hydroformylation of alkenes is an outstanding reaction in the chemical industry. In 2012 more than $2.5*10^9$kg aldehydes or “oxo-products” where produced with help of the hydroformylation process (183). In 1930 Smith et al. (184) reported the formation of oxygen containing compounds were reported at temperatures above 200°C during the conversion of water gas and ethylene with help of Fe and Co catalysts. These compounds were interpreted as intermediate products in the synthesis of hydrocarbons and not as oxo-products which are obtained from an alone standing reaction (184). As an alone standing reaction, hydroformylation was discovered by Roelen at Ruhrchemie company, Oberhausen in the end of 1937 (185) and the hydroformylation process was registered as patent in 1938 by the discoverer (186). The general reaction scheme is shown in Figure 26.

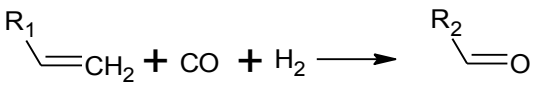

Figure 26: General scheme of the hydroformylation reaction.

Alkenes are converted in presence of synthesis gas and a metal- (e.g. Fe or Ag) or a transition metal catalyst (Rh, Co, Ni, Pd) to the aldehyde (187). The first catalytic cycle for the Co-hydrotetracarbonyl $HCo(CO)_4$ catalyzed hydroformylation reaction was published by Heck and Breslow in 1961 (188). Through the reaction, the alkene is extended with one carbon atom. Aldehydes are typically intermediate products e.g. in surfactant or plasticizer industry (189). The hydroformylation of alkenes leads to several in part high boiling byproducts like ketones and polyketones (190) and (191) or alkanes, alcohols, alkyl formats and branched aldehydes or alcohols (192), (193), (194) and (195). In literature only a few studies on the influence of ligands or reaction conditions on hydroformylation side products can be found (192) and (194); in dependency of the catalyst, ligand and the reaction conditions several byproducts like iso - aldehydes can occur (15). The ligand basicity of an organophosphine ligand has an influence on side product formation; organophosphine ligands

showing a high basicity form a smaller amount of alcohols and paraffines than organophosphine ligands possessing a low basicity at equal reaction conditions (192). Markert et al. (195) found via investigation of the hydroformylation of 1-dodecene that the main side reaction is the isomerization. The isomerization itself is reversible; however, these isomers are as well as 1-dodecene reactants for hydrogenation and hydroformylation and therefore the background for any other side product formation, namely branched aldehydes, branched alcohols and dodecane. The hydroformylation of cyclic compounds like cyclohexene is likewise possible (196). Alongside hydroformylation of alkenes other starting substances can be hydroformylated, like the hydroformylation of styrene exemplified for the hydroformylation of vinylarenes (197), (198) and (199). If e.g. vinylarenes are hydroformylated enantiomerically pure it is talked about asymmetric hydroformylation (200). Asymmetric hydroformylation of vinylarenes can lead to 2-aryl propionic acids. These acids are widely used in pharmaceutical industry to synthesize nonsteriodal anti-inflammatory drug belonging to the profen class (201). One other approach is to combine the hydroformylation with several other reactions e.g. the hydrogenation (202) and (203). A feedstock to produce long chain alcohols are aldehydes. Hence it is obvious to combine two reaction steps to yield the alcohol directly utilizing the mild reaction conditions and the high selectivities (202).

3.2 Catalysts for hydroformylation

The hydroformylation can be catalyzed by many metals or transition metals in combination with a broad variety of ligands. Universally catalysts applied for hydroformylation exhibit the chemical structure $H_aM_b(CO)_cL_d$ (187). Thereby “M” connotes a transition metal atom. In literature even bimetallic catalysts can be found, consisting of two different transition metal atoms (204). It has been found that bimetallic catalysts can contribute in further development active catalysts for hydroformylation especially since they are in some cases more active than their monometallic analogue (205). The metal atom must be able to form a carbonyl complex with CO, through the

modification with different ligands L_d the e.g. selectivity can be influenced. For catalytic hydroformylation a lot of metals are suitable but not surprisingly there exists an order in hydroformylation activity: $Rh \gg Co \gg Ir > Ru > Os > Pt > Pd > Fe > Ni.$ Alongside the multifaceted varieties of different catalysts for hydroformylation the evolution of industrial applied catalyst can be divided into several steps. The industrial process originally developed by Roelen at Ruhrchemie company and realized later also by Badische Anilin & Soda Fabrik (BASF) and Imperial Chemical Industries (ICI) used the simple catalyst cobalttetracarbonylhydrogen $HCo(CO)_4$ (206). Later it was found by Shell Company that the implementation of a phosphine modified Co catalyst system could improve the process significantly in terms of lowering the operating pressure and temperature (183). Nevertheless the chemo- and regio-selectivity realized with Co catalyst is limited (183) and therefore the important milestone in progress of industrial as well as lab-scale hydroformylation is the introduction of Rh complex catalyst namely Tris(triphenylphosphine)rhodium carbonyl hydride $RhH(CO)(PPh_3)_3$ or RhTPP by (207). Rh-TPP was later modified via sulfonation with oleum to the well-known Rh-tris(m-sulfophenyl)phosphine trisodium salt (Rh-TTPS) (208). This highly water soluble ligand [approximately 1.1 kg/L], for years the only industrial usable and inexpensive ligand, was applied in the Ruhrchemie process (209). Both ligands are depicted in Figure 27.

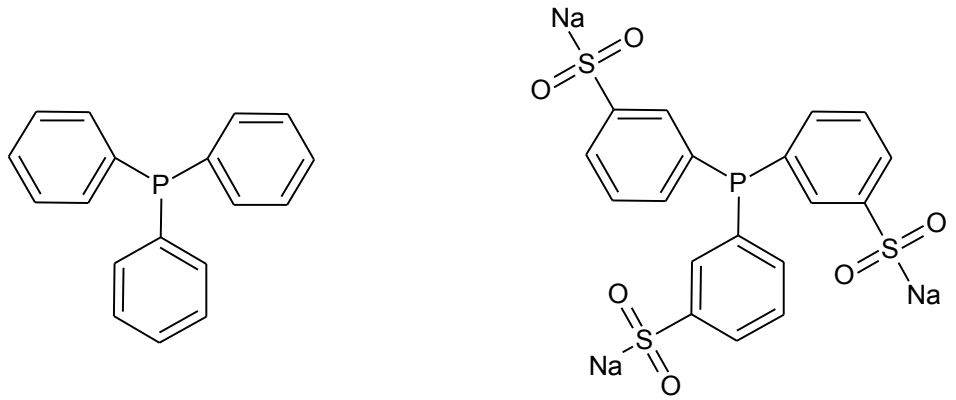

Figure 27: Chemical formula of the TPP (left side) and TPPTS ligand (right side).

Phosphine ligands like SulfoXantPhos or BIPHEPHOS having a more complex chemical structure depicted in Figure 28 are also applied in hydroformylation with good results (195), (210) and (211). Application hindering could be with such ligands the more laborious synthesis and increased

instability compared to more “simple” ligands like Rh-TPP or Rh-TPPS, which can be synthesized easily. In addition to that latter ligands are more reactive and stable. Furthermore, with phosphine ligands hydrolysis and alcoholysis as well consecutive reaction with the product itself can appear (212). Today Rh catalysts are commonly used in industry as well as in academic research (15), (16), (18), (19), (195), (213), (214), (215) and (216); although the cost for the Rh catalyst system of course is higher but nevertheless it offers also some considerable advantages like high selectivity and catalyst activity, low reaction temperatures and pressures (mild reaction conditions).

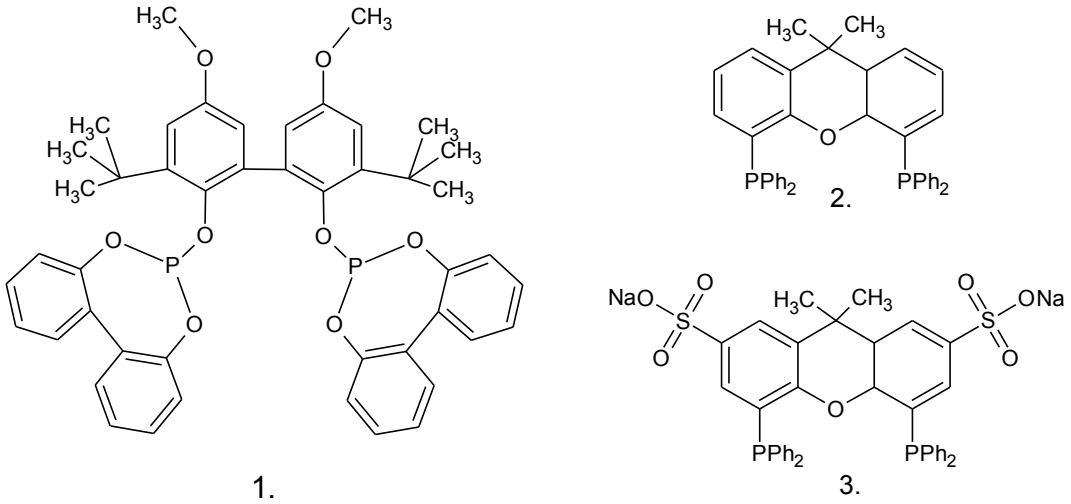

Figure 28: Phosphine ligands for hydroformylation: 1. BIPHEPHOS ligand, 2. XantPhos ligand and 3. SulfoXantPhos ligand.

Of course this has to be accompanied with a sophisticated catalyst recycling concept, e.g. implemented within the Ruhrchemie/Rhône-Poulenc oxo process (Ruhrchemie process) (213). Alongside other transition metals for catalysis of hydroformylation were investigated: Iridium is also able to catalyze hydroformylation. Although Ir-complexes are in some cases more stable than the correlated Rh-complexes (217) the turn over frequency (TOF) is less than with Rh catalyst and the ratio of n-aldehyde to iso-aldehyde (n:i ratio) is little with 74:26 (218) assumed that the n-aldehyde is the desired product. The TOF is referred to the number of moles a catalyst can convert to the educt per second. As one of the first alternatives to the in the early years of hydroformylation widely applied Co catalysts Ruthenium was found being able to catalyze the reaction (219). The activity and

selectivity was increased compared to the conventional Co catalysts as well it was possible to operate the reaction under mild reaction conditions (220). Drent and Budelzaar (221) have shown that Palladium is also a promising catalyst for hydroformylation of propene and 1-octene under mild reaction conditions. Through neat variation of ligands it is possible to achieve a good aldehyde yield up to 95%. One other suitable transition metal for catalysis of oxo-synthesis is Pt. The first patents for hydroformylation with Pt catalyst were granted in 1966 to Slaugh and Mullineaux (222) and Wilkinson (223). The metal with the lost activity relating hydroformylation catalyze activity is iron. Of course Fe has several advantages since it is easily available, not cost intensive despite to the previously introduced transition metals and rife in nature but it could not enforce due several disadvantages hindering the hydroformylation. Pergola et al. (204) reported a lack of long term stability and in addition to that the n:i ratio was very poor with 36:64. Summarizing all alternative transition metals one has to come to the conclusion that until now there are no practicable alternatives to Rh or Co catalysts in the field of hydroformylation (183).

3.3 Industrial hydroformylation

Large amounts of oxo-products were produced in industry and nearly all obtained aldehydes are used as feedstock for further processing. Theoretically alcohols, carboxylic acids or aldol products can be produced. But according to Protzmann and Wiese (224) mainly three product groups are produced: Short chain aldehydes are used to produce solvents, e.g. butanol. Aldehydes with a medium chain length (C_5 to C_{12}) are converted into plasticizers and long chain aldehydes (C_{13} to C_{17}) are usually applied for producing surface active substances. At present different approaches for industrial hydroformylation are representing the state of the art. The way alkenes are hydroformylated in industry depends strongly on the chain length.

3.3.1 Industrial hydroformylation of short chain alkenes

The hydroformylation of short chain alkenes were continuously improved the last decades. Until the beginning of the sixties, in industry short chain alkenes were hydroformylated at high pressures and temperatures with help of Co catalysts (185), (213) and (225). A typical process is represented by the BASF process: Propene is converted with synthesis gas at temperatures between 140°-180°C and pressures between 265-295bar in liquid phase. After reaction the Co catalyst is transferred through chemical reaction into an aqueous Co-salt solution and recycled within the aqueous phase. Not converted educt and synthesis gas was not recycled, but combusted. The n:iso ratio is 3:1 (206). As a follow up processes the low pressure (LPO) oxo-processes were introduced as a reaction to the 1973 oil crisis and the increased energy efficiency requirements. The Union Carbide Company (UCC) developed the first LPO process known as the UCC-process (187). The process shows several improvements to the former BASF process. A recycle stream to recycle not converted olefin was introduced in the process to counter increased raw material costs. Through the application of a novel Rh-catalyst temperatures and pressures could be decreased to prevent high costs for energy. According to Beller et al. (187) this process has two different forms of appearance. For both, the catalyst is dissolved in a solution of high boiling aldehydes inside the reactor. Within the UCC gas recycle process the product is evaporated from the reactor and partly condensed for further purification. The not condensed part is recycled with the not converted educt and synthesis gas into the reactor. To avoid large volumes one proceeded to remove a liquid stream containing product, educt and catalyst solution. The product is removed from the stream with help of strip column. The pressure in this UCC liquid recycle process is around 18bar at temperatures 85°-90°C. Parallel to Union Carbide BASF developed a similar LPO gas recycling process operating at approximately 110°C and 15-17bar (187). The major improvement to hydroformylation of short chain alkenes was the introduction of aqueous biphasic catalysis to industrial hydroformylation by the Ruhrchemie process in 1984, which is state of the art until today (2), (214) and (216). The process flow chart is depicted in

Figure 29. Propylene and synthesis gas are introduced in the continuous stirred reactor where the aqueous catalyst solution is located. Before the synthesis gas is used to strip not converted propylene and synthesis gas from the product stream. Hence the excellent water soluble Rh-TPPTS catalyst is immobilized in the aqueous phase no catalyst removal from the product stream is necessary. This catalyst is additional not sensitive to catalyst poison sulfur, which allows the operation with synthesis gas without further acid gas removal (213). After phase separation the aqueous catalyst phase is recycled and the product phase is purified into a fraction of n- and iso-aldehyde. Typical process parameters are temperatures between 110° and 130°C and pressures between 40 and 60bar (187).

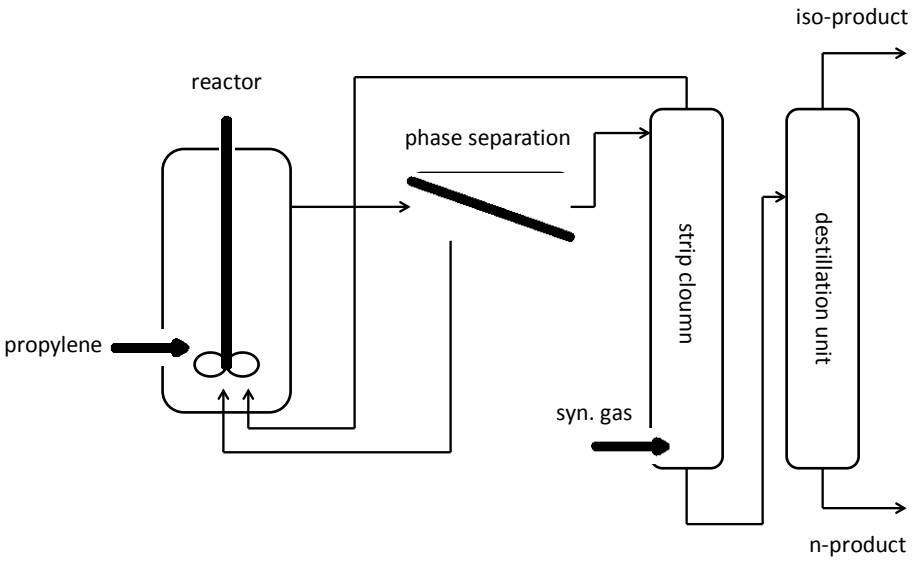

Figure 29: General flow chart of the Ruhrchemie hydroformylation process.

3.3.2 Industrial hydroformylation of long chain alkenes

Industrial hydroformylation of long chain alkenes until today means homogeneous Co catalyzed reaction under harsh reaction conditions (16), (187) and (226). At present three different approaches are adopted. For all three processes the reaction is carried out equal in a homogenous phase at high temperatures and pressures, e.g. 175°C and 290-300bar. Unequal is the catalyst recycling concept.

The Co catalyst is oxidized with acetic acid and the now water soluble Co compound is washed out (BASF). At Ruhrchemie the Co catalyst is removed by thermal Co carbonyl degradation. Only within the EXXON process the catalyst is recycle is possible without changing the coordination or oxidation state in the way that sodium cobalt carbonylate is recovered from the product and transferred into the active catalyst form cobalt carbonyl hydride (187).

3.4 Hydroformylation in microemulsions

Based on the Ruhrchemie process described in 3.3.1 for hydroformylation of short chain alkenes combining the advantages of homogenous catalysis, primarily no mass transfer limitation and mild reaction conditions, with the advantages of heterogeneous catalysis, mainly excellent catalyst recycling or catalyst immobilization, a similar process for long chain alkenes could be supposable. Furthermore, the immobilized catalyst simplifies the product purification. However, one has to face the problem that the water solubility of alkenes decreases dramatically with increasing the carbon chain length as it is depicted in Figure 18 and described by Cornils et al. (2), Haumann et al. (15), Cornils and Kuntz (208) and Kohlpaintner et al. (214). Additionally the alkene reactivity decreases slightly with increasing chain length, just as well in monophasic hydroformylation (227). Therefore the Ruhrchemie oxo-process is not applicable for alkenes with a chain length exceeding five (228) respectively six (16) and (154) carbon atoms. It is now one of the classical problems of chemical engineering occurring: An aqueous catalyst phase, which is absolutely necessary for reaction, has to be brought in contact with a hydrophilic product phase. Different strategies to overcome this dilemma are discussed in literature. One is the addition of a cosolvent (229), likewise the use of a supercritical fluid could be helpful (230). As well as the application of an ionic liquids is discussed (231). Beside this the addition of a surfactant could prove helpful. Menger et al. (232) introduced in 1973 as one of the first the possibility of reactions, here ester hydrolysis, performed in micellar media. The idea spread and until today a large number of different applications in micellar media or

microemulsions were examined in different workgroups (181), (233), (234), (235), (236) and (237). Haumann et al. (15), Ünveren and Schomäcker (18), Miyagawa et al. (154) and Hamerla et al. (216) applied microemulsions as reaction media for hydroformylation of alkenes with a carbon chain length ≥ 8 under mild conditions. Haumann et al. (15) investigated the hydroformylation of 1-dodecene with help of a surfactant containing system at 75°C and several pressures, the conversion of alkene to aldehyde increased with increased pressure at constant temperature T=75°C. Secondary the conversion was investigated at different temperatures and fixed pressure, giving the result that conversion at low temperatures was low. With increasing temperature the conversion reaches a maximum declining with further increased temperature. This could be a hint that hydroformylation of long chain alkenes is performing improved in the Winsor III system as shown in Figure 19. The TOF was below industrial processes. Further investigation was done by Miyagawa et al. (154) with hydroformylation of 1-tetradecene, 1-dodecene and 1-octene. They could confirm the presumption that reaction takes place favored in the three phase area given that reaction rates in the three phase area are higher than in Winsor I and Winsor II system. This is in good agreement with the results obtained by Tjandra et al. (238) and it was later confirmed by Rost et al. (19) and Hamerla et al. (216). Also the reactivity among different isomeric olefins drops in the following alignment: terminal olefin ≫ internal olefin > cyclic olefin ≫ branched olefin. Ünveren and Schomäcker (18) investigated the hydroformylation of 1-octene in microemulsions and micellar media. They concluded that the amount of added surfactant has no influence on hydroformylation selectivity. Hamerla et al. (216) compared the hydroformylation of 1-dodecene in a microemulsion with hydroformylation in a homogenous reference system. The reaction was performed at 110°C and later temperature was shifted to 80°C following the product influence on the Winsor III system. Operating pressure was set to 40bar with a syngas CO_2/H_2 1:1 ratio. Nevertheless, TOF in the homogeneous reference system was about six times higher than TOF in the multiphase system. Almost total conversion could be reached after approximately 180 min. However, the high TOF was bought by a worse n:i ratio [n:i = 94:6, homogeneous system and n:i = 98:2, multiphase system] and with a high accumulation of

branched olefin. According to Müller et al. (153) and Rost et al. (19) a continuous operating process could be designed as depicted Figure 30 in consisting of a reactor section, a separator and an additional purifying step with the following specifications. In the reactor olefin is converted with synthesis gas and help of catalyst continuously to linear aldehyde. The reactor is temperate in the Winsor III temperature region meaning that the process starts at 110°C with a stepwise decreased temperature to follow the Winsor III system. For this experiment the nonionic surfactant Marlophen NP9® was used and the pressure was kept constant at 40bar with a syngas CO_2/H_2 1:1 mixture. The temperature adaption is necessary since the aldehyde is influencing the LLE in the system Marlophen NP9® + water + technical grade 1-dodecene according to Rost et al. (19).

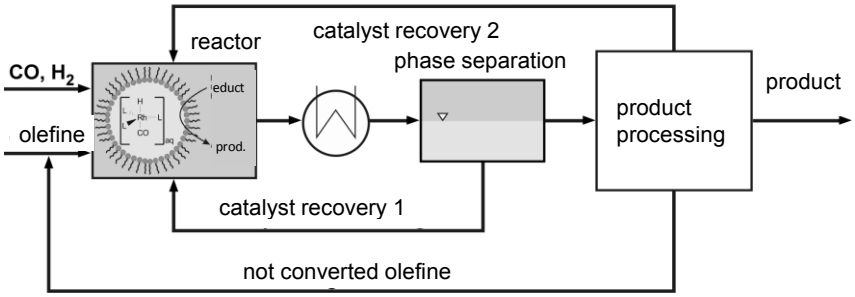

Figure 30: Novel concept for a continuous hydroformylation of long chain alkenes.

After reaction the mixture is cooled down until the Winsor I region is reached. Through phase separation it is separated into one aqueous phase containing the catalyst and one hydrophobic phase containing the product and not converted educt. With help of a further purification step product and educt can be separated. Not converted olefin is recycled. Likewise a second catalyst recovery stream is applied in order to guarantee nearly complete catalyst recycling. To recycle nearly the complete catalyst is obligatory due to the tremendous high price of Rh (15) and (19). Even if the process concept is convincing, one has to focus on a few challenges that can appear in nearly all systems containing surfactants. These systems tend to emulsify, a long term stable emulsion can be formed

and phase separation becomes impossible. According to Miyagawa et al. (154) this effect can be reduced by choosing a more hydrophobic surfactant. However, the Winsor III temperature range is shift likewise, which may cause other problems e.g. concerning reaction or conversion. Also problems with foam may appear. They can be counteracted by anti-foaming agents, but one has to consider always that all these additives can influence the phase behavior dramatically. As a result of that the whole process can be infeasible due to altered phase change temperatures or even not any more existing phase change temperatures.

3.5 Other approaches for hydroformylation

As it was illustrated in chapter 3.4 that one alternative for hydroformylation of long chain alkenes is the hydroformylation in microemulsions or micellar media. Alongside this approach and the homogenous catalysis illustrated in chapter 3.3 other processes are discussed in literature. Behr and coworkers studied intensively the application of thermomorphic solvent systems (TMS) (189), (210), (211), (239), (240), (241), (242), (243) and (244) for different approaches. Basically the TMS is composed of at least two solvents, one polar solvent and one apolar solvent namely the educt. The third component is represented by the product. It combines the advantages of homogeneous catalysis with simple catalyst removal typically achieved in heterogeneous catalysis. Using the hydroformylation as an example, a TMS can be applied in the following way: At low temperatures the polar catalyst phase and the non-polar educt phase is separated due to the low temperature. The two phases are heated up and above the UCST the two phases affiliate. Within the now homogeneous phase the reaction takes places. Subsequent reaction the mixture is cooled down and separated into two phases, one containing product and one containing catalyst. This approach was tested successfully for hydroformylation of long chain alkenes e.g. the hydroformylation of 1-dodecene (189). Schäfer et al. (211) presented moreover a detailed experimental analysis of the involved phase equlibria in the TMS system diemtehylformamide (DMF) + decane as well as a

modeling of the latter via application of the perturbed chain polar statistical associating fluid theory (PCP-SAFT). Kiedorf et al. (245) characterized in a comprehensively study the reaction network with at least six parallel important side reactions like isomerisation, hydrogenation and hydroformylation. Supplementary a kinetic model was developed for designing and optimizing new reactor concepts for hydroformylation (245). Another possibility for catalyst immobilization is the usage of an ionic liquid. The supported ionic liquid phase (SILP) catalysis firstly reported by Riisager et al. (246) is an auspicious alternative and several publications concerned with this technique in the last years (247) (248), (249), (250) and (251). The basic concept is to dissolve the catalyst in an ionic liquid (IL) and then coat with this mixture an extremely porous material e.g. silica. The catalyst is now fixed within the pores with help of the ionic liquid as a thin film (one nanometer ore even thinner) physisorbed at the surface (251). Since ILs possess an extremely low vapor pressure the catalyst phase does not migrate into the gaseous phase and therefore the catalyst loss is negligible. The SILP technique is successfully applied for hydroformylation of olefins under mild reaction conditions (temperatures ≈120°C, total pressures approximately 12 bar) up to a chain length of five carbon atoms (248). Also the hydroformylation of a technical C_4-stream was investigated of long time period of 30 days (250). Within this period no selectivity loss to the desired product n-pentanal could be recognized and selectivity exceeded anytime 99% (250). Similar results were obtained during hydroformylation of 1-propene and 1-butene (247) and (249). However, one important drawback for application of SILP systems is the dilution of the ionic liquid phase through formed high boiling side products. To overcome this problem the high boiling side products have to be removed from the IL catalyst phase under vacuum (248).

Furthermore, hydroformylation with supercritical fluids appeared as one of the latest development for hydroformylation of long chain alkenes in literature (252), (253), (254), (255) and (256). Blanchard and Brennecke (257) showed that organic compounds could be removed from IL's by supercritical CO_2. Webb et al. (253) and Webb et al. (254) developed on this basis a continuous process for hydroformylation of long chain alkenes. The catalyst is thereby immobilized in an IL phase and

synthesis gas and educt is passing through the reactor with a stream of supercritical CO_2. After reaction the supercritical CO_2 can be removed by lowering the pressure and the catalyst plus the ionic liquid remains in the reactor. By recompression of CO_2 the supercritical fluid can be recycled (253). This approach is successfully applied for alkenes up to a chain length of twelve carbon atoms (254). The achieved selectivities with this procedure were with 92% under mild reaction conditions below the selectivities reached in e.g. microemulsions or TMS systems (256). Summarizing the requirements necessary to develop any hydroformylation process as introduced in chapter 3 it is obvious that the knowledge about the phase behavior is the basis. It is not only the basis for process development and design it is also the basis for understanding process control. Given that for the reaction the microemulsion is favored and therefore the temperature range for the three phase region must be known. For estimating e.g. the catalyst loss also the composition in each phases have to be known. One can consider at a first approach that the catalyst loss is influenced by the loss of water within the product phase. The catalyst loss is one if the important bottleneck for the application of high performing Rh-catalysts. Furthermore, the surfactant loss with the product stream needs also to be estimated since the surfactant can influence the product purification.

4. Experimental methods

4.1 Materials

For the experiments all chemicals were used as delivered without any further purification. The pure surfactants $C_{12}E_4$, $C_{12}E_6$, $C_{12}E_8$ were purchased by Sigma Aldrich with a purity ≥ 98% and stored to the exclusion of light below 5°C. The technical surfactant Genapol X080® was likewise purchased by Sigma Aldrich and stored in a brown glass flask at room temperature. For experiments three different lot numbers BCBC8877V, BCBG0985V and BCBH5447V were used. 1-dodecene delivered by Sigma Aldrich was used in GC quality (purity ≥ 99%) for pure substances LLE measurement and in technical quality (purity ≥ 95%) for technical grade LLE measurement. Acetonitrile, methanol and 1-propanol in HPLC isocratic quality as well as Na_2SO_4 were purchased by Carl Roth. Water was demineralized from the Berlin water supply and used after boiling. For volumetric Karl-Fischer water detection water free methanol and Karl-Fischer Roti®hydroquant CS solution from Carl Roth was used. For calibration demineralized water as well as hydranal di sodium tartrate dehydrate ($C_4H_2O_6Na_2 * 2H_2O$) purchased by Riedel de Haën was utilized. Combi coulomat fritless solution (Merck) was used for coulometric water detection. For studying the aldehyde influence on the LLE tridecanal purchased by Alpha Aesar with a purity ≥ 96% was used. The catalyst influence on the LLE was studied with help of the SulfoXantPhos catalyst. The precursor [Rh(aca)$(CO)_2$] was contributed by Umicore, the Ligand was purchased by Molisa and synthesized according to (258). The amount of formed peroxides in the surfactant solution was determined using the Merckoquant peroxide test, purchased by Merck chemicals.

4.2 Sampling

For tie line measurement in surfactant containing systems all samples were prepared in pressure tight glass flasks in order to prevent sample evaporation, which causes variance in composition,

during tempering. The samples were temperate in a water bath type Haake N3 or in an oil bath type Huber MPC with accuracy of $\pm$ 0.1°C. All samples were weighted with an accuracy of at least $\pm$ 0.0001g. In order to prevent errors generated by cutting the interface especially in systems evolving three or more phases a tiny hollow needle was put in the glass flask before equilibration. With help of this needle one was able to sample directly from the bottom phase without penetrating the other phases; before sampling the needle was flushed by air. Furthermore, during sampling the temperature was kept constant with help of a double walled glass vessel. The probe was put in the solubility promoter 1-propanol to prevent demixing through cooling down and then used for further investigation. For Kahlweit's fish detection and for cloud point curve detection in the binary subsystems $C_{12}E_8$ + pure 1-dodecene, $C_{12}E_8$ + water, Genapol X080® + technical 1-dodecene and Genapol X080® + water the samples were also prepared in pressure tight glass flasks and temperate in a water bath type Haake N3 or in an oil bath type Huber MPC with accuracy of $\pm$ 0.1°C. Again the weight accuracy was at least $\pm$ 0.0001g.

4.3 Detection of surfactant

After sampling and dilution with 1-propanol the mass fraction of pure surfactant $C_{12}E_8$ and the mass fraction of technical grade surfactant Genapol X080® was detected with help of HLPC (Agilent 1200 series equipped with a Knauer Eurosphere II 100-5 C-18 column) at isocratic conditions. As eluent in both cases 80% acetonitrile and 20% water with a 1mMol Na_2SO_4 per liter as an additive and a flow rate 1mL/min was used. For detection the Diode array detector (DAD) was applied at a wavelength set to 191nm. The peak area was analyzed with help of Agilent Chem Station software. For calibration samples with a different mass fraction were prepared and the peak area plotted against mass fraction. In Figure 31 the calibration curve for the surfactant $C_{12}E_8$ is shown. The correlation coefficient is R^2=0.999 and the connection between peak area A and surfactant mass

fraction is $A[AUs] = 685675[AUs]w_{C_{12}E_8}$. The similar detection method was applied for detection of Genapol X080®.

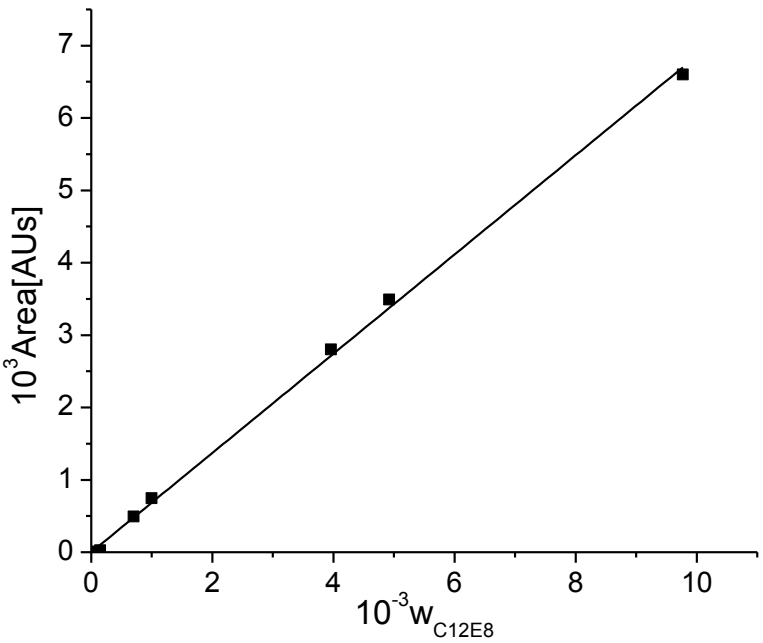

Figure 31: Calibration curve for the surfactant $C_{12}E_8$.

In Figure 32 the calibration curve for the surfactant Genapol X080® is depicted.

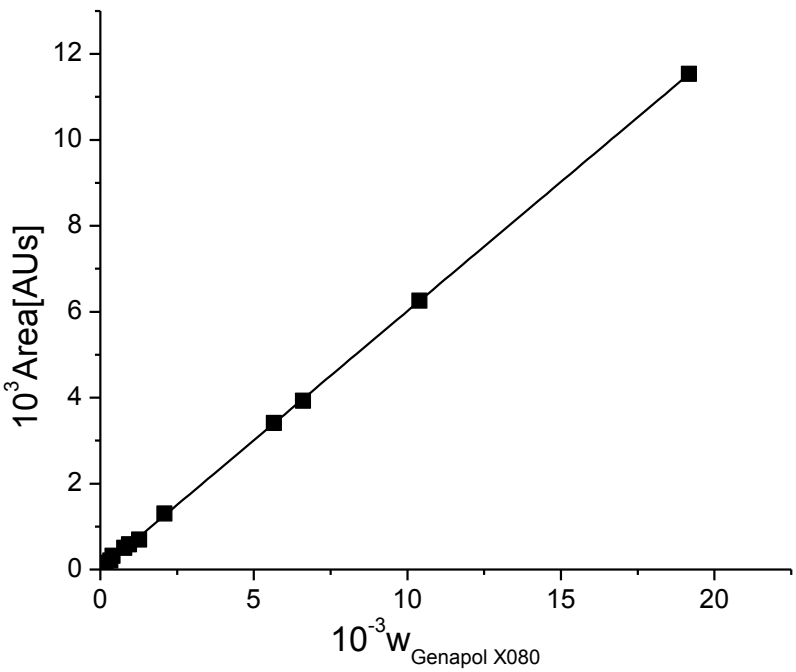

Figure 32: Calibration curve of surfactant Genapol X080®.

The correlation coefficient is R^2=0.9999 and the connection between peak area A and surfactant mass fraction is $A[AUs] = 601523[AUs]w_{Genapol\ X080®}$. It is a challenge to measure the surfactant mass fractions in the different excess phase according to their extreme low absorption in the UV/vis spectrum. However, HPLC measurement is a method of choice hence other surveying methods (e.g. gas chromatography) are not applicable according to surfactant's thermal instability.

4.4 Detection of 1-dodecene

The 1-dodecene mass fraction for pure and technical grade was detected by HPLC (Agilent 1200 series) after the sample was diluted with 1-propanol to prevent demixing. As a stationary phase the column Agilent Eclipse XDB-C18 and as eluent 100% methanol with a flow rate of 1mL/min was applied. The DAD detector was set to the wavelength 200nm. The peak area was analyzed with help of Agilent Chem Station software. For calibration samples with different mass fraction were prepared and the peak area plotted against mass fraction. In Figure 33 the calibration curve for the pure 1-dodecene is shown.

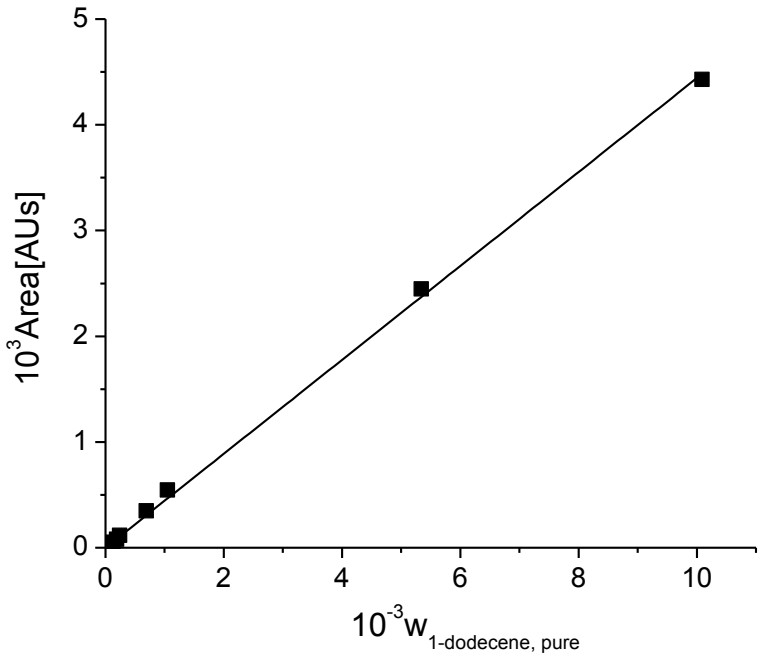

Figure 33: Calibration curve for pure 1-dodcene.

Again, the correlation coefficient was R^2=0.999. The connection between peak area A and surfactant mass fraction can be calculated by $A[AUs] = 44162[AUs]w_{1-dodecene,pure}$. The same method was applied for measuring the mass fraction of technical grade 1-dodecene. In Figure 34 the calibration curve for technical grade 1-dodecene is depicted. Here the correlation coefficient is R^2=0.9999. The connection between peak area A and surfactant mass fraction is given by $A[AUs] = 749703[AUs]w_{1-dodecene,technical\ grade}$.

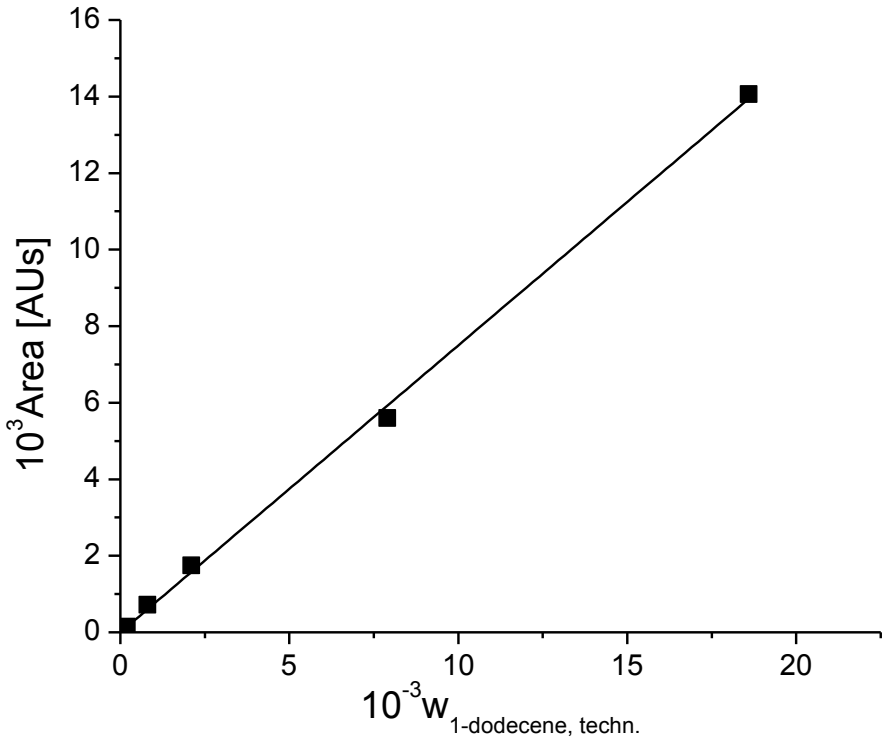

Figure 34: Calibration curve for technical 1-dodecene.

The 1-dodecene concentration in water was detected also with help of HPLC. Given that one can expect an extreme low solubility far beyond any standard analytical methods, a gas stripping technique from literature (259) and (260) was modified. After this additional step of enrichment one was able to measure the 1-dodecene mass fraction in water. In Figure 35 the gas stripping apparatus is depicted.

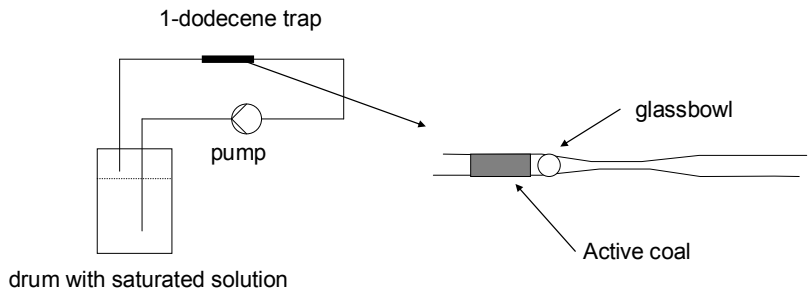

Figure 35: Gas stripping apparatus for 1-dodecene enrichment.

10kg of 1-dodecene saturated water were stripped by inert gas (air) within this apparatus (Figure 35) for 48h. For pumping the strip gas the oil free vacuum pump Neuberger KNF Laboport was applied. 1-dodecene was adsorbed at active coal located in a glass tube modified to a capillary with help of a Bunsen-burner. The 1-dodecene was resolved by a small amount of 1-propanol and used for further HPLC measurements.

4.5 Detection of water

For water detection the Karl-Fischer water detection method was used (261). For water mass fraction above w_{water}=0.0001 the volumetric water detection (Mettler DL18) was used, for smaller mass fractions the columetric detection (Mettler-ToledoC20) was utilized. Hence there is a direct connection between the amount of water and the current flow for coulometric Karl Fischer water detection no further calibration is needed. Contrary for volumetric water detection a calibration curve is necessary. Hence, a connection exists between the amount of used Karl Fischer solvent and the amount of water within the sample. For preparing the calibration water and di sodium tartrate dihydrate with a fixed amount of crystal water ($w_{water} = 0.1566$) was used. In Figure 36 the calibration curve for volumetric Karl Fischer water detection is plotted.

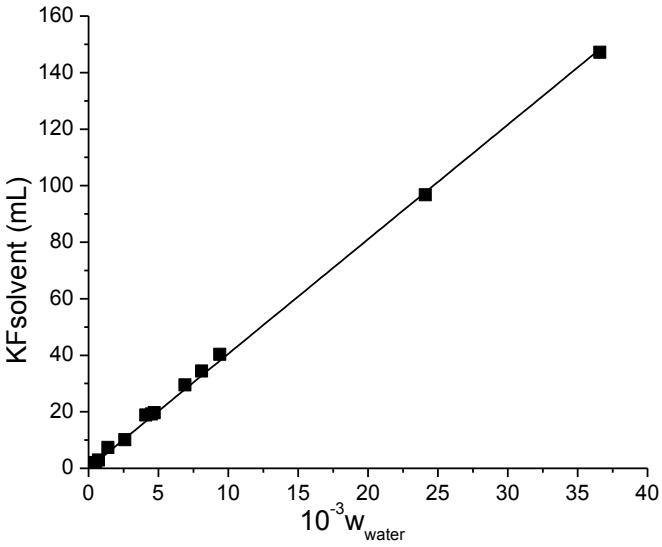

Figure 36: Calibration curve for volumetric Karl Fischer water detection.

The correlation coefficient was R^2=0.9999 and the connection between used KF solvent and water mass fraction is $KFsolvent[mL] = 4052[mL]w_{water}$.

4.6 Measurement of Kahlweit's fish

The phase change temperature was detected by slowly heating up and by slowly cooling down, the average of both temperatures was set as the phase change temperature. The maximum difference between these two temperatures was 1°C. For a first overview the cloud point temperature was detected roughly (≈1°C) by a nested interval method. The visual method was used to detected the Kahlweit's fish for the ternary systems $C_{12}E_8$ + water + 1-dodecene, pure (system A), $C_{12}E_6$ + water + 1-dodecene, pure, $C_{12}E_4$ + water + 1-dodecene, pure and in the system Genapol X080® + water + 1-dodecene, technical grade (system B) at a constant oil water ratio $\alpha = \frac{m_{water}}{m_{hydrophobic\ components}} = 0.5$ in dependency of temperature and surfactant mass fraction $\gamma = \frac{m_{surfactant}}{m_{total}}$. The samples were prepared in the following way: Firstly surfactant was added to the water and secondly 1-dodecene

was introduced to the mixture. In order to prevent thermal decomposition the samples were replaced after 48h.

4.7 Detection of surfactant decomposition

To investigate the surfactant decomposition qualitatively, an infra-red (IR) spectrum of fresh and decomposed surfactant were measured with a Fourier transform infrared spectrometer (FTIR-spectrometer) purchased by Shimadzu instruments (IR Prestige-21). Each spectrum was measured twenty five times and the average of each measurement was calculated and plotted as transmission over wave number. The amount of formed peroxides from surfactant decomposition was determined by using peroxides test stripes with an accuracy of $\pm 5 \frac{mg}{L}$.

4.8 Measurement error

To obtain the analytical error by means of standard deviation was not practical due to the large number of samples within this study. For the calculation at least ten independent samples for every feed concentration are necessary and of course they have to be measured. This increases the analytical effort as well as the usage of e.g. extreme high price pure surfactant. At the end of the day this becomes not practical due to financial and temporal restrictions. To overcome this problem each compound was measured three times from one sample and the average was set as the concentration of this particular compound. Furthermore, it is difficult to obtain a standard deviation for an optical method because the results are depending strongly on the experimenter. In case of the tie lines one has to consider the following effect: Sampling can cause here a significant influence on the measurement error, the measurement caused by analytical equipment e.g. HPLC or balance is negligible small. To keep the sampling error as small as possible the in 4.2 described technique was applied. Nevertheless a few methods can be used for estimation of the analytical error. At first the

mass balance has to be fulfilled, this is verified by plotting the feed concentration and the measured tie lines in one diagram. Beside the graphical check of the mass balance it also can be checked by calculating. Given that the system A is in the Winsor II state at 90°C, it can be assumed that almost the whole amount of surfactant is dissolved in the 1-dodecene rich phase. One is able to calculate the mass balance and compare it to the experimental results. For a system composed of 0.8191g 1-dodecene, 1.0921g water and 0.0416g $C_{12}E_8$ the mass fraction of $C_{12}E_8$ within the oil phase can be calculated $w_{C_{12}E_8} = \frac{0.0416g}{0.0416g+0.8191g} = 0.0483$. This result is in perfect agreement with the mass fraction obtained by HPLC measurement $w_{C_{12}E_8} = 0.0452$. Second the solubility behavior at constant surfactant feed concentration for system A and system B was checked. As predicted the surfactant solubility is increasing with increasing temperature within the oil phase and decreasing with increasing temperature within the aqueous phase.

5. Results and discussion

In general, thermodynamic data are obtained with help of components as pure as possible to study e.g. in the case of surfactants the influence of ethoxylate chain length on the LLE as it is discussed in Chapter 2.4. However, to apply those systems for industrial processes one is limited to apply technical grade surfactants since they are available in bulk scale. Of course the composition of a technical grade surfactant can vary from one charge to another, but generally in any technical surfactant is always the major component given and also the type of side products should not change. Therefore it is clear that investigation of bulk scale surfactants in comparison of thermodynamic data is necessary.

5.1 Kahlweit's fish

With the detection of the Kahlweit's fish the phase and aggregation behavior of a surfactant containing mixture can be determined at a glance. This diagram provides a quick overview about coexisting phase numbers at different temperatures depending on γ at a specific α value. Hence, at low temperatures the surfactant is mostly located in the aqueous bottom phase; the surfactant solubility in the non-polar phase is minor which is confirmed by a small phase volume of the latter phase (Winsor I behavior). Anyhow with increasing the temperature the Winsor III system is evolving with the microemulsion as middle phase. If γ is also increased the system is existent as a single phase system (Winsor IV). At high temperatures the phase behavior is switching to Winsor II. Here the surfactant is concentrated mostly in the 1-dodecene rich phase, confirmed by an increased phase volume of the latter phase. Figure 37 depicts the gauged Kahlweit's fish for system A. Of course in literature are some data for Kahlweit's fish of surfactant containing systems especially for alkane containing systems (19), (22), (84), (137), (235), (262), (263) and (264). For alkene containing systems Rost et al. (19) published a fish diagram measured at $\alpha = 0.5$ for the system water + Marlophen

NP9® + 1-dodecene. The used surfactant is a technical grade surfactant of the alky phenyl polyethoxylate type described in section 2.1.1 and technical grade 1-dodcene. However, after careful inquiry no Kahlweit's fish data for system A containing alkenes and C_iE_j type surfactants could be found.

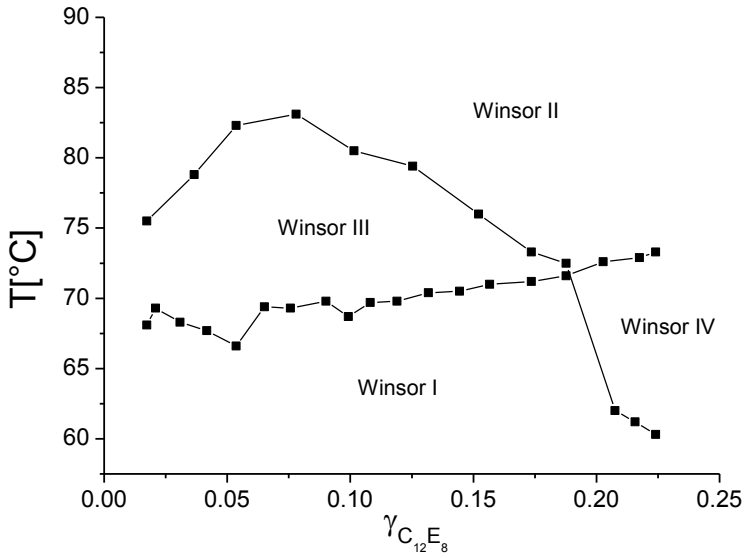

Figure 37: Kahlweit's fish for system A at α equal to 0.5.

The phase change temperatures are given in Table 2.

Table 2: Experimental determined phase transition temperatures for system A gauged with the optical method. T_1: phase transition from Winsor I to Winsor III; T_2: Phase transition from Winsor III to Winsor II; T_3: Phase transition from Winsor I to Winsor IV; T_4: Phase transition from Winsor IV to Winsor II at given γ and fixed $\propto = 0.5$.

T_1/°C	T_2/°C	T_3/°C	T_4/°C	$\gamma_{C_{12}E_8}$
68.1	75.5			0.0174
69.3				0.0209
68.3				0.0308
	78.8			0.0366
67.7				0.0417
66.6	82.3			0.0536
69.4				0.0651
69.4				0.0757

	83.1			0.078
69.8				0.0901
68.7				0.0992
	80.5			0.1015
69.7				0.1081
69.8				0.119
	79.4			0.1254
70.4				0.1317
70.4				0.1444
	76			0.1521
71				0.1566
71.2	73.3			0.1736
71.6	72.5			0.1877
		62	72.6	0.2075
		61.2	72.9	0.2157
		60.4	73.3	0.2241

5.1.1 Influence of the ethoxylate chain length

In order to estimate the phase and aggregation behavior of technical surfactants, which are always a mixture of different ethoxylate chain length, it is required to determine the ethoxylate unit's influence on the LLE. In general it is known that with increasing the number of etholxylate units and fixed number of carbon atoms in the hydrophobic chain the Winsor III system is shifted to higher temperatures. Vice versa the Winsor III system is shifted to lower temperatures with decreasing the ethoxylate chain length at a given hydrophobic component. The influence of different ethoxylate chain lengths on three phase temperature intervals in systems containing alkanes, nonionic surfactants C_iE_j and water could be found in the literature: (22), (84), (149), (150) and (151). Until today no fish diagrams with alkenes and surfactants of the C_iE_j type in dependency of the j-number

are available in literature for the authors knowledge. In Figure 38 is the influence of the ethoxylate chain length on the three phase body at constant α is depicted.

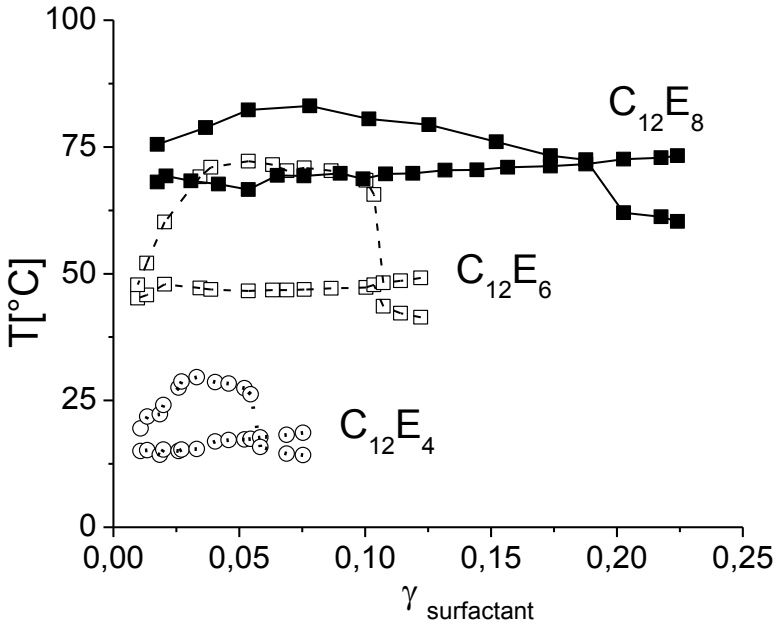

Figure 38: Kahlweit's fish at constant oil-water ratio $\propto = 0.5$ for $C_{12}E_8$ (solid squares and solid line), $C_{12}E_6$ (open squares and dashed line) and $C_{12}E_4$ (open circles and dotted line) at different surfactant mass fraction γ in dependency of temperature.

In good agreement to the results obtained with alkanes the three phase body of the fish is shifted to lower temperatures with decreasing the number of ethoxylate units at constant i-number. Likewise the shape of the fish's body is shrinking meaning that the Winsor III phase evolves at a narrow γ margin. This implicates that the phase inversion temperature (PIT) is also shifted to lower γ and lower temperatures. In the phase change temperatures are given in Table 3, respectively Table 4.

Table 3: Phase change data for the system water + $C_{12}E_4$ + pure 1-dodecene; T_1: phase transition from Winsor I to Winsor III; T_2: Phase transition from Winsor III to Winsor II; T_3: Phase transition from Winsor I to Winsor IV; T_4: Phase transition from Winsor IV to Winsor II at given γ and fixed $\alpha = 0.5$.

T_1/°C	T_2/°C	T_3/°C	T_4/°C	$\gamma_{C_{12}E_4}$
15	19.5			0.0108
15.2	21.8			0.0135
14.3	22.3			0.0185

15.3	24.1			0.0199
15	27.5			0.0259
15.3	28.7			0.0271
15.4	29.6			0.0331
16.9	28.6			0.0405
17.2	28.3			0.0458
17.3	27.4			0.0521
17.4	26.2			0.0545
		15.8	17.7	0.0584
		14.5	18.2	0.0688
		14.2	18.6	0.0753

Table 4: Phase change data for the system water + $C_{12}E_6$ + 1-dodecene; T_1: phase transition from Winsor I to Winsor III; T_2: Phase transition from Winsor III to Winsor II; T_3: Phase transition from Winsor I to Winsor IV; T_4: Phase transition from Winsor IV to Winsor II at given γ and fixed $\alpha = 0.5$.

T_1/°C	T_2/°C	T_3/°C	T_4/°C	$\gamma_{C_{12}E_6}$
45.2	47.8			0.0097
45.8	52.1			0.0133
47.9	60.2			0.0204
47.2	69.1			0.0344
46.9	71			0.0387
46.6	72.2			0.0536
46.8	71.5			0.0632
46.8	70.3			0.0689
46.9	70.9			0.0758
47.1	70.3			0.0865
47.3	68.4			0.1004
47.8	65.6			0.1035
		43.6	48.2	0.1072
		42.2	48.6	0.1141
		41.4	49.2	0.1221

5.1.2 Influence of technical grade substances

As accentuated for technical processes only technical grade surfactants can be applied. According to Haumann et al. (15), Rost et al. (19) and Hamerla et al. (216) adequate temperatures for hydroformylation are between 75°C and 80°C with a starting temperature 110°C. Kahlweit and Strey (22) pointed out that moderate pressure changes influence the LLE insignificant. In literature a fish diagram for the system technical surfactant Marlophen NP9® + 1-dodecene + water could be found (19). In general this system is a system suitable for hydroformylation processes, but the Marlophen NP® type surfactants causing wastewater treatment and environmental problems and therefore they are restricted in European Union (35) contrary to the C_iE_j type surfactants. Given that $C_{12}E_8$ possesses a three phase area in the relevant temperature range further investigation with a technical surfactant with $C_{12}E_8$ as a major component are necessary. Beside this, in literature (16) some data points for the system 1-dodecene and different Marlipal® type surfactants are existent. These data provide information just at one concentration point in dependency of temperature. Figure 39 shows the influence of technical grade surfactant Genapol X080® with the major component $C_{12}E_8$ and technical grade 1-dodecene on the LLE in terms of Kahlweit's fish measured at $\alpha = 0.5$.

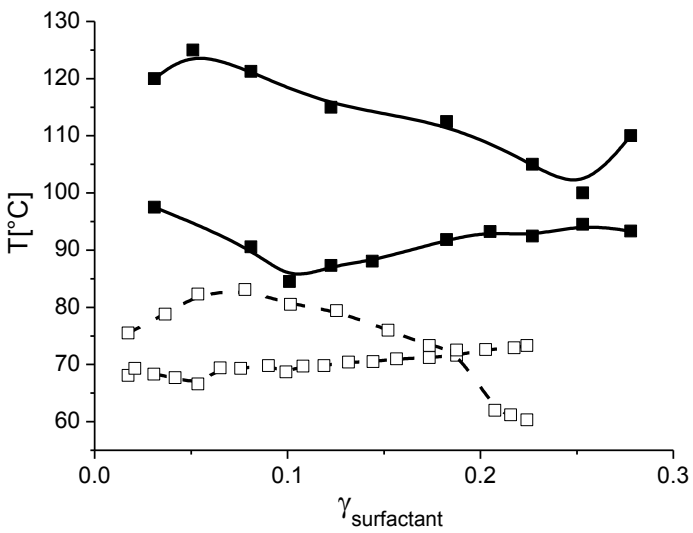

Figure 39: Kahlweit's fish for system A (open squares and dashed line) compared to system B (solid squares and solid lines) at constant $\alpha = 0.5$.

The technical grade surfactant has an exceeding influence on the LLE. Winsor III area is shifted to higher temperatures and the dimension of the three phase body is increased. Up to $\gamma_{\text{Genapol X080®}}$=0.27 no Winsor IV system could be found. The Winsor IV system will occur at higher surfactant concentrations. However, these high surfactant concentrations are not relevant for hydroformylation. In Table 5 the phase change temperatures are given.

Table 5: Phase change temperatures for system B; T_1: phase transition from Winsor I to Winsor III; T_2: Phase transition from Winsor III to Winsor II at given γ and fixed $\alpha = 0.5$.

T/°C	T/°C	$\gamma_{\text{Genapol X080®}}$
97.5	120	0.0031
	125	0.0051
90.5	121.3	0.0081
84.5		0.0101
87.3	115	0.1226
88.1		0.144
91.9	112.5	0.1825
93.3		0.205
92.5	105	0.227
94.5	100	0.253
27.8	93.4	0.278

5.1.3 Influence of the aldehyde

Hitherto the LLE for a system suitable for hydroformylation was investigated, meaning the system consists of three different components: Educt, water for dissolving the catalyst and surfactant responsible for contact between catalyst and educt. However, during the reaction product is formed in a non-negligible amount. Having in mind that the produced aldehyde exhibits non polar and more polar parts within the molecule, thus showing similarities with a classical co-solvent, the investigation

on the LLE becomes evident. Therefore at three different aldehyde ratios $\beta = \frac{w_{tridecanal}}{w_{tridecanal}+w_{1-dodecene}}$ ($\beta = 0.25,\ \beta = 0.5\ and\ \beta = 1$) the product influence on LLE was studied. Hamerla et al. (216) adjusted the reaction temperatures after reaction onset from 110°C to 80°C in order to keep the reaction rate high, which is confirmed by results of (19). They measured the influence of increased aldehyde content within the hydrophobic phase in the system Marlophen NP9® + water + 1-dodecene, technical. However, due to restrictions of the phenyl type surfactants, further investigation for systems containing ethylene glycol type surfactants, which are used as replacements are performed. In Figure 40 the influence of increased tridecanal fraction related to the hydrophobic phase is depicted.

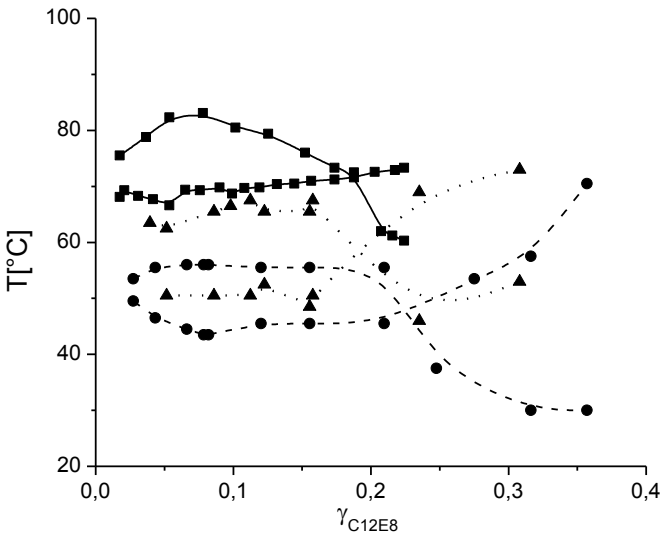

Figure 40: Influence of tridecanal to system A (squares and solid line: $\beta_{tridecanal} = 0$; triangles and dotted line: $\beta_{tridecanal} = 0.25$; circles and dashed line $\beta_{tridecanal} = 0.5$).

With increasing β the Winsor III system is shifted to lower temperatures. This behavior can explain the observation regarding the reaction rate obtained by Rost et al. (19) and Hamerla et al. (216). The Winsor III phase temperature is decreasing around 40°C if β is increased up to 0.5. For $\beta = 1$ the three phase area is sunken below the surfactant's melting point. Beside this the Winsor IV system is expanding. For application of this system in a technical scale the reactor temperature has to be

adjusted during the process in dependency of the aldehyde concentration in the reactor. Furthermore, the hold-up in the reactor has to be controlled since the Winsor III temperature is decreasing with increasing aldehyde concentration witch leads in extreme case to a slowdown of the hydroformylation reaction given that the reaction rate is maximal within the Winsor III region according to Rost et al. (19) and Hamerla et al. (216). In Table 6 the phase change temperatures are given for $\beta = 0.25$ and in Table 7 for $\beta = 0.5$.

Table 6: Phase change temperatures for system A, $\boldsymbol{\beta = 0.25}$; T_1: phase transition from Winsor I to Winsor III; T_2: Phase transition from Winsor III to Winsor II; T_3: Phase transition from Winsor I to Winsor IV; T_4: Phase transition from Winsor IV to Winsor II at given γ and fixed $\boldsymbol{\alpha = 0.5}$.

T_1/°C	T_2/°C	T_3/°C	T_4/°C	$\gamma_{C_{12}E_8}$
	63.5			0.03946
50.5	62.5			0.05151
50.5	65.5			0.08596
	66.5			0.098
50.5	67.5			0.11242
52.5	65.5			0.12268
48.5	65.5			0.1556
50.5	67.5			0.15772
		46	69	0.2352
		53	73	0.30817

In Table 7 the phase change temperatures are given for system A, $\beta = 0.5$.

Table 7: Phase change temperatures for system A, $\beta = 0.5$; T_1: phase transition from Winsor I to Winsor III; T_2: Phase transition from Winsor III to Winsor II; T_3: Phase transition from Winsor I to Winsor IV; T_4: Phase transition from Winsor IV to Winsor II at given γ and fixed $\alpha = 0.5$.

T_1/°C	T_2/°C	T_3/°C	T_4/°C	$\gamma_{C_{12}E_8}$
49.5	53.5			0.02726
46.5	55.5			0.0433
44.5	56			0.0663
43.5	56			0.07857
43.5	56			0.08209
45.5	55.5			0.12024
45.5	55.5			0.15553
45.5	55.5			0.20974
		37.5		0.24762
			53.5	0.27525
		30	57.5	0.31631
		30	70.5	0.35696

5.1.4 Influence of the Rh - SulfoXantPhos catalyst

The next step is the investigation of the Rh catalyst influence. Although the catalyst concentration according to Hamerla et al. (216) is very low, $w_{Rh\text{ - }SulfoXantPhos} \approx 2*10^{-5}$, according to Figure 28 the catalyst plus ligand has a complex amphiphilic structure which can influence the LLE. In Figure 41 this influence is depicted.

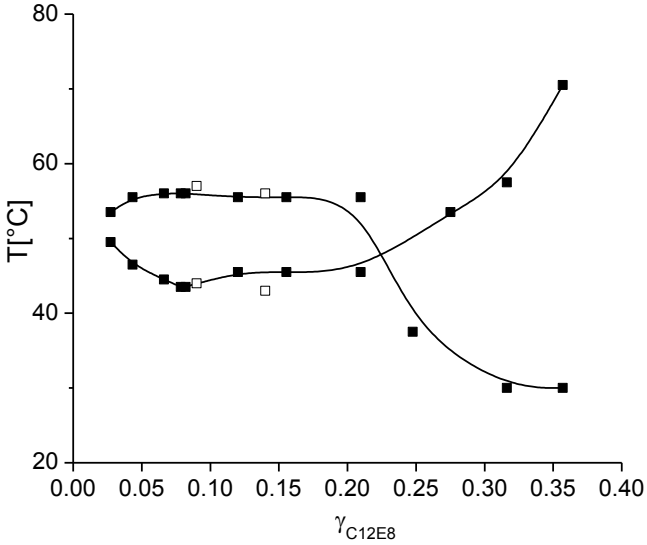

Figure 41: Influence of the Rh – SulfoXantPhos catalyst on the LLE of system A with $\alpha = 0.5$ and $\beta = 0.5$. Black squares and line system A without Rh – SulfoXantPhos catalyst; open squares system A with Rh – SulfoXantPhos catalyst, $w_{Rh-SulfoXantPhos}$=2*10^{-5}.

The influence of the catalyst is negligible in system A with $\alpha = 0.5$ and $\beta = 0.5$. The phase change temperatures for the catalyst containing system are given in Table 8.

Table 8: Phase change temperatures for system A with $\alpha = 0.5$ and $\beta = 0.5$ containig $w_{Rh-SulfoXantPhos}$=2*10^{-}5. T_1 phase transition from Winsor I to Winsor III; T_2: Phase transition from Winsor III to Winsor II at given γ.

T_1/°C	T_2/°C	$\gamma_{C_{12}E_8}$
44	57	0.09
43	56	0.14

5.2 Cloud point curve measurements

Beside measurements in the ternary systems in term of the "Kahlweit's fish" the detection of the binary subsystems is necessary for a detailed investigation of the phase behavior within the ternary systems A and B. To obtain the influence of the technical grade surfactant at first a cloud point curve

for the system $C_{12}E_8$ and water and then a cloud point curve for the system Genapol X080® + water was detected.

5.2.1 $C_{12}E_8$ + water

The first binary subsystem investigated was the binary subsystem water and $C_{12}E_8$. This subsystem was gauged with the optical method. A water + $C_{12}E_8$ mixture was prepared and the cloud point temperature was detected roughly at first by a nested interval method. After that the cloud point temperature was detected more precisely by heating up the solution and cooling down slowly. The average was set as the cloud point temperature. The binary subsystem showed a LCST behavior, which is quite common for systems belonging to the type C_iE_j + water. In Figure 42 the demixing behavior is depicted.

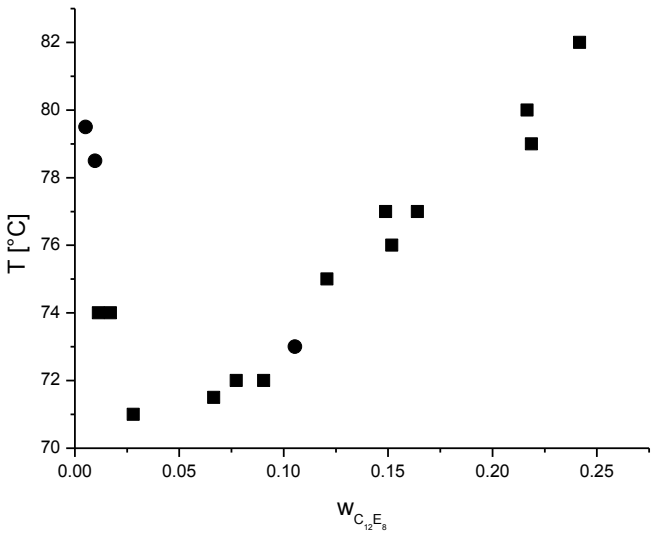

Figure 42: Experimental cloud point temperatures for the system $C_{12}E_8$ + water (squares: samples with peroxide formation; circles system without peroxide formation).

In Table 9 and Table 10 the experimental demixing temperatures are given.

Table 9: Experimental cloud point temperatures without peroxide formation related to the $C_{12}E_8$ + water binary subsystem.

$w_{C_{12}E_8}$	T/°C
0.0113	74
0.0171	74
0.028	71
0.0665	71.5
0.0773	72
0.0905	72
0.1208	75
0.1489	77
0.1518	76
0.1641	77
0.2166	80
0.2187	79
0.2417	82

Table 10: Experimental cloud point temperatures with peroxide formation related to the $C_{12}E_8$ + water binary subsystem.

$w_{C_{12}E_8}$	T/°C
0.0052	79.5
0.0097	78.5
0.1054	73

At any cloud point temperature the system disaggregates into two phases, one surfactant rich phase and one surfactant poor phase. Nevertheless the surfactant concentration in both phases is always

above the CMC (129). The CMC for the latter system depends strongly on temperature. At low temperatures the CMC decreases with increasing the temperature but with further temperature raise the CMC starts to increase Figure 16. With increasing the temperature the hydrophobicity increases as well and according to Chen et al. (128) the hydration of the hydrophilic head group is decreased. The hydration of this molecule part is responsible for the micelle formation. At high temperatures another effect has to be taken into account: The increased temperature causes a breakdown in the structured water molecules surrounding the hydrophobic tail, which is in disfavor of the formation of micelles. These two opposing effects cause the minimum in the CMC (128). The phase behavior in the binary system $C_{12}E_8$ + water at region where liquid crystalline phases occur was not investigated because for hydroformylation process this concentration range is irrelevant. After several hours at high temperatures thermal decomposition of surfactant was noticed and peroxides were formed. A rough estimation of the peroxide content with test stripes results in a peroxide concentration below 25mg per liter in all solutions. To exclude an effect of the formed peroxides on the LLE three cloud points with fresh solution were measured again and as depicted in Figure 42 no influence of peroxide formation on the LLE could be recognized. For the system $C_{12}E_8$ + water several data could be found in literature (90), (91), (265) and (266). In Figure 43 the measured cloud point curve is compared to literature data.

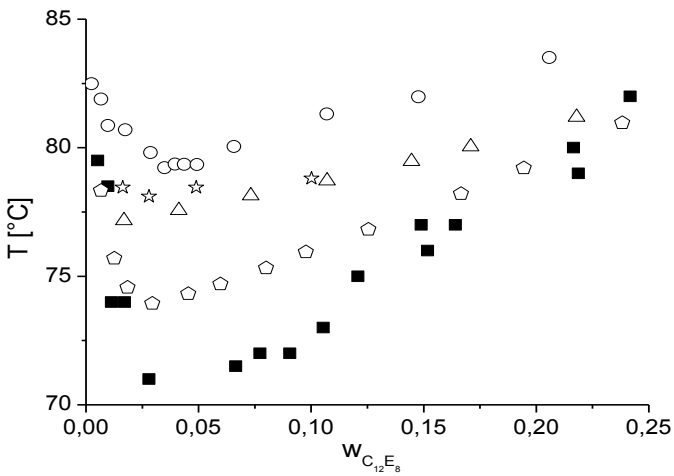

Figure 43: LLE data for the system $C_{12}E_8$ + water (open circles: (91); stars: (265); open triangles: (90); open pentagons: (266); solid squares: this work).

The cloud point curve obtained in this work is much lower than other literature data (90), (91), (265) and (266). An influence of chemicals with a different degree of purification could be excluded, given that all research groups used the same highly purified $C_{12}E_8$ surfactant. The difference can be explained by the experimental procedure: Mitchell at al. (90) and Fujimatsu et al. (91) applied for their experiments a continuously increase of temperature (2°C/min and 1.3°C/min). This large scale heating rate can be used to detect roughly the LLE in this type of systems but not for an exact determination. Unfortunately no further statement about the data measured by Shinoda et al. (265) could be given since no information about experimental details and procedure is provided in the paper. The data measured in this work is in good agreement with data obtained by Degiorgio et al. (266) in the diluted and concentrated regions of LLE. Nevertheless differences near the critical point occur. These differences occur due to the measurement technique. Degiorgio et al. (266) used a light scattering technique with an extreme low heating rate (0.1°C/min), in this work the visual method was applied. Having in mind the critical opalescence it is obvious that both methods show slightly differences in the region near the critical point.

5.2.2 $C_{12}E_8$ + 1-dodecene

The next binary subsystem is the system $C_{12}E_8$ + pure 1-dodecene. This system shows above the surfactant melting point no demixing behavior and therefore the two substances are completely miscible.

5.2.3 Genapol X 080® + water

For estimating the influence of technical grade substances the LLE in the binary system Genapol X080® + water was investigated and in Figure 44 the LLE for $C_{12}E_8$ + water and Genapol X 080® + water is plotted.

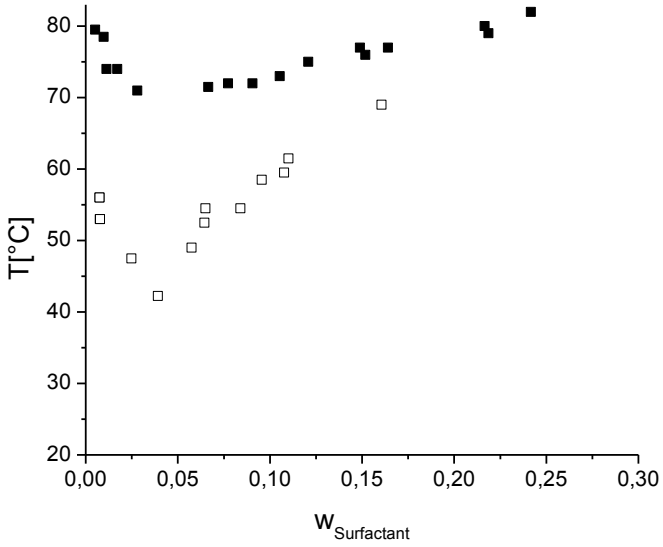

Figure 44: Cloud point curve for the system $C_{12}E_8$ +water (solid squares) and Genapol X080® + water (open squares).

Both systems show the for the alky polyglycol ether type surfactants typical LCST demixing behavior. However, when technical grade substances are applied the demixing temperatures are shifted to much lower temperatures. The temperatures differ for more than 20°C. Beside this the cloud point curve shape has a more narrow form when technical grade substances are used. In Table 11 the demixing temperatures for system B are given. The cloud point data in literature (267) and (268) differ in a wide range as depicted in Figure 45. For a solution containing 1% Genapol X080® (w/v) two different cloud points could be found (268) reported 34.5°C and (267) 75°C. Unfortunately Sosa Ferrera et al. (267) gave no further information about the experimental procedure to obtain the demixing temperature.

Table 11: Demixing temperatures for the system Genapol X080® + water.

$W_{Genapol\ X080®}$	T/°C
0.00751	56
0.00753	56
0.00774	53
0.00788	53
0.02485	47.5

0.03919	42
0.0575	49
0.06444	52.5
0.06496	54.5
0.08406	54.5
0.09559	58.5
0.10779	59.5
0.11012	61.5
0.16055	69

Shi et al. (268) measured the demixing curve with a specific heating rate of 1°C/10min.. Taking into account that the equilibration time for this type of systems is in the range of several hours one can assume that in this particular case the solid liquid equilibrium (SLE) curve was investigated. This assumption is confirmed by the melting point for the technical grade surfactant, which is the temperature range between 30°C and 40°C measured with help of the optical method.

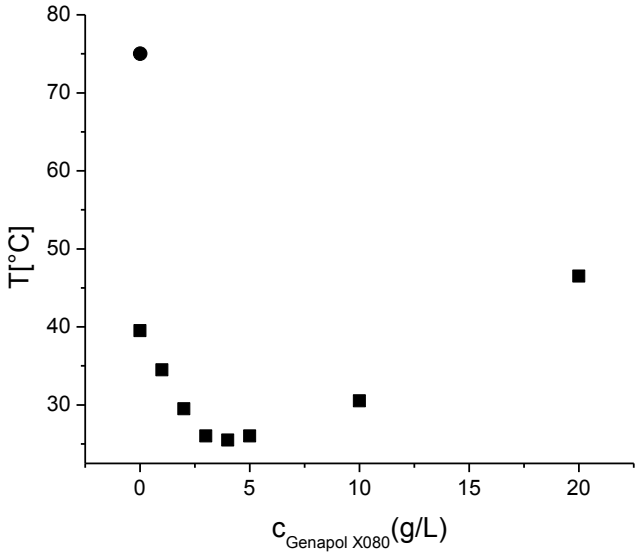

Figure 45: Cloud point curve for the system Genapol X080® + water (squares: (268) and circle: (267)).

5.2.4 Genapol X080® + technical 1-dodecene

The last binary subsystem investigated with the optical method is the binary system Genapol X080® + technical 1-dodecene. Above the melting range of the technical surfactant mixture both substances are completely miscible and show no demixing behavior. This is in good agreement with the results obtained for $C_{12}E_8$ and pure 1-dodecene.

5.3 Tie line and solubility measurements

5.3.1 1-Dodecene + water

The binary subsystem 1-dodecene + water exhibits a broad miscibility gap. The solubility of water in pure 1-dodecene is shown in Figure 46 and experimental data is given in Table 12.

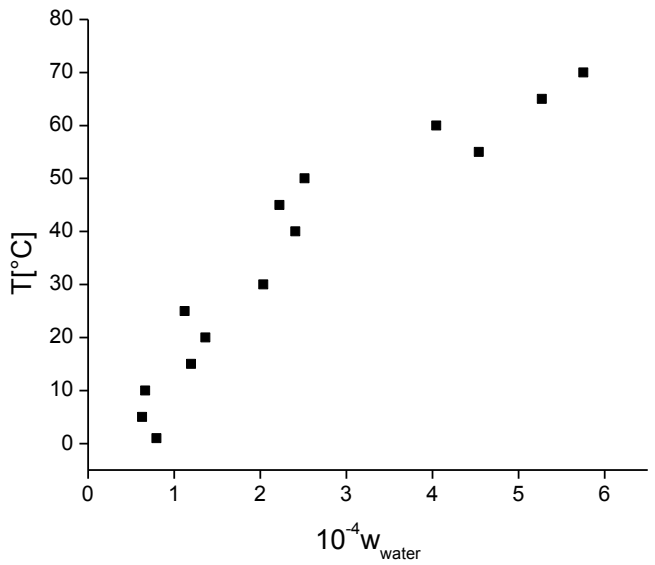

Figure 46: Experimental temperature dependent water solubility in pure 1-dodecene.

In the temperature range between the freezing and the boiling point of the mixtures the temperature has hardly influence on the solubility of water in 1-dodecene.

Table 12: LLE data for the 1-dodecene rich side in the 1-dodecene + water binary subsystem in dependency of temperature.

$10^{-4}w_{water}$	T/°C
0.8	1
0.6	5
0.7	10
1.2	15
1.4	20
1.1	25
2	30
2.4	40
2.2	45
2.5	50
4.5	55
4	60
5.3	65
5.8	70

With help of the special enrichment procedure it was possible to gain through HPLC measurement the solubility of 1-dodecene in water at room temperature (T≈25°C). Since a large amount of water (≈10kg) has to be temperate for this experiment it was only possible to operate this experiment at room temperature. To verify this experiment the recovery rate was checked in the following way: With help of dilution series a stock solution of 1-dodecene in 1-propanol was prepared and a small amount of this solution was put into water, resulting a 1-dodecene mass fraction below the maximal solubility of 1-dodecene in water. The amount of 1-dodecene was detected and the recovery rate was 95%. In Figure 47 the solubility of several alkanes and alkenes at 25°C are given.

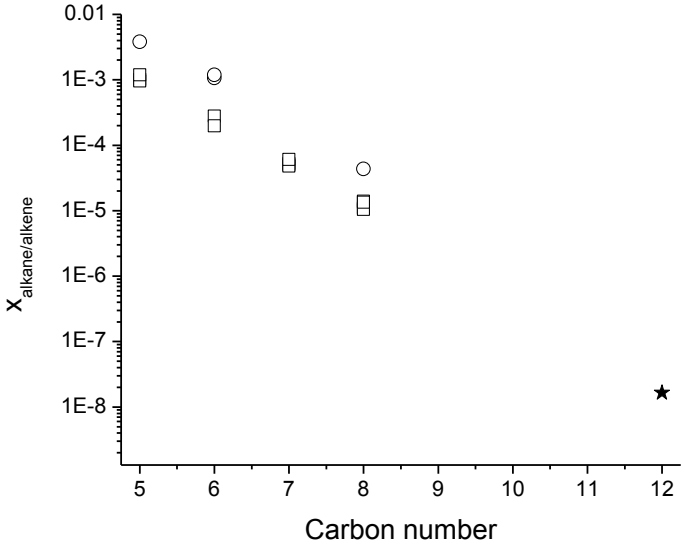

Figure 47: Solubility of several alkanes (open squares: (146)) and alkenes (open circles: (146), star: this work) in dependency of chain length at room temperature (25°C).

The solubility of alkanes or alkenes is decreasing with increasing the chain length. The solubility of 1-dodecene in water agrees well with the homologue series. The solubility of 1-dodecene in water is $w_{pure1-dodecene} = 1.8 \cdot 10^{-7}$, respectively $x_{pure\ 1-dodecene} = 1.65 \cdot 10^{-8}$.

5.3.2 Technical 1-dodecene + water

For the binary system technical 1-dodecene + water the water solubility in technical 1-dodecene was measured. As expected from measurements with pure 1-dodecene the temperature has hardly influence on water solubility in the alkene. Figure 48 depicts the water solubility in technical 1-dodecene compared with the water solubility in pure 1-dodecene.

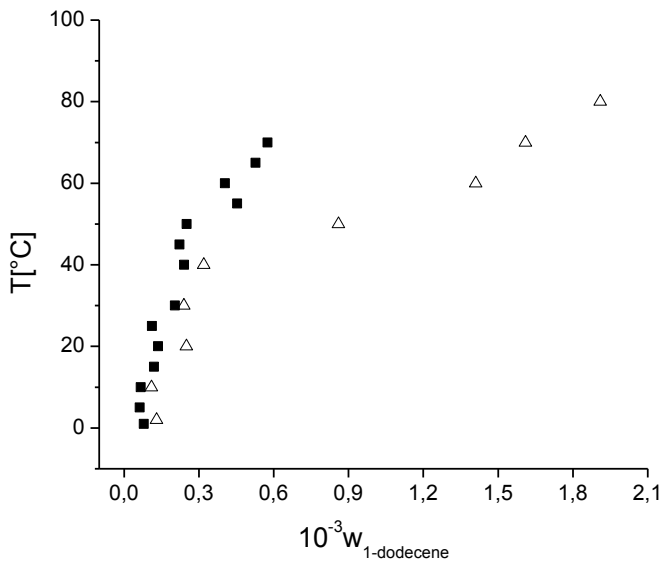

Figure 48: Water solubility in pure 1-dodecene (squares) and water solubility in technical 1-dodecene.

In both cases the water solubility within the alkene rich phase differs marginal across the entire temperature range and therefore there is little difference in the solubility of water in pure and in technical grade surfactant. The data points are given in Table 13.

Table 13: Water solubility in technical grade 1-dodecene.

$10^{-3}w_{technical\ 1\text{-}dodecene}$	T/°C
0.13	2
0.11	10
0.25	20
0.24	30
0.32	40
0.86	50
1.41	60
1.61	70
1.91	80

The solubility of technical grade 1-dodecene in water was measured due to the complex enrichment procedure only at room temperature. The procedure was similar to the measurement of pure 1-dodecene solubility in water and the solubility is equal to $w_{technical\,1-dodecene} = 1.75 \cdot 10^{-7}$, respectively $x_{technical\,1-dodecene} = 1.6 \cdot 10^{-8}$ which in the range of the solubility for pure 1-dodecene in water.

5.3.3 $C_{12}E_8$ + 1-dodecene + water

In the ternary system $C_{12}E_8$ + 1-dodecene + water the Kahlweit's fish was detected by the optical method at a specific α as depicted in Figure 37. However, this information provides no information about the mass fractions of different substances in the different coexisting phases. To obtain detailed information about the phase composition tie lines were measured with help of HPLC in a temperature range between 30°C and 90°C in 10°C steps, each. At temperatures between 30°C and 60°C system A shows the classical Winsor I phase behavior, the surfactant is mostly dissolved in the aqueous phase. Figure 49 shows the LLE for system A at 30°C. The experimental data for the Winsor I system is given in Table 14.

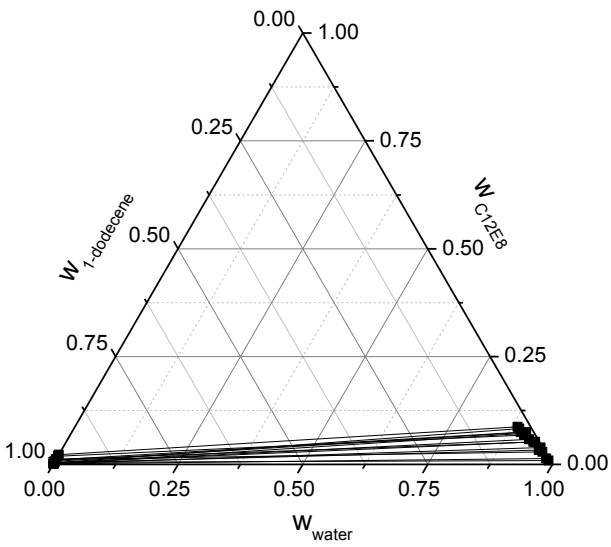

Figure 49: Tie lines for system A at 30°C.

The tie lines are expanded to the surfactant rich site and the surfactant containing aqueous phase is in equilibrium with a nearly pure oil phase. If the temperature is increased the general phase behavior for system A is not changing. Figure 50 depicts the tie lines for system A at 40°C.

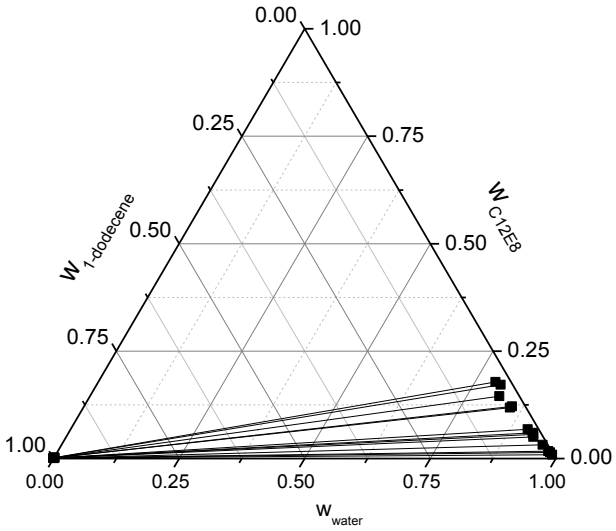

Figure 50: Tie lines for system A at 40°C.

By further increase of temperature up to 50°C the general picture stays the same as depicted in Figure 51.

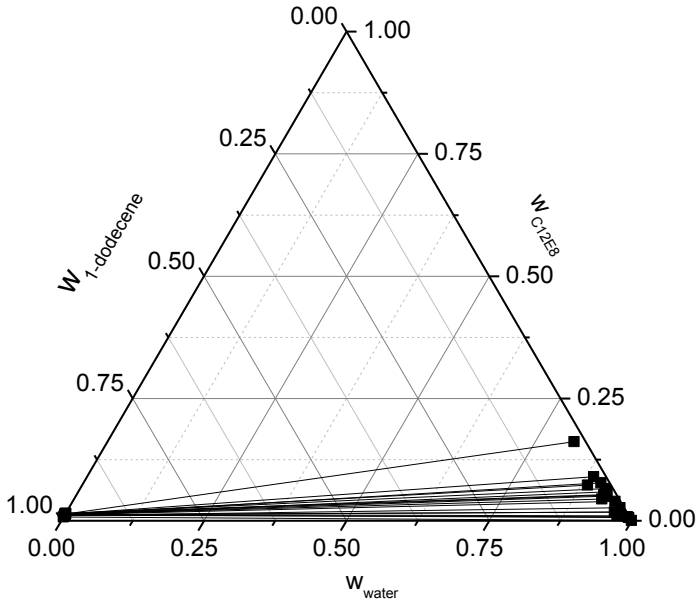

Figure 51: Tie lines for system A at 50°C.

At 60°C system A shows again Winsor I phase behavior, shown in Figure 52.

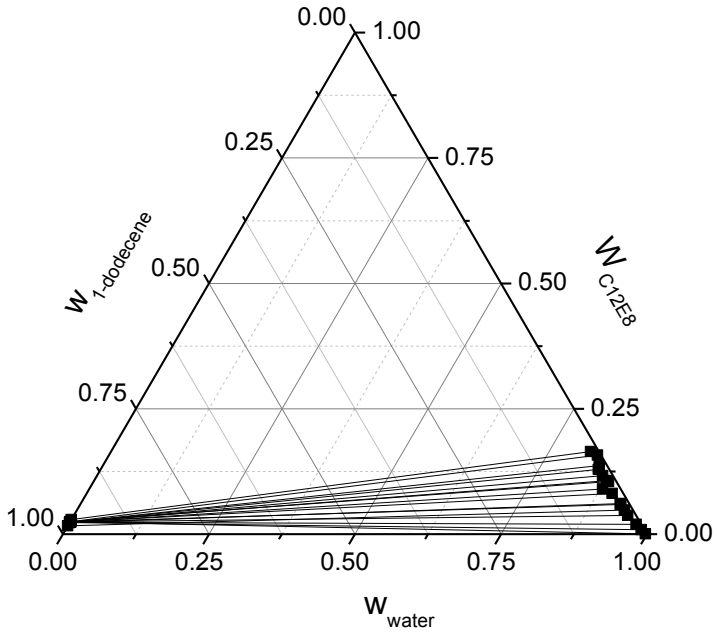

Figure 52: Tie lines for system A at 60°C.

Table 14: LLE data for system A at temperatures 30°C, 40°C, 50°C and 60°C. Superscript I denotes the oil rich phase and superscript II denotes the aqueous phase.

T/°C	$w^{I}_{H_2O}$	$w^{I}_{C_{12}E_8}$	$w^{II}_{H_2O}$	$w^{II}_{C_{12}E_8}$
30	< 0.0001	0.0009	0.9108	0.0723
30	< 0.0001	0.0119	0.9396	0.0519
30	< 0.0001	0.0190	0.9096	0.0679
30	< 0.0001	0.0109	0.8989	0.0747
30	< 0.0001	0.0113	0.9653	0.029
30	< 0.0001	0.0038	0.9243	0.0579
30	< 0.0001	0.0033	0.9561	0.033
30	< 0.0001	0.0039	0.9358	0.039
30	< 0.0001	0.0020	0.9568	0.039
30	< 0.0001	0.0046	0.988	0.0086
30	< 0.0001	0.0074	0.91	0.0749

30	0.0009	0.0037	0.8925	0.0827
30	0.0001	0.0227	0.8866	0.087
40	< 0.0001	0.0008	0.9576	0.0322
40	< 0.0001	0.0009	0.9304	0.0502
40	< 0.0001	0.0012	0.9814	0.0145
40	< 0.0001	0.0012	0.9885	0.0089
40	< 0.0001	0.0013	0.9272	0.0562
40	< 0.0001	0.0010	0.9237	0.0598
40	< 0.0001	0.0011	0.9762	0.0174
40	< 0.0001	0.0012	0.91	0.0681
40	0.0008	0.0016	0.8493	0.1185
40	0.0003	0.0015	0.8042	0.172
40	0.0011	0.0017	0.8523	0.1214
40	< 0.0001	0.0019	0.7909	0.178
40	0.0012	0.0015	0.8152	0.1453
50	0.0001	0.0113	0.9881	0.0083
50	0.0002	0.012	0.9606	0.0178
50	0.0001	0.0125	0.9279	0.0504
50	0.0001	0.0109	0.9662	0.0264
50	< 0.0001	0.0134	0.08184	0.1616
50	< 0.0001	0.0118	0.9274	0.0594
50	< 0.0001	0.0129	0.9252	0.0449
50	< 0.0001	0.0123	0.9509	0.0394
50	< 0.0001	0.0121	0.9076	0.0776
50	< 0.0001	0.0134	0.8884	0.09
50	< 0.0001	0.0122	0.9916	0.0064
50	< 0.0001	0.0075	0.9993	0.0005

50	< 0.0001	0.0138	0.8863	0.073
50	< 0.0001	0.0132	0.9692	0.0098
50	< 0.0001	0.015	0.9208	0.0660
50	< 0.0001	0.0145	0.9255	0.0521
50	< 0.0001	0.0152	0.9245	0.0533
60	< 0.0001	0.0233	0.9860	0.0088
60	< 0.0001	0.0244	0.9251	0.0590
60	< 0.0001	0.0167	0.9374	0.0481
60	< 0.0001	0.0231	0.9247	0.0608
60	< 0.0001	0.0242	0.9484	0.0371
60	< 0.0001	0.0236	0.9717	0.0193
60	< 0.0001	0.0242	0.9970	0.0005
60	< 0.0001	0.0236	0.8793	0.0900
60	< 0.0001	0.0248	0.8822	0.1045
60	< 0.0001	0.0238	0.8656	0.1167
60	< 0.0001	0.0241	0.8998	0.0810
60	< 0.0001	0.0245	0.8775	0.1066
60	< 0.0001	0.0239	0.8499	0.1367
60	0.0013	0.0236	0.8525	0.1291
60	0.0016	0.0249	0.8367	0.1574
60	< 0.0001	0.0291	0.8214	0.1645

At 70°C system A changes the phase behavior, a third phase is evolving and the system is now in the Winsor III region. In Figure 53 the Gibbs's triangle for 70°C and 80°C is plotted.

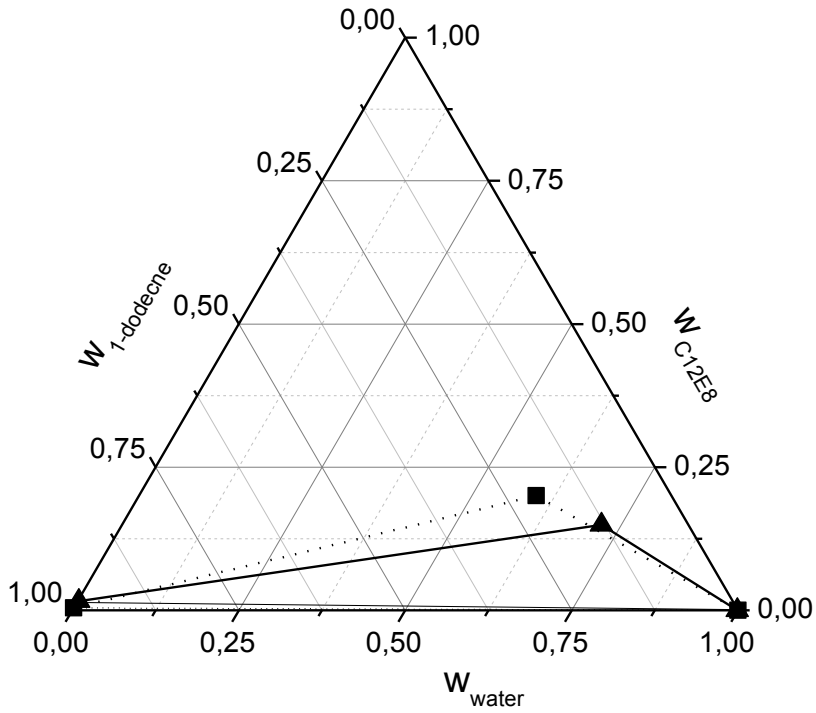

Figure 53: LLE for system A at 70°C (triangles and solid line) and 80°C (squares and dotted line).

At these two temperatures the microemulsion is in equilibrium with two almost pure excess phases, one water excess phase at the bottom and one oil excess phase on top. The top of the three phase body is moving with increasing temperature towards the 1-dodecene side due to the increased solubility of $C_{12}E_8$ in the oil rich phase. The phase change temperatures obtained from the tie line measurement in system A are in good accordance with the data obtained from the Kahlweit's fish measurement in Figure 37. In Table 15 the data for the three phase equilibrium are given.

Table 15: LLE data for system A at temperatures 70°C and 80°C. Superscript I denotes the oil rich phase, superscript II denotes the microemulsion phase and superscript III denotes the aqueous phase.

T/°C	$w^{I}_{H_2O}$	$w^{I}_{C_{12}E_8}$	$w^{II}_{H_2O}$	$w^{II}_{C_{12}E_8}$	$w^{III}_{H_2O}$	$w^{III}_{C_{12}E_8}$
70	0.0015	0.0163	0.7200	0.1494	0.9991	0.0003
80	< 0.0001	0.0041	0.5969	0.1999	0.9998	0.0002

At 90°C the phase behavior of system A has changed again, the surfactant is now mostly located in the oil rich phase. This behavior is called Winsor II phase behavior. The tie lines for system A at 90°C are plotted in Figure 54 the data is given in Table 16. Again, the phase change temperatures fit to the phase change temperatures obtained by the measurement of the Kahlweit's fish for system A plotted in Figure 37.

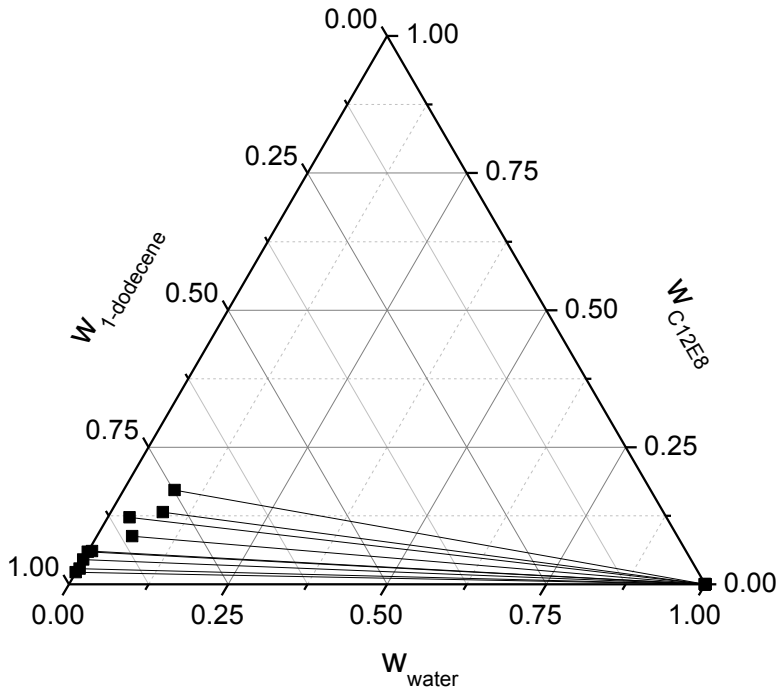

Figure 54: Tie lines for system A at 90°C.

Table 16: LLE data for system A at 90°C. Superscript I denotes the oil rich phase and superscript II denotes the aqueous phase.

T/°C	$w^{I}_{H_2O}$	$w^{I}_{C_{12}E_8}$	$w^{II}_{H_2O}$	$w^{II}_{C_{12}E_8}$
90	0.0003	0.0591	0.9999	0.0001
90	0.0024	0.0287	0.9999	0.0001
90	0.0555	0.0876	0.9999	0.0001
90	< 0.0001	0.0452	0.9999	0.0001
90	0.0061	0.0603	0.9999	0.0001
90	0.0861	0.1316	0.9999	0.0001

90	0.0345	0.122	0.9999	0.0001
90	< 0.0001	0.22	> 0.9999	< 0.0001
90	0.0803	0.1719	0.9999	0.0001

The obtained results depicted from Figure 49 to Figure 54 and Table 14 to Table 16 show an excellent agreement with the expected phase behavior. With increasing the temperature at a constant surfactant feed concentration, the solubility of $C_{12}E_8$ must decrease in the aqueous phase and increase in the oil rich phase, since the surfactant solubility in the latter phase is increasing with temperature. In Figure 55 the $C_{12}E_8$ mass fraction is plotted at a constant feed concentration within the aqueous phase in dependency of temperature.

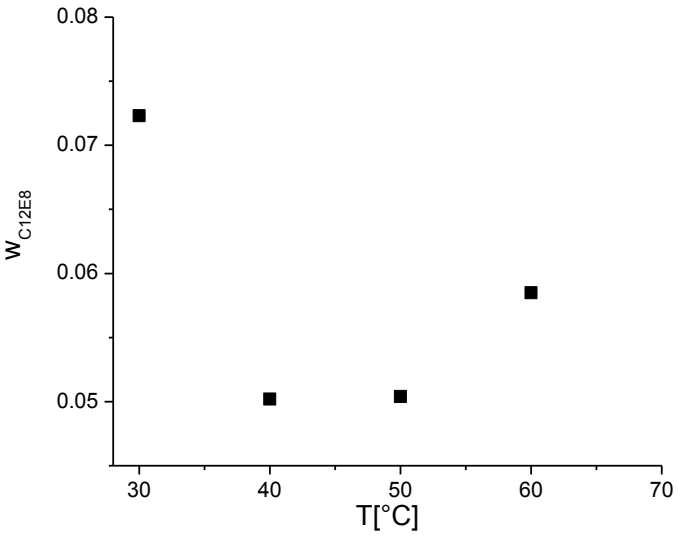

Figure 55: $C_{12}E_8$ weight fraction in the aqueous phase at a constant feed ($w_{C_{12}E_8} \approx 0.04$) in dependency of temperature.

Vice versa the $C_{12}E_8$ solubility in the oil rich phase is increasing with increasing temperature as shown in Figure 56. The data plotted in Figure 55 and Figure 56 are not only useful for estimation of the measurement quality. They can help to estimate in a first approximation the catalyst loss if one assume that the catalyst + ligand is following the surfactant in the solubility behavior. For operating

the technical process e.g. in a miniplant these data can set the basis for choosing the different temperatures for phase separation, reactor temperature and so on. Furthermore, the surfactant loss with the product phase can be estimated and the amount of surfactant make up can be valued. Alongside a big amount of surfactant in the product stream can affect the product purification in a negative way. It is also possible to estimate the amount of recycled product within the aqueous phase; of course this amount has to be as low as possible for an economic process.

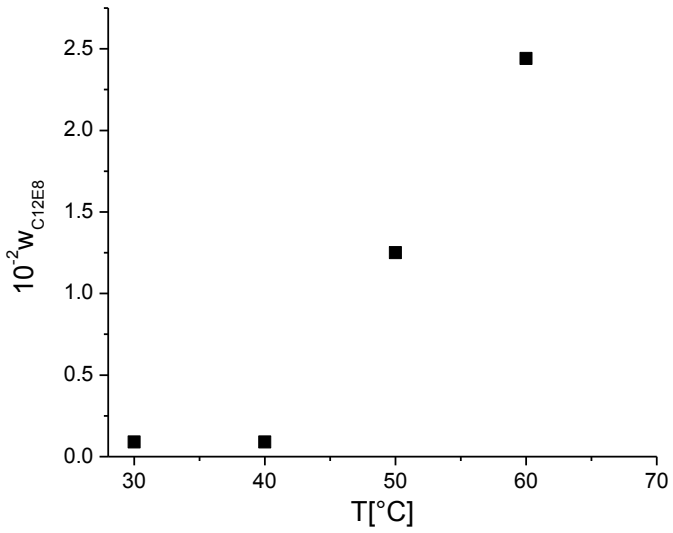

Figure 56: $w_{C_{12}E_8}$ in the oil rich phase at a constant feed ($w_{C_{12}E_8} \approx 0.04$) in dependency of temperature.

5.3.4 Genapol X080® + technical 1-dodecene + water

The next step is the investigation of the phase equilibrium in the pseudo ternary system Genapol X080® + technical 1-dodecene + water in order to compare it with the LLE data for system A. As depicted in Figure 57 at 30°C only a slight difference between system B and system A can be recognized. Both systems are in the Winsor I phase region.

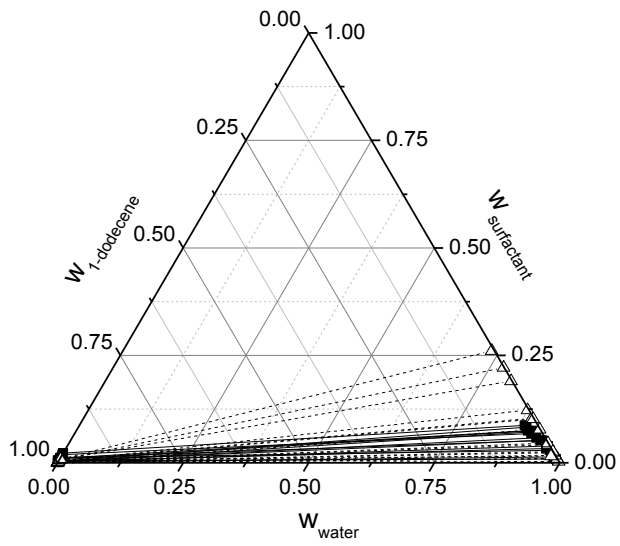

Figure 57: Tie lines for system A [squares and solid line] and system B [open triangles and dashed line] at 30°C.

With increasing the temperature up to 40°C the overall phase behavior for both systems does not change as depicted in Figure 58.

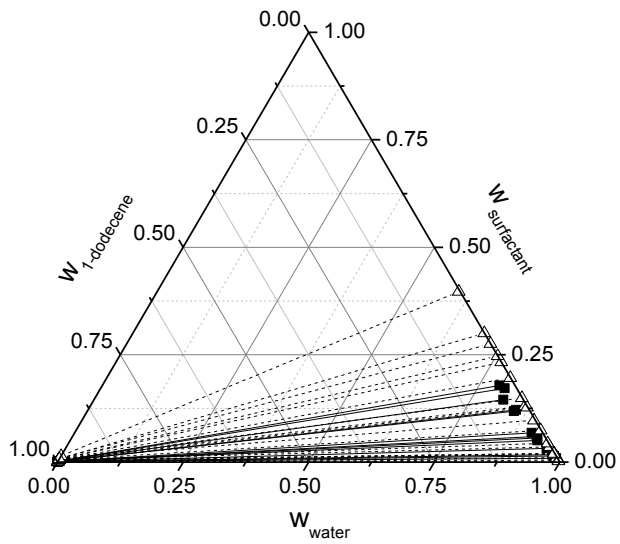

Figure 58 Tie lines for system A [squares and solid line] and system B [open triangles and dashed line] at 40°C

The surfactant is mostly located in the aqueous phase for system A as well for system B. With further rise of temperature up to 50°C both systems stay in the Winsor I region as it is clearly visible in Figure 59.

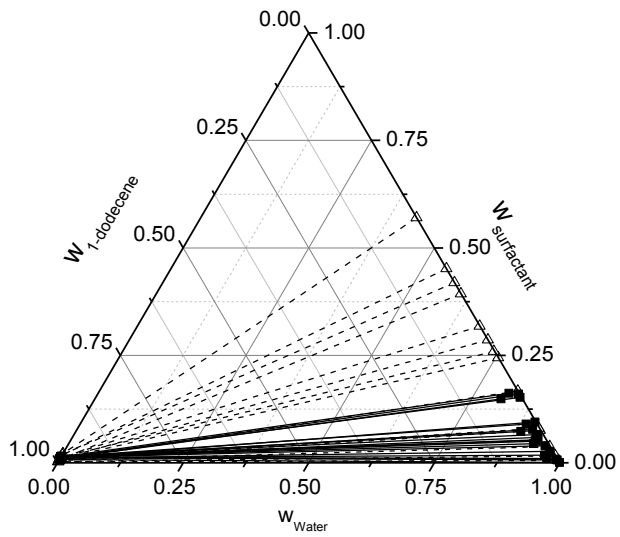

Figure 59: Tie lines for system A [squares and solid line] and system B [open triangles and dashed line] at 50°C.

Equally at 60°C no significant difference in the phase and aggregation behavior of system A and system B could be recognized. In Figure 60 the Gibbs's triangle at 60°C is shown.

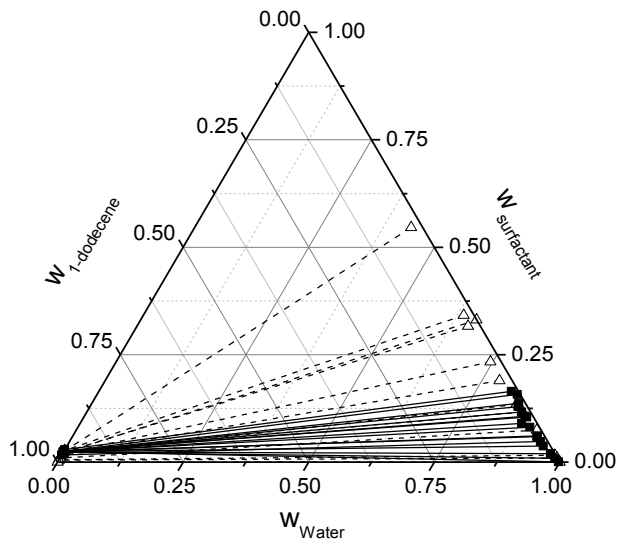

Figure 60: Tie lines for system A [squares and solid line] and system B [open triangles and dashed line] at 60°C.

At 70°C the phase behavior for system A has changed and now the surfactant is mostly dissolved in the middle phase. However, in system B now three phase equilibrium is evolving with one water and one 1-dodecene excess phase. In Figure 61 the triangle for both systems is plotted. At high surfactant concentrations a one phase region could be found.

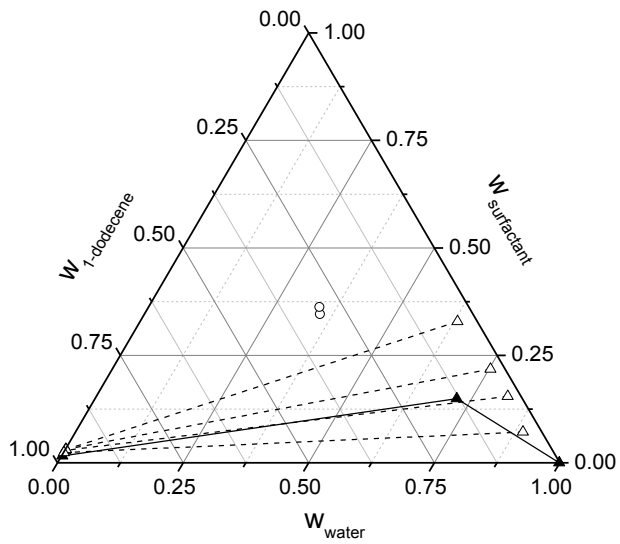

Figure 61: Tie lines for system A [solid triangles and black line] and system B [open triangles and dashed line] as well as one phase compositions for system B [open circles] at 70°C.

At this temperature the technical grade surfactant is able to solubilize a noteworthy amount of technical grade 1-dodecene within the aqueous phase. At 80°C system A remains still in the Winsor III region and until this temperature there is no change in the phase behavior of system B as depicted in Figure 62.

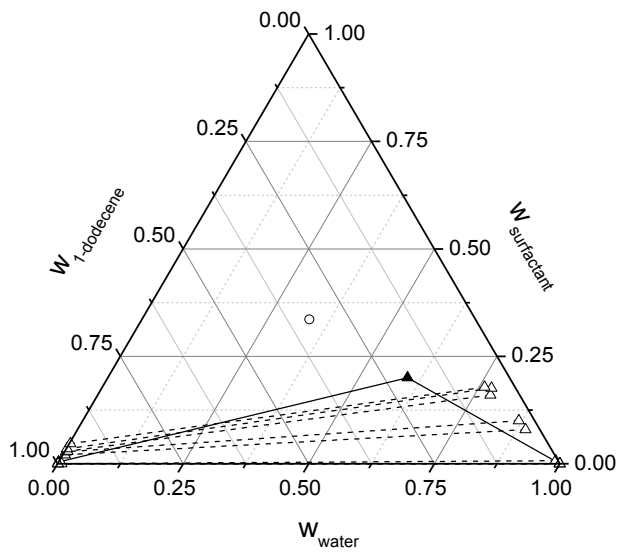

Figure 62: Tie lines for system A [solid triangles and black line] and system B [open triangles and dashed line] as well as one one phase composition for system B [open circles] at 80°C.

The measured data points for the Winsor I of system B are given in Table 17 and for the Winsor IV region in Table 18.

Table 17: Measured LLE data for system B in the Winsor I phase region. Superscript I denotes the oil rich phase and superscript II denotes the aqueous phase.

T/°C	$w^{I}_{H_2O}$	$w^{I}_{Genapol\,X080®}$	$w^{II}_{H_2O}$	$w^{II}_{Genapol\,X080®}$
30	< 0.00001	0.0005	0.99668	0.00303
30	< 0.00001	0.0002	0.99031	0.00951
30	< 0.00001	0.0006	0.98996	0.00951
30	< 0.00001	0.001	0.98219	0.01697
30	< 0.00001	0.0031	0.95552	0.04179
30	< 0.00001	0.002	0.97515	0.023514
30	< 0.00001	0.0019	0.95351	0.04531
30	< 0.00001	0.0017	0.97319	0.02615
30	< 0.00001	0.0019	0.92103	0.07771
30	< 0.00001	0.005	0.89247	0.10356
30	< 0.00001	0.0034	0.87452	0.12252
30	< 0.00001	0.0028	0.89587	0.10211
30	< 0.00001	0.0074	0.80787	0.19012
30	< 0.00001	0.0063	0.9747	0.01531
30	0.001	0.0068	0.7774	0.22174
30	0.002	0.00838	0.73453	0.26063
40	0.00019	0.00126	0.9888	0.09933
40	0.00014	0.00086	0.9951	0.00466
40	0.00015	0.00062	0.99644	0.00249
40	0.00017	0.0039	0.98078	0.01794
40	0.00023	0.00402	0.97842	0.0201
40	0.00018	0.00402	0.8657	0.13012
40	0.0002	0.00402	0.96228	0.03542
40	0.00021	0.00513	0.95377	0.04406
40	0.0002	0.00504	0.97843	0.0194
40	0.00023	0.00455	0.92505	0.07396

40	0.00026	0.00804	0.9003	0.09685
40	0.00024	0.00548	0.80343	0.19607
40	0.00023	0.00486	0.87133	0.12725
40	0.00023	0.00861	0.72444	0.27516
40	0.00024	0.00511	0.85006	0.14922
40	0.00022	0.00587	76706	0.23278
40	0.00025	0.00636	0.75263	0.24709
40	0.00015	0.01423	0.60065	0.39702
40	0.00022	0.00175	0.69928	0.30045
50	0.00021	0.00512	0.96089	0.03794
50	0.00018	0.00231	0.99459	0.00506
50	0.00027	0.00667	0.92233	0.07595
50	0.00026	0.00840	0.75531	0.24429
50	0.00028	0.00754	0.8327	0.16699
50	0.00024	0.0032	0.98303	0.01604
50	0.00027	0.00861	0.71385	0.28589
50	0.00029	0.01214	0.71385	0.25589
50	0.00026	0.00775	0.91753	0.08034
50	0.00025	0.01242	0.6819	0.3177
50	0.00044	0.0194	0.58084	0.41916
50	0.00042	0.02107	0.42959	0.57024
50	0.00038	0.01864	0.54831	0.45169
50	0.00037	0.00664	0.60653	0.39312
60	0.00039	0.00528	0.982	0.01628
60	0.00048	0.00932	0.91716	0.07488
60	0.00034	0.01653	0.84694	0.1342
60	0.00046	0.0184	0.78504	0.18957
60	0.00054	0.02042	0.7456	0.23307
60	0.00051	0.02234	0.6594	0.3164
60	0.00055	0.02044	0.6687	0.33086
60	0.00087	0.02537	0.43127	0.54611
60	0.00058	0.02751	0.63761	0.34175
60	0.0005	0.02377	0.86766	0.11678

60	0.00036	0.00484	0.98961	0.00936
60	0.00037	0.00004	0.99983	≤0.00001
70	0.00146	0.02878	0.81917	0.15459
70	0.00097	0.03133	0.75298	0.21819
70	0.00133	0.03108	0.6321	0.32872
70	0.00105	0.02344	0.89081	0.07189
80	0.0082	≤0.00001	0.98805	0.00701
80	0.00444	0.02044	0.89219	0.07931
80	0.00305	0.20801	0.8685	0.10033
80	0.00579	0.02881	0.78189	0.16
80	0.0016	0.03518	0.77617	0.1758
80	0.00228	0.0466	0.76086	0.17828
80	0.00078	≤0.00001	≤0.99999	≤0.00001

Table 18: Phase composition for system B in the Winsor IV region at 70°C and 80°C.

T/°C	$w^{I}_{H_2O}$	$w^{I}_{Genapol\,X080®}$
70	0.34927	0.34609
70	0.34056	0.36218
80	0.33373	0.33553

At 90°C system B has reached the Winsor III region with the microemulsion as the middle phase and in system A the Winsor II phase behavior is existent. This is in good agreement with Kahlweit's fish depicted in Figure 39. In Figure 63 the phase behavior for system B is compared to the phase behavior in system A.

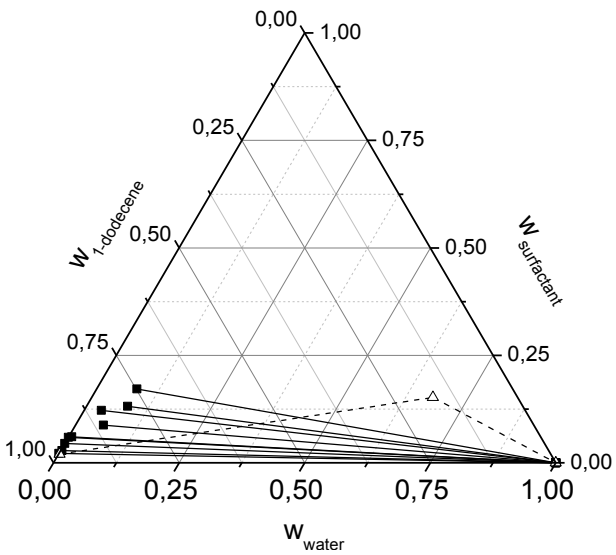

Figure 63: Tie lines for system A [solid squares and black line] and system B [open triangles and dashed line] at 90°C.

In Table 19 the measured data points are given.

Table 19: LLE data for system B at 90°C. Superscript I denotes the oil rich phase, superscript II denotes the microemulsion phase and superscript III denotes the aqueous phase.

T/°C	$w^{I}_{H_2O}$	$w^{I}_{Genapol\ X080®}$	$w^{II}_{H_2O}$	$w^{II}_{Genapol\ X080\ ®}$	$w^{III}_{H_2O}$	$w^{III}_{Genapol\ X080\ ®}$
90	0.00234	0.01997	0.67941	0.15203	0.99981	< 0.00001

In addition to the determination of the phase compositions in the three phase area at 90°C tie lines for the binary system attached to the three phase area at the technical 1-dodecene side were measured at 85°C and 90°C. It was not possible to determine tie lines for the binary system attached to the three phase area at the Genapol X080® side due to the tremendous equilibration time. The knowledge of the binary systems attached to the ternary LLE is necessary for the application of these systems. Given that the optimal reaction temperature for hydroformylation is between 80°C and 90°C it is necessary to have a nearly complete overview about the phase behavior in whole concentration range. The measured tie lines are plotted in Figure 64 and Figure 65 the data points are given in Table 20.

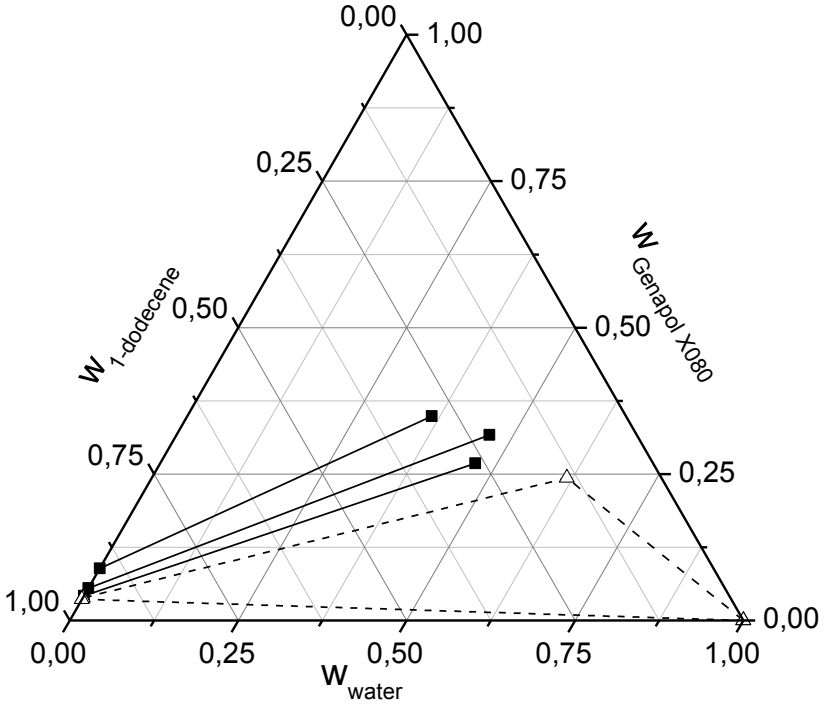

Figure 64: Tie lines [solid squares and black line] attached to the three phase LLE [dashed line and open triangles] at 85°C.

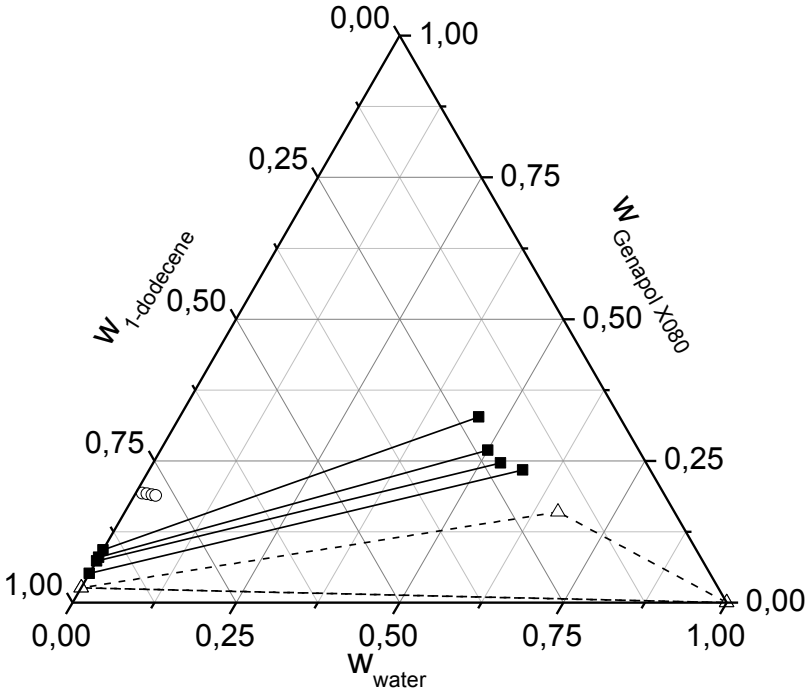

Figure 65: Tie lines [solid squares and black line] attached to the three phase LLE [dashed line and open triangles] at 90°C. Open circles specify single phase compositions.

Table 20: Phase compositions for the binary systems attached to the three phase region at temperatures 85°C and 90°C.

T/°C	$w^{I}_{H_2O}$	$w^{I}_{Genapol\,X080®}$	$w^{II}_{H_2O}$	$w^{II}_{Genapol\,X080®}$
85	< 0.0001	0.0501	0.4647	0.3168
85	< 0.0001	0.089	0.363	0.3488
85	< 0.0001	0.0421	0.4678	0.2685
90	< 0.0001	0.0513	0.5711	0.2338
90	< 0.0001	0.0737	0.5311	0.2465
90	< 0.0001	0.0931	0.4574	0.3273
90	< 0.0001	0.08	0.5007	0.2689

Measurements at higher temperatures than 90°C were not possible due to boiling retardation. As demonstrated in 5.3.3 the solubility of $C_{12}E_8$ within the aqueous phase is decreasing with increasing temperature. The same behavior is expected for the technical grade surfactant. In Figure 66 the surfactant solubility in the aqueous phase at constant feed mass fraction is plotted.

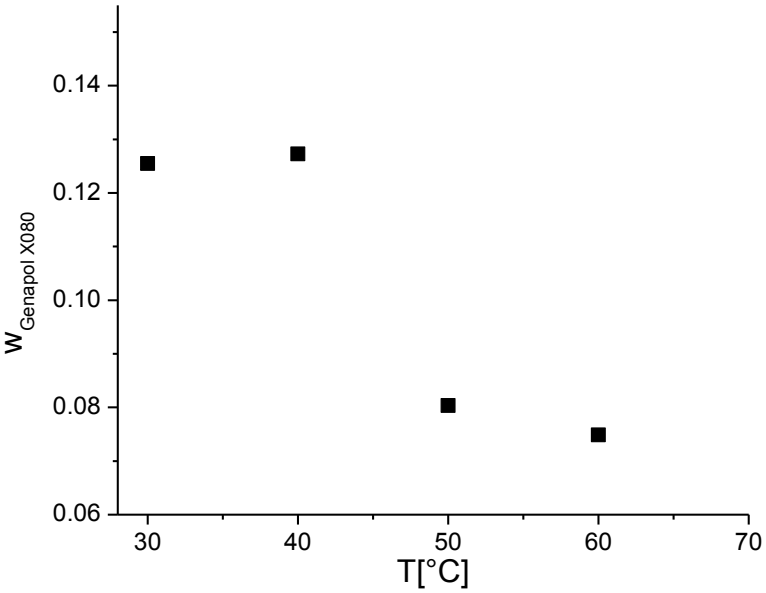

Figure 66: $w_{Genapol\ X080}$ in the aqueous phase at a constant feed ($w_{Genapol\ X080}$ ≈0.04) in dependency of temperature.

When temperature is increasing the solubility of surfactant in the aqueous phase is decreasing this is in good agreement with the results obtained from measurements with the pure substances. Vice versa the solubility of the technical surfactant has to be enhanced in the oil rich phase. This is the case as depicted in Figure 67. The data plotted in Figure 66 and Figure 67 can be used for verifying the catalyst loss in a technical scale process. The data obtained in 5.3.3 gave a first hint about the estimation of catalyst loss in the oil rich phase as well as the surfactant loss with the product phase. It turned out that there are large differences in the phase behavior in system A and system B. Therefore it is necessary to estimate the catalyst loss and the surfactant loss with technical grade substances again. In addition to that the amount of product which cannot be separated in the phase separation step can be estimated, too.

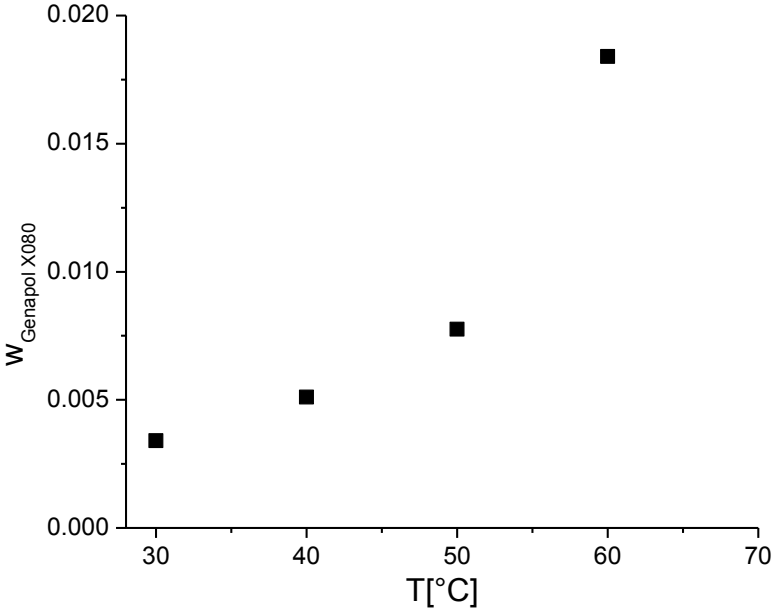

Figure 67: $w_{Genapol\ X080}$ in the oil rich phase at a constant feed ($w_{Genapol\ X080}$ ≈0.04) in dependency of temperature.

In addition to that the mass balance has to be fulfilled. The mass balance was checked by plotting a single tie line and the corresponding feed point as shown in Figure 68.

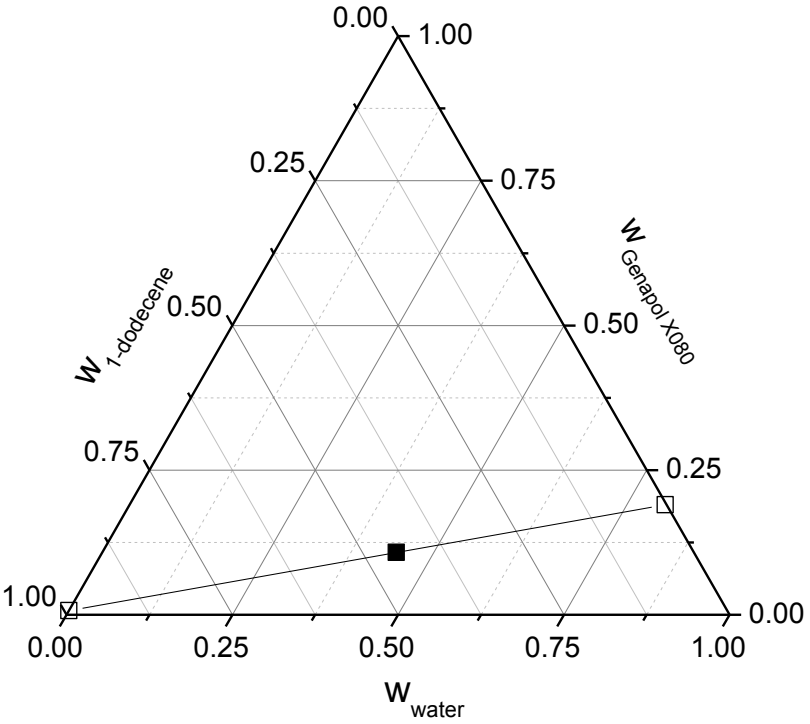

Figure 68: Single tie line (solid line), phase compositions within the coexisting phases (open squares) and feed weight fraction (solid square) at 30°C for system B.

5.3.5 Four phase LLE in the system Genapol X080® + 1-dodecene + water

Let us assume a system containing three pure substances. According to Gibbs's phase rule this system can have a four phase LLE having in mind that under these circumstances the degree of freedom is one: $F = 2 - \pi + n = 2 - 4 + 3 = 1$. F denotes the degree of freedom, π the number of phases and n the number of components. Furthermore, in laboratory experiments usually the pressure is fixed to atmospheric pressure or in addition pressure has no influence on the system, then the degree of freedom is reduced to zero. In general systems of the type nonionic surfactant + water + oil are not depending on pressure in moderate pressure regions (22). Therefore in a three component system finding a four phase LLE is a rare coincidence or practical impossible. Nevertheless in system B a four phase LLE was investigated as depicted in Figure 69, because this

system is a true multicomponent system. To verify the four phase LLE the sample was shaked and the fourth phase evolved again. Furthermore, the experiment was repeated several times.

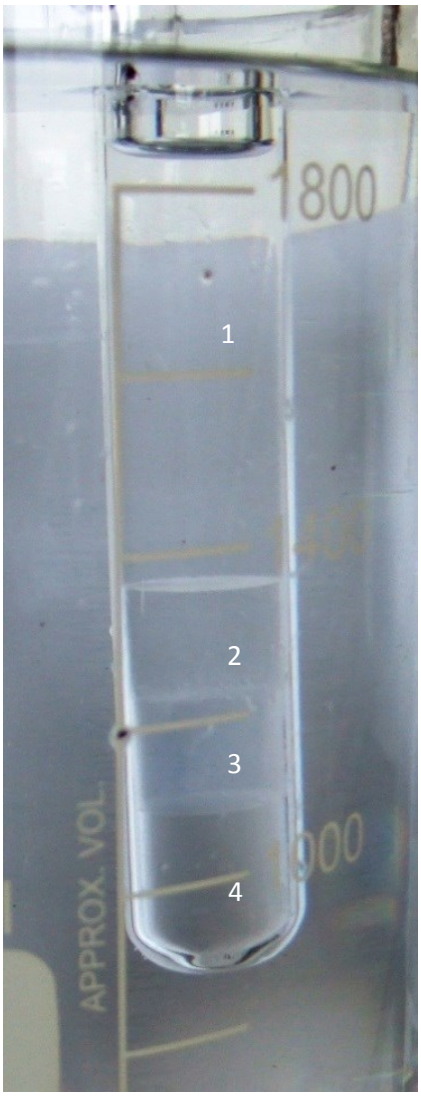

Figure 69: Four phase liquid liquid equilibrium in system B at 90°C.

The microemulsion splits into two transparent phases in opposition to Schulman and Riley (269) who described the microemulsion as a stable, optically transparent phase. This can happen having in mind a system containing technical grade surfactant is in no case a three component system. Moreover it is a multicomponent system since the technical grade surfactant contains not converted fatty alcohol, surfactants with a different degree of ethoxylation and not converted ethylenoxide. Likewise in technical surfactants a lot of additives could be part of the formulation. This result is also of importance for the technical application within the miniplant. On the one hand the four phase LLE

can influence the hydroformylation reaction significantly on the other hand new problems with phase separation can occur. If the separator is configured to separate a system containing three liquid phases it would be very difficult to separate four phases. Here always two phases are leaving the separator together, which has influence of product and catalyst loss.

5.4 Comparison of pure and technical grade surfactant and 1-dodecene

When technical grade substances are used the number and type respectively the nature of impurities become more and more evident. Of course this thesis is not targeting a detailed analysis of amount and structure of surfactant impurities a few hints can be obtained by the performed studies. Beside this for hydroformylation process for e.g. in a miniplant one has to concern these hints and furthermore, one must take the long term stability of surfactant into account. A look on the HPLC chromatogram allows a first evaluation. In Figure 70 the chromatogram for Genapol X080® and $C_{12}E_8$ dissolved in 1-propanol with a nearly similar mass fraction is plotted.

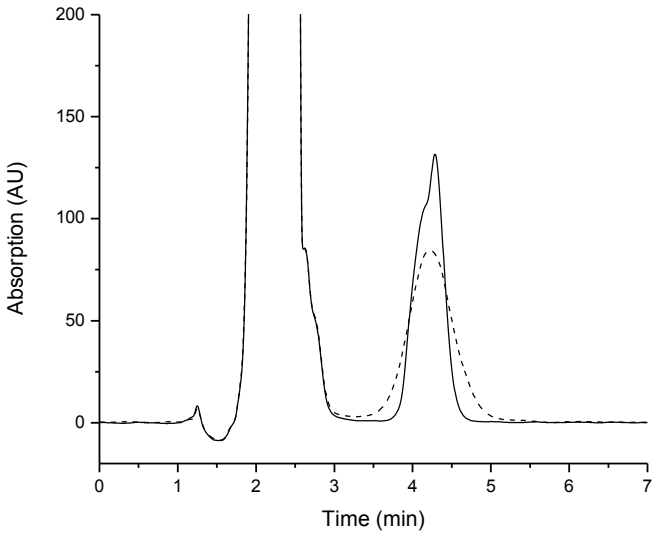

Figure 70: Chromatogramm of Genapol X080® (dashed line, $w_{Genapol\ X080®}$=0.00054) and $C_{12}E_8$ (solid line, w_{C12E8}=0.00058) dissolved in 1-propanol.

There are significant differences determinable. The Genapol X080® peak is broad compared to the peak belonging to the pure substance. This is caused by a broad ethoxylate chain length distribution. Beside this the surfactant decomposes while heating. A hint his given by FTIR measurement depicted in Figure 71.

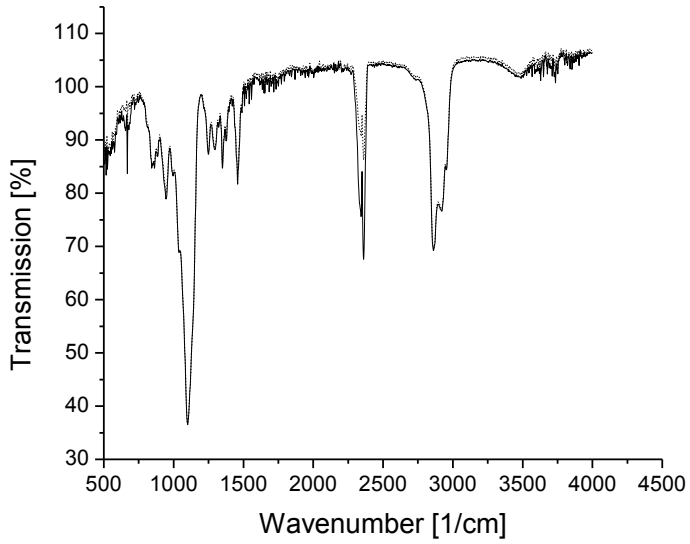

Figure 71: FTIR spectrum for fresh Genapol X080® (dashed line) and Genapol X080® heated for 48h at 90°C (solid line).

After heating the surfactant a clear increase of the peak within the area between wavenumber 2300 and 2400 $\frac{1}{cm}$ can be recognized. Normally the band between wavenumber 3300 and 2250 $\frac{1}{cm}$ can refer to associated OH-groups. Through decomposition of the ethoxylate chain the number of these groups is increasing. Beside this through surfactant decomposition peroxides are formed. These peroxides can be determined after several hours of heating. The amount of formed peroxides after 48h hours heating is around 20 mg per liter solution. In case of 1-dodecene also differences in the HPLC chromatogram could be recognized as depicted in Figure 72.

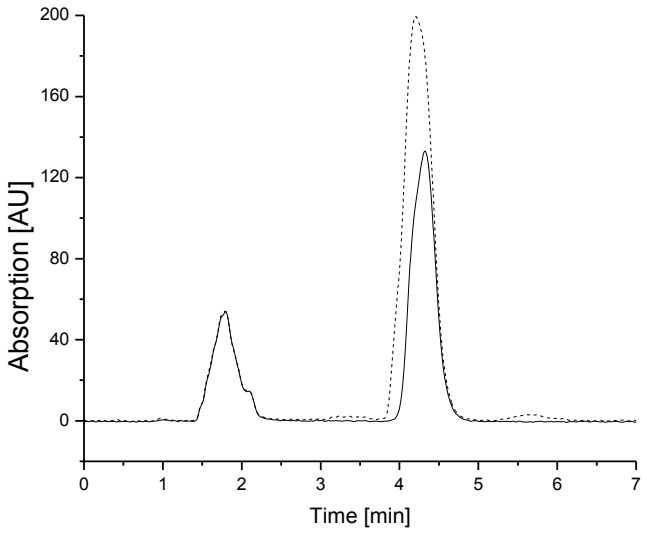

Figure 72: Chromatogram of technical 1-dodecene (dashed line, $w_{1\text{-dodecene, technical}}$=0.00058) and pure 1-dodecene (solid line, $w_{1\text{-dodecene, pure}}$=0.00051).

5.5 Calculation of the binary phase and aggregation behavior: The Nagarajan and Ruckenstein model

Despite ternary systems containing surfactants, which cannot be modeled with acceptable accuracy at the moment, the binary subsystem water + surfactant can be modeled with help of the micelle formation model. The modeled LLE as well as the predicted CMC taken from Dorn et al. (270) are compared with the cloud point curve obtained in this work given in Figure 73. The results are in good agreement with the experimental data. One micelle poor phase is in equilibrium with a micelle rich phase. The free enthalpy of mixing **Eq. (4)** can be calculated with help of the size distribution function **Eq. (15)** and $\Delta\mu_0 g$ as function of aggregation number and temperature. Taking a g^e-model **Eq. (5)** into account with help of three adjustable parameters the equilibrium conditions **Eq. (17)** and **Eq. (18)** can be solved.for the surfactant C12E8 according to Dorn et al. (270) the following paramaters were used: $C_1 = 0.874$, $C_2 = -287.5$ and $\gamma = 141.625$. $(\mu_{0g})_{ster}$ was fitted to CMC data obtained at room temperature. Furthermore, the temperature dependency of the CMC was well described.

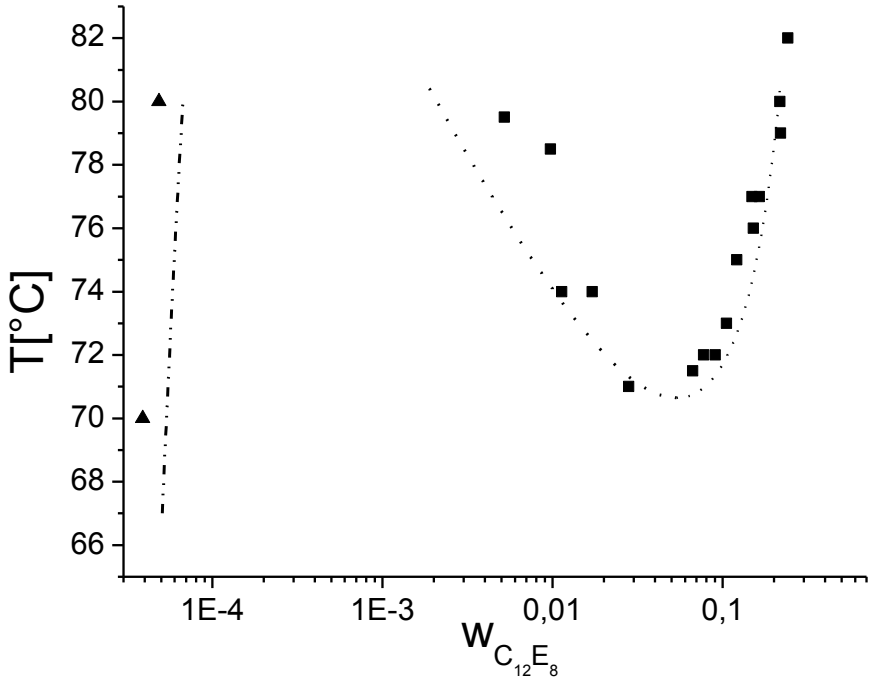

Figure 73: Calculated LLE for the system $C_{12}E_8$ and water (dotted line modeled cloud point curve from (270), squares this work). Triangles experimental CMC data from (129), dashed line predicted CMC from (270).

6. Summary and Outlook

Caused by the high potential of surfactant containing systems in the field of chemical engineering the knowledge about the phase and aggregation behavior is fundamental. To perform any large scale process without knowing about the phase behavior is not recommendable. Therefore the measurement of new thermodynamic data is of major importance as the prediction of LLE for the system water + nonionic surfactant + oil is still not satisfying. Within this work the LLE for the system $C_{12}E_8$ + water + 1-dodecene was measured across a wide temperature range. Several analytical problems had to be managed and solved within the framework of this investigation. Around one hundred samples were prepared for phase prism measurement witch implies around 500 single measurements to detect the phase composition. New methods to handle this huge amount of samples in an efficient way were developed. Through application of HPLC it was possible not only to detect the thermal instable component surfactant but also to detect 1-dodecene with one analytical device. This makes the time efficient measurement of these systems in principal feasible. Moreover, the sampling has to be carried out at constant temperature. Furthermore, during sampling several interfaces have to be pushed through with a needle in order to take a small amount of probe of each phase. Especially in the three or four phase LLE this can cause a relevant measurement error. To reduce this error a new approach for sampling from the bottom phase was implied and tested successfully. One other challenge is the measurement of trace components concerning the binary subsystem water + 1-dodecene. The water solubility of 1-dodecene is far beyond any standard analytical method. A gas stripping technique was modified and through this additional step of enrichment the measurement with standard analytical equipment was possible for the first time. One other important issue is the surfactant quality. To obtain thermodynamic data generally pure substances are used. For the most LLE measurements with e.g. bulk chemicals the difference between measurements with pure substances and technical grade substances is small or negligible. In case of surfactants this is not true. A technical grade surfactant cannot be considered as pure

substance with some impurities. It is a true multicomponent system containing in general surfactant molecules with a broad degree of ethoxylation, not converted fatty alcohols and ethylenoxide. The influence of the surfactant with different degree of ethoxylation and the influence of the technical grade surfactant were measured by means of the Kahlweit's fish. Additional the influence of the technical grade surfactant on the phase composition was studied. The surfactant quality can influence the LLE drastically. Not only the temperature a three phase LLE is evolving is shifted to much higher temperatures also the number of coexisting phases is increasing. To the authors knowledge for the first time a four phase LLE was reported in a system containing technical grade surfactant + water + oil. The developed methods for rapid measurement of the phase composition in system containing the pure substances could be adopted for measurements in system containing technical grade substances. Furthermore, for technical application e.g. the hydroformylation not only the phase equilibria of technical grade surfactant + water + educt are of relevance also the influence of the product has to take into account in order to operate the process correct. The phase prism including the binary subsystems was therefore measured with technical surfactant Genapol X080® and technical grade 1-dodecene. The product and catalyst influence on the system was successfully studied in terms of the Kahlwet's fish. Thereby no catalyst influence on the LLE was detectable. The formed aldehyde is lowering the temperature of the Winsor III system significantly and with a further increased amount of product the temperature of the Winsor III system can be decreased below the melting range of the technical grade surfactant. For this reason the reaction temperature has to be adapted during the process. Given that the prediction of LLE in systems forming a microemulsion is still not sufficient the focus beside the further development of thermodynamic models should be in sophistication of measurement.

7. Literature

1. **Dwars, T., Paetzold, E. and Oehme, G.** Reaktionen in micellaren Systemen. *Angew. Chem.* 2005, 117, 7338-7364.

2. **Cornils, B., Herrmann, W., A. and Eckl, R., W.** Industrial aspects of aqueous catalysis. *J. Mol. Catal. A* 1997, 116, 27-33.

3. **El Fouih, Y. and Bouallou, C.** Recycling of carbon dioxide to produce ethanol. *Energy procedia* 2013, 37, 6679-6686.

4. **Preston, W.** The modern soap industry. *J. Chem. Educ.* 1925, 2, 1035-1044.

5. **Edser, C.** Status of global surfactant markets. *Focus surfactants* 2008, 11, 1-2.

6. **Qian, C. and Mc Clements, D., J.** Formation of nanoemulsions stabilized by model food-grade emulsifiers using high-pressure homogenization: Factors affecting particle size. *Food Hydrocolloids* 2011, 25, 1000-1008.

7. **Liang, R., Xu, S., Shoemaker, C., Li, Y., Zhong, F. and Huang, Q.** Physical and antimicrobial properties of peppermint oil nanoemulsions. *J. Agric.Food Chem.* 2012, 60, 7548-7555.

8. **Liang, R., Shoemaker, C., Yang, X., Zhong, F. and Huang, Q.** Stability and bioaccessibility of β-carotene in nanoemulsions stabilized by modified starches. *J. Agric. Food Chem.* 2013, 61, 1249-1257.

9. **Takada, H. and Nozoye, H.** Atomic force microscopy studies of AgBr emulsion grains. *Langmuir* 1993, 9, 3305-3309.

10. **Sis, H. and Chander, S.** Improving froth characteristics and flotation recovery of phosphate ores with nonionic surfactants. *Miner. Eng.* 2003, 13, 587–595.

11. **Hung, K.-C., Chen, B.-H. and Liya, E., Y.** Cloud-point extraction of selected polycyclic aromatic hydrocarbons by nonionic surfactants. *Sep. Purif. Technol.* 2007, 57, 1-10.

12. **Dorsey, J., G., Cooper, W., T., Siles B., A., Foley, J., P. and Barth H., G.** Liquid chromatography: theory and methodology. *Anal. Chem.* 1996, 68, 515R-568R.

13. **Lipshutz, H., B., Petersen, T., B. and Abela, R., A.** Room-temperature Suzuki-Miyaura couplings in water facilitated by nonionic amphiphiles. *Org. Lett.* 2008, 10, 1333-1336.

14. **Rispens, T. and Engberts, J., B., F., N.** Micellar catalysis of Diels-Alder reactions: Substrate positioning in the micelle. *J. Org. Chem.* 2002, 67, 7369-7377.

15. **Haumann, M., Koch, H., Hugo, P. and Schomäcker, R.** Hydroformylation of 1-dodecene using Rh-TPPTS in a microemulsion. *Appl. Catal. A* 2002, 225, 239-249.

16. **Haumann, H., Yildiz, H., Koch, H. and Schomäcker, R.** Hydroformylation of 7-tetradecene using Rh-TPPTS in a microemulsion. *Appl. Catal. A* 2002, 236, 173–178.

17. **Haumann, H., Koch, H. and Schomäcker, R.** Hydroformylation in microemulsions: conversion of an internal long chain alkene into a linear aldehyde using a water soluble cobalt catalyst. *Catal. Today.* 2003, 79-80, 43-49.

18. **Ünveren, H., H., Y. and Schomäcker, R.** Rhodium catalyzed hydroformylation of 1-octene in microemulsion: comparison with various catalytic systems. *Catal. Lett.* 2006, 110, 195-201.

19. **Rost, A., Müller, M., Hamerla, T., Y., Kasaka, Wozny, G. and Schomäcker, R.** Development of a continuous process for the hydroformylation of long-chain olefins in aqueous multiphase systems. *Chem. Eng. Process. Intensif.* 2013, 67, 130-135.

20. **Griffin, W., C.** Classification of surface active agents by HLB. *J. Soc. Cosmet. Chem.* 1949, 1, 311-326.

21. **Dörfler, H., D.** *Grenzflächen und kolloid-disperse Systeme.* 2. Ed., Berlin, Springer, 2002.

22. **Kahlweit, M. and Strey, R.** Phasenverhalten ternärer Systeme des Typs H_2O - Öl - nichtionisches Amphiphil (Mikroemulsionen). *Angew. Chem.* 1985, 97, 655-669.

23. **Helin, F., A., J., Gyenge M., Beadele, D., A., Boyd, J., H., Mayhew, R., L and Hyatt, R., C.** Nonionic, anionic and cationic emulsifiers in GR-S polymerizations. *J. Ind. Eng. Chem.* 1953, 45, 1330-1336.

24. **Schoeller, C. and Wittwer, M.** *Assistants for the textile and related industry. 1970578,* USA, 1934.

25. **Kennedy, H., T., Burja, E., O. and Boyklin, R., S.** An investigation of the effects of wettability on the recovery of oil by water flooding. *J. Phys. Chem.* 1955, 59, 867-869.

26. **Fox, E., J. and Jackson, W., A.** Sorption of surface active agents from aqueous solutions by phosphate rock. *J. Agric. Food. Chem.* 1955, 3, 38-42.

27. **Snell, D., F. and Snell, C., T.** Syndets and surfactants. *J. Chem. Educ.* 1958, 35, 271-278.

28. **Gotch, A., J., Loar G., W., Reeder A., J. and Glista, E., E.** Formation of single-phase microemulsions in toluene+water+nonionic surfactant systems. *Langmuir* 2008, 24, 4485-4493.

29. **Krogh, K., A., Halling-Sorensen, B., Mogensen, B., B. and Vejrup K.** Environmental properties and effects of nonionic surfactant adjuvants in pesticides: A review. *Chemospher.* 2003, 50, 871-901.

30. **Traverso-Soto, J., M., Lara-Martin, P., A., Leon, V., M. and Gonzales-Mazo, E.** Analysis of alcoho lpolyethoxylates and polyethylene glycols in marine sediments. *Talanta* 2013, 110, 171-179.

31. **Steindorff, A., Balle, G., Horst, K. and Michel, R.** *Glycol and polyglycol ethers of isocyclic hydroxyl compounds. 2213477,* USA, 1940.

32. **Hellmann, H.** Abbau von Alkylphenolethoxilaten in Waschmitteln. Nachweis durch IR-Spektroskopie und Dünnschicht-Chromatographie. *Fresenius J. Anal. Chem.* 1985, 322, 42-46.

33. **Giger, W., Brunner, P., H. and Schaffner, C.** 4-Nonylphenol in sewage sludge: Accumulation of toxic metabolites from nonionic surfactants. *Science* 1984, 225, 623-625.

34. **Gültekin, I. and Ince, N., H.** Synthetic endocrine disruptors in the environment and water remediation by advanced oxidation processes. *J. Environ. Manage.* 2007, 85, 816-832.

35. **Cox, P. and Drys, G.** Directive 2003/53/EC of the european parliamnet and of the council of 18 June 2003. *Official Journal of the European Union* 2003, L178/24-L178/27.

36. **Hoffmann, B. and Platz, G.** Phase and aggregation behaviour of alkylglycosides. *Curr. Opin. Colloid Interface Sci.* 2001, 6, 171-177.

37. **von Rybinski, W. and Hill, K.** in *Novel surfactants, preparation, application and biodegrability.* New York , 2003, 114, 35-95.

38. **Holmberg, K.** *Novel Surfactants, Preparation, Application and Biodegrability.* New York , 2003, 114.

39. **Fukuda, K., Söderman, O., Lindman, B. and Shinoda, K.** Microemulsions formed by alkyl polyglucosides and an alkyl glycerol ether. *Langmuir* 1993, 9, 2921-2925.

40. **Nilsson, F., Söderman, O. and Johansson, I.** Physical-chemical properties of the n-octyl beta-D-glucoside/water system. A phase diagram, self-diffusion NMR, and SAXS study. *Langmuir* 1996, 12, 902-908.

41. **von Rybinski, W.** Alkyl glycosides and polyglycosides. *Curr. Opin. Colloid Interface Sci.* 1996, 1, 587-597.

42. **Kahl, H., Enders, S. and Quitzsch, K.** Experimental and theoretical studies of the system n-decyl-beta-D-maltopyranoside+water. *Coll. Surf. A* 2001, 183-185, 661-679.

43. **Kahl, H. and Enders, S.** Thermodynamics of carbohydrate surfactant containing systems. *Fluid Phase Equilib.* 2002, 194-197, 739-753.

44. **Kahl, H. and Enders, S.** Aggregation behaviour of n-alkyl-beta-d-glucopyranoside + water + alcohol mixtures. *Fluid Phase Equilib.* 2007, 261, 221-229.

45. **von Rybinski, W. and Hill, K.** Alkyl polyglycosides properties and applications of a new class of surfactants. *Angew. Chem. Int. Ed.* 1998, 37, 1328-1345.

46. **Silva, F., V., M., Goulart, M., Justion, J., Neves, A., Santos, F., Caio, J., Lucas, S., Newton, A., Sacoto, A., Barbosa, E., Santos, M., S. and Rauter, A., P.** Alkyl deoxy-arabino-hexopyranosides: Synthesis, surface properties, and biological activities. *Bioorg. Med. Chem.* 2008, 16, 4083-4092.

47. **Fischer, E.** Über die Glycoside der Alkohole. *Ber. Dtsch. Chem. Ges.* 1893, 26, 2400-2412.

48. **Böhme A.G.,** *Verwendung von hochmolekularen synthetischen Glucosiden als Saponinersatz, als Emulgierungs-, Reinigungs- und Netzmittel. 593422,* Deutschland, 1934.

49. **Harland, H., Y.** *Glucoside as plasticizers for water soluble animal and vegetable adhesives. 2422328,* USA, 1947.

50. **Ames, G., R.** Long-Chain derivates of monosaccharides and oligosaccharides. *Chem. Rev.* 1960, 60, 541-553.

51. **Drummond, C., J., Fong, C., Krodkiewski, I., Boyd, B., J. and Baker, I., J., A.** Sugar fatty acid esters. *Novel surfactants preparation, applications and biodegrability.* 2. Ed., New York , 2003, 114, 95-128.

52. **Parker, J., K., James, K. and Hurford, J.** Sucrose ester surfactants - a solventless process and the pruducts thereof. *ACS Symp. Ser.* 1977, 7, 97-114.

53. **Svensson, M. and Brinck, J.** Surfactants based on sterols and other alicyclic compounds. *Surfactant Sciences* New York , 2003, 217-239.

54. **Baade, St. and Mueller-Goymann, C., C.** Lidocaine and soyasterole-PEG-16-ether - investigations on the interaction between an amphiphilic drug and a nonionic surfactant in aqueous solution. *Colloid. Polym. Sci.* 1994, 272, 228-235.

55. **Folmer, B.** Fatty acid monoethanol amide ethoxylates. *Novel surfactants preparation, application and biodegrability.* 2. Ed., New York, 2003, 114, 241-256.

56. **Khan, A., Kaplun, A., Talmon, Y. and Hellsten, M.** Microstructural study of aqueous solutions of octadecylamide oligo(oxyethylene)ether. *J. Colloid Interface Sci.* 1996, 181, 191-199.

57. **Menger, F., M. and Littau, C., A.** Gemini surfactants: Synthesis and properties. *J. Am. Chem. Soc.* 1991, 131, 1451-1452.

58. **FitzGerald, P., A., Carr, M., W., Davey T., W., Serelis, A., K., Such C., H. and Warr, G., G.** Preparation and dilute solution properties of model gemini nonionic surfactants. *J. Colloid Interface Sci.* 2004, 275, 649-658.

59. **van Doren, H., A., Smity, E., Pestman, J., M., Engberts, J., B., F., N. and Kellog, R., M.** Mesogenic sugars. From aldoses to liquid crystals and surfactants. *Chem. Soc. Rev.* 2000, 29, 183-199.

60. **Johnsson, M., Wagenaar, A., Stuart, M., C., A., Engberts, J., B., F., N.** Sugar based gemini surfactants with pH dependent behavior: Vesicle to micelle transition, critical micelle concentration and vesicle surface charge reversal. *Langmuir* 2003, 19, 4609-4618.

61. **Johnsson, M. and Engberts, J., B., F., N.** Novel sugar based gemini surfactants: aggregation properties in aqueous solution. *J. Phys. Org. Chem.* 2004, 17, 934-944.

62. **Komorek, U. and Wilk, K. A.** Surface and micellar properties of new nonionic gemini aldonamide-type surfactants. *J. Colloid Interface Sci.* 2004, 271, 206-211.

63. **Yoshimura, T., Ishihara, K. and Esumi, K.** Sugar based gemini surfactants with peptide bonds - synthesis, adsorption, micellisation and biodegradability. *Langmuir* 2005, 21, 10409-10415.

64. **Paddon-Jones, G., Regismond S., Kwetkat, K. and Zana, R.** Micellisation of nonionic surfactant dimers and of the corresponding surfactant monomers in aqueous solution. *J. Colloid Interface Sci.* 2001, 243, 496-501.

65. **Smith, G., D.** Commercial surfactants: An overview. *Solution chemistry of surfactants.* New York , Plenum Press, 1979, 195-218.

66. **Holmberg, K., Jönsson, B., Kronberg, B. and Lindmann, B.** *Surfactants and polymers in aqueous solution.* 2. Ed., John Wiley & Sons, New York, 2002.

67. **Wang, X. and Rackaitis, M.** Geling nature of aluminium soaps in oils. *J. Colloid Interface Sci.* 2009, 331, 335-342.

68. **McRoberts, T., S. and Schulman, J., H.** Role of the hydroxyl group in the gealtion of aluminium soaps in hydrocarbons. *Nature* 1948, 162, 101-102.

69. **Glazer, J., Mc Roberts, T., S. and Schulman, J., H.** The preparation of a stable aluminium dodecanoate (laurate) with no geling properties in hydrocarbons. *Chem. Soc. Rev.* 1950, 2082-2083.

70. **Ludke, W., O., Wiberley, S., E., Goldenson, J. and Bauer, W., H.** Mechanism of peptization of aluminium soap-hydrocarbon gels based upon infrared studies. *J. Phys. Chem.* 1955, 59, 222-225.

71. **Kekicheff, P., C., Grabielle-Madelmont and Ollivon, M.** Phase diagram of sodium dodecyl sulfate-water system; 1. A calorimetric study. *J. Colloid Interface Sci.* 1989, 131, 112-132.

72. **Kekicheff, P.** Phase diagram of sodium dodecyl sufate-water system; 2. Complementary isoplethal and isothermal study phase studies. *J. Colloid Interface Sci.* 1989, 131, 133-152.

73. **Laughlin, R., G.** *The aqueous phase behavior of surfactants.* Academic Press, Waltham, 1994.

74. **Mukerjee, P. and Mysels, K., J.** Critical micelle concentrations of aqueous surfactant systems. *Nat. Stand. Ref. Data Ser. - Nat. Bur. Stand.* 1971, 36, 1-227.

75. **Yoshimura, T. and Esumi, K.** Synthesis and surface properties of anionic gemini surfactants with amide groups. *J. Colloid Interface Sci.* 2004, 276, 231-238.

76. **Evans, D., J., Allison, D., G., Brown, M., R., W. and Gilbert, P.** Effect of growth-rate on resistance of Gram-negative biofilms to cetrimide. *J. Antimicrob. Chemother.* 1990, 26, 473-478.

77. **Anderson, M., T., Martin J., E., Odinek. J., G. and Newcomer P., P.** Effect of methanol concentration on CTAB micellization and on the formation of surfactant-templated silica (STS). *Chem. Mater.* 1998, 10, 1490-1500.

78. **Krishnaswamy, R., Gosh, S., K., Lakshmanan, S., Raghunathan, V., A. and Sood, A., K.** Phase behavior of concentrated aqueous solutions of setyltrimethylammonium bromide (CTAB) and sodium hydroxy naphthoate (SHN). *Langmuir* 2005, 21, 10439-10443.

79. **Warr, G., G., Zemb, T., N. and Drifford, M.** Liquid-liquid phase separation in cationic micellar solutions. *J. Phys. Chem.* 1990, 94, 3086-3092.

80. **Chevalier, Y., Storet, Y., Pourchet, S. and Le Perchec, P.** Tensioactive properties of zwitterionic carboxybetaine amphiphiles. *Langmuir* 1991, 7, 848-853.

81. **Laughlin, R., G.** Fundamentals of the zwitterionic hydrophilic group. *Langmuir* 1991, 7, 842-847.

82. **Weers, J.,G., Rathman, J., F., Axe, F., U., Chrichlow, C., A., Foland, L., D., Scheuing, D., R., Wiersema, R., J. and Zielske, A., G.** Effect of the intramolecular charge separation distance on the solution properties of betaines and sulfobetaines. *Langmuir* 1991, 7, 854-867.

83. **Shinoda, K., Yamamata, K. and Knioshita, K.** Surface chemical properties in aqueous solutions of nonionic surfactants: Octyl glycol ether, alpha-octyl glycerol ether and octyl glucoside. *J. Phys. Chem.* 1959, 63, 648-650.

84. **Kahlweit, M., Lessner, E. and Strey, R.** Influence of the properties of the oil and the surfactant on the phase behavior of systems of the type H_2O-oil-nonionic surfactant. *J. Phys. Chem.* 1983, 87, 5032-5040.

85. **Brown, W., Pu, Z. and Rymden, R.** Size and shape of nonionic amphiphile micelles: NMR and self diffusion and static quasi-elastic light-scattering measurements $C_{12}E_5$, $C_{12}E_7$, $C_{12}E_8$ in aqueous solution. *J. Phys. Chem.* 1988, 92, 6086-6094.

86. **Kahlweit, M., Strey, R., Firman, P., Haase, D. and Schomäcker, R.** General patterns of the phase behavior of mixtures of H_2O nonpolar solvents, amphiphiles and electrolytes 1. *Langmuir* 1988, 4, 499-511.

87. **Kato, T., Anzai, S. and Seimiya, T.** Light scattering from semi dilute solutions of nonionic surfactants $C_{12}E_5$ and $C_{12}E_8$ and the scaling law. *J. Phys. Chem.* 1990, 94, 7255-7259.

88. **Murthy, A., K.** Aqueous and nonaqueous microemulsions with high molecular weight alkenes. *Coll. Poly. Sci.* 1993, 271, 209-216.

89. **Bossev, D., P., Kline, S., R., Israelachvili, J., N. and Paulaitis, M., E.** Pressure-induced freezing of the hydrophobic core leads to a L_1, H_1 phase transition for $C_{12}E_5$ micelles in D_2O. *Langmuir* 2001, 17, 7728-7731.

90. **Mitchell, D., J., Tiddy, G., J., T., Waring, L., Bostock, T. and McDonald, M., P.** Phase behaviour of polyoxyethylene surfactants with water. *J. Chem. Soc. Farady Trans. 1.* 1983, 79, 975-1000.

91. **Fujimatsu, H., Ogasawara, S. and Kuroiwa, S.** Lower critical solution temperature (LCST) and theta temperature of aqueous solutions of nonionic surface active agents of various polyoxyethylene chain lengths. *Coll. Polym. Sci.* 1988, 266, 594-600.

92. **Yamazaki, R., Iizuka, K., Hiraoka, K. and Nose, T.** Phase behavior and mechanical properties of mixed poly(ethylene glycol) mono-dodecyl ether aqueous solutions. *Macromol. Chem. Phys.* 2005, 206, 439-447.

93. **Dong, R. and Hao, J.** Complex fluids of poly(oxyethylene) monoalkyl ether nonionic surfactants. *Chem. Rev.* 2010, 110, 4978-5022.

94. **Puvvada, S. and Blankschtein, D.** Molecular-thermodynamic approach to predict micellization, phase bahvior and phase separation of micellar solutions. I. Application to noionic surfactants. *J. Chem. Phys.* 1989, 92, 3710-3724.

95. **Nagarajan, R. and Ruckenstein, E.** Theory of surfactant self-assembly: A predictive molecular thermodynamic approach. *Langmuir* 1991, 7, 2934-2969.

96. **Lang, J., C. and Morgan, R., D.** Nonionic surfactant mixtures I. Phase equilibria in $C_{10}E_4$-H_2O and closed loop coexistence. *J. Chem. Phys.* 1980, 73, 5849-5861.

97. **Zheng, L., Suzuki, M. and Inoue, T.** Phase behavior of an aqueous mixture of octaethylene glycol dodecyl ether revealed by DSC, FT-IR and 13C NMR measurements. *Langmuir* 2002, 18, 1991-1998.

98. **Israelachvili, J., N., Mitchell, D., J. and Ninham, B., W.** Theory of self-assembly of hydrocarbon amphiphiles into micelles and bilayers. *J. Chem. Soc. Faraday Trans. 2.* 1976, 72, 1525-1568.

99. **Zheng, L., Suzuki, M., Inoue, T. and Lindman, B.** Aqueous phase behavior of hexaethylene glycol dodecyl ether studied by differential scanning calorimetry, Fourier transform infrared spectoscopy and 13C NMR spectoscopy. *Langmuir* 2002, 18, 9204-9210.

100. **Naegeli, C.** Theorie der Gärung. Ein Beitrag zur Molecularphysiologie. *Oldenburg*, München, 1879.

101. **Zsigmondy, R. and Bachmann, W.** Über Gallerten. *Kolloid-Z.* 1912, 11, 145-157.

102. **Laing, M., E. and McBain, J., W.** The investigation of sodium oleate solutions in the three physical states of curd, gel and sol. *J. Chem. Soc. Trans.* 1920, 117, 1506-1528.

103. **Davies, D., G. and Bury, C., R.** Partial specific volume of potassium n-octoate in aqueous solution. *J. Chem. Soc.* 1930, 2263-2267.

104. **Lawrence, A., S., C.** Soap micelles. *Trans. Faraday. Soc.* 1935, 31, 189-195.

105. **Hoar, T., P. and Schulman, J., H.** Transparent water in oil dispersions: The olephatic hydro micelle. *Nature* 1943, 152, 102-103.

106. **Preston, W., C.** Some correlating principles of deteregent action. *J. Phys. Chem.* 1948, 52, 84-97.

107. **Ginn, M., E. and Harris, J., C.** Correlation between critical micelle concentration and fatty soil removal. *J. Am. Oil Chem. Soc.* 1961, 38, 605-609.

108. **Tanford, C.** *The hydrophobic effect.* Wiley and Sons, New York, 1980.

109. **Ruckenstein, E.** Thermodynamically stable dispersions: Micellisation, solubilistaion and microemulsions. *Annals New York Academy of Science.* 1983, 404, 224-246.

110. **Kahlweit, M., Strey, R. and Busse, G.** Microemulsions: A qualitative thermodynamic approach. *J. Phys. Chem.* 1990, 94, 3881-3894.

111. **Ramadan, M., S., Evans, F., D. and Lumry, R.** Why micelles form in water and hydrazine: A reexamination of the origin of hydrophobicicty. *J. Phys. Chem.* 1983, 87, 4538-4543.

112. **Evans, F., D., Yamauchi, A., Wel, G., J. and Bloomfield, V., A.** Micelle size in ethylammonium nitrate as determined by classical and quasi elastic light scattering. *J. Phys. Chem.* 1983, 87, 3534-3537.

113. **Rico, I. and Lattes, A.** Formamide a water substitute. 12. Krafft temperature and micelle formation of ionic surfactants in formamide. *J. Phys. Chem.* 1986, 90, 5870-5872.

114. **Garibri, H., Palepu, R., Tiddy, G, J., T., Hall, D., G., G. and Wyn-Jones, E.** The use of surfactant selective electrodes in non aqueous solvents. *J. Chem. Soc. Chem. Commun.* 1990, 1990, 115-116.

115. **Rudolph, E., S., J., Langeveld, J., H., de Loos, T., W. and de Swaan Arons, J.** Phase behaviour of water+nonionic surfactant systems: experiments and modelling applying the Peng–Robinson equation of state with the Wong–Sandler mixing rules and the UNIQUAC gE-model. *Fluid Phase Equilib.* 2000, 173, 81-96.

116. **Garcia-Lisbona, M., N., Galindo, A., Jackson, G. and Burgess, A., N.** An examination of the cloud point curves of liquid-liquid immiscibility in aqueous solutions of alkyl polyoxyethylene surfactants using the SAFT-HS approach with transferable parameters. *J. Am. Chem. Soc.* 1998, 120, 4191-4199.

117. **Browarzik, C. and Browarzik, D.** Liquid–liquid equilibrium calculation in binary water + nonionic surfactant C_iE_j systems with a new mass-action law model based on continuous thermodynamics. *Fluid Phase Equilib.* 2005, 235, 127-138.

118. **Tanford, C.** Theory of micelle formation in aqueous solution. *J. Phys. Chem.* 1974, 78, 2469-2479.

119. **Ruckenstein, E. and Nagarajan, R.** Critical micelle concentration and the transition point for micellar size distribution. *J. Phys. Chem.* 1981, 85, 3010-3014.

120. **Nagarajan, R. and Ruckenstein, E.** Relation between the transition point in micellar size distribution, the CMC, and the cooperativity of micellization. *J. Colloid Int. Sci.* 1983, 91, 500-506.

121. **Puvvada, S. and Blankschtein, D.** Molecular-thermodynamic approach to predict micellisation, phase behavior and phase separation of micellar solutions. I Application to nonionic surfactants. *J. Chem. Phys.* 1990, 92, 3710-3724.

122. **Enders, S. and Häntzschel, D.** Thermodynamics of aqueous carbohydrate surfactant solutions. *Fluid Phase Equilib.* 1998, 153, 1-21.

123. **Blankschtein, D., Thurston, G., M. and Benedeck, G., B.** Theory of phase separation in micellar solutions. *Phys. Rev. Lett.* 1985, 54, 955-958.

124. **Nagarajan, R.** Modelling solution entropy in the theory of micellisation. *Colloids and Surfaces A.* 1993, 71, 39-64.

125. **Corkill, J., M., Goodman, J., F., Walker, T. and Wyer, J.** The multiple equilibrium model of micelle formation. *Proc. R. Soc. Ser. .* 1969, 312, 243-255.

126. **Mukerjee, P.** The size distribution of small and large micelles. *J. Phys. Chem.* 1972, 76, 565-570.

127. **Ueno, M., Takasawa, Y., Miyashige, H., Tabata, Y. and Meguro, K.** Effects of alkyl chain length on surface and micellar properties of octaethyleneglycol-n alkyl ethers. *Coll. Poly. Sci.* 1981, 259, 761-766.

128. **Chen, L.-J., Lin, S.-Y. and Huang, C.-C-.** Effect of hydrophobic chain length of surfactants on enthalpy-entropy compensation of micellisation. *J. Phys. Chem. B* 1998, 102, 4350–4356.

129. **Chen, L.-J., Lin, S.-Y., Huang, C.-C. and Chen, E.-M.** Temperature dependence of critical micelle concentration of polyoxyethylenated non-ionic surfactants. *Coll. and Surf. A* 1998, 135, 175-181.

130. **de Mul, M., N., G., Davis, H., T., Evans, D., F., Bhave, A., V. and Wagner, J., R.** Solution phase bahvior and solid phase structure of long chain sodium soaps mixtures. *Langmuir* 2000, 16, 8276-8284.

131. **Raut, J., S., Naik, V., M.; S., Singhal and Juvekar, V., A**. Soap: the polymorphic genie of hierarchically structured soft condensed-matter products. *Ind. Eng. Chem. Res.* 2008, 47, 6347-6353.

132. **Klein, R., Dutton, H., Diat, O., Tiddy, G., J., T. and Kunz, W.** Thermotropic phase behavior of choline soaps. *J. Phys. Chem. B* 2011, 115, 3838-3847.

133. **Dörfler, H., D. and Hieke, A.** Influence of the chain length of K-soaps on the phase diagram and structural parameters of nonaqueous liquid crystals and the gel phase in K-soap/glycerol binary systems. *Coll. Poly. Sci.* 2000, 278, 90-95.

134. **Nagarajan, R. and Ruckenstein, E.** Molecular theory of microemulsions. *Langmuir* 2000, 16, 6400-6415.

135. **Winsor, P. A.** Hydrotropy, solubilisation and related emulsification processes. Part I. *Trans. Faraday Soc.* 1948, 44, 376-398.

136. **Friberg, S.** Microemulsions, hydrotropic solutions and emulsions - a question of phase equilibria. *J. Amer. Oil. Chem. Soc.* 1971, 48, 578-581.

137. **Kahlweit, M., Strey, R., Haase, D. and Firman, P.** Properties of the three phase bodies in the H_2O-oil-nonionic surfactant amphiphile mixtures. *Langmuir* 1988, 4, 785-790.

138. **Sassen, C., L., Filemon, L., M., de Loos, T., W. and de Swaan Arons, J.** Influence of pressure and eletrolyte on the phase behavior of water+oil+nonionic surfactant systems. *J. Phys. Chem.* 1989, 93, 6511-6516.

139. **Bonkhoff, K., Hirtz, A. and Findenegg, G. H.** Interfacial tensions in the three phase region of nonionic surfactant+water+alkane systems: Critical cloud point effects an aggregation behavior. *Physica A* 1991, 172, 174-199.

140. **Aveyard, R., Binks, B., P., Fletcher, P., D., I. and Ye, X.** Solubilisation of water in alkanes using nonionic surfactants. *J. Chem. Biotechnol.* 1992, 54, 231-236.

141. **McFann, G., J. and Johnston, K., P.** Phase behavior of nonionic surfactant/oil/water system containing light alkanes. *Langmuir* 1993, 9, 1942-1948.

142. **Bagger-Jörgensen, H., Olsson, U. and Iliopoulos, I.** Phase behavior of nonionic microemlsion upon additon of hydrophobically modiefied polyelectrolyte. *Langmuir* 1995, 11, 1934-1941.

143. **Rudolph, E., S., J., Bovendeert M., J., de Loos, T., W. and de Swaan Arons, J.** Influence of methane on the phase behavior of oil+water+nonionic surfactants systems. *J. Phys. Chem. B* 1998, 102, 200-205.

144. **Salager, J., L., Anton, R., E., Sabatini, D., A., Harwell, J., H., Acosta, E., J. and Tolosa, L., I.** Enhancing solubilisation in microemulsions - state of the art and current trends. *J. Surf. Deterg.* 2005, 8, 3-21.

145. **Nave, S., Testard, F., Coulombeau, H., Baczko, K., Larpent, C. and Zemb, T.** Ternary phase diagram of thermoreversible chelating nonionic surfactant. *Phys. Chem. Chem. Phys.* 2009, 11, 2700-2707.

146. **Sörensen, J. M. and Arlt, W.** *Liquid-liquid equilibrium data collection.* Dechema, 1979. Vol. 5.

147. **Griffiths, R., B.** Thermodynamic model for tricritical points in ternary and quaternary fluid mixtures. *J. Chem. Phys.* 1974, 60, 195-206.

148. **Kohnstamm, P.** Thermodynamik der Gemische. Springer, Berlin, 1926, 223-274.

149. **Kahlweit, M., Leßner, E. and Strey, R.** Über das Phasenverhalten ternärer Systeme des Typs H_20 - Öl - nichtionisches Tensid. *Coll. Poly. Sci.* 1983, 261, 954-964.

150. **Kahlweit, M., Strey, R., Haase, D., Kunieda, H., Scmeling, T., Faulhaber, B., Borkovec, M., Eicke, H.-F., Busse, G., Eggers, F., Funck, T., H., Richmann, H., Magid, L., Söderman, O., Stilbs, P., Winkler, J., Dittrich, A. and Jahn, W.** How to study microemulsions. *J. Coll. Interf. Sci.* 1987, 118, 436-453.

151. **Sottmann, T. and Strey, R.** Evidence of corresponding states in ternary microemulsions of water-alkane-C_iE_j. *J. Phys. Condens. Matter.* 1996, 8, A39-A48.

152. **Nowothnik, H., Blum, J. and Schomäcker, R.** Suzuki-Kupplung in dreiphasigen Mikroemulsionssystemen. *Angew. Chem.* 2011, 123, 1959-1962.

153. **Müller, M., Kasaka, Y., Müller, D., Schomäcker, R. and Wozny, G.** Process design for the separation of three liquid phases for a continuous hydroformylation process in a miniplant scale. *Ind. Eng. Chem. Res.* 2013, 52, 7259-7264.

154. **Miyagawa, C., C., Kupka, J. and Schumpe, A.** Rhodium catalyzed hydroformylation of 1-octene in micro emulsions and micellar media. *J. Mol.Catalys.* . 2005, 234, 9-17.

155. **Lang, J., C. and Widom, B.** Equilibrium of three liquid phases and approach to the tricritical point in benzene-ethanol-water-ammonium sulfane mixtures. *Physica A* 1975, 81, 190-213.

156. **Vulfson, E., N.** Enzymatic synthesis of surfactants, surfactants in lipid industry. *Royal Chem. Soc.* 1992, 118, 16-37.

157. **Asmer, H., J., Lang, S., Wagner, F. and Wray, V.** Microbial production, structure, elucidation, and bioconversation of sophrose lipids. *J. Am. Oil Chem. Soc.* 1988, 65, 1460-1466.

158. **Uchida, Y., Misawa, S., Nakhara, T. and Tabuchi, T.** Factors affecting the production of succinoyl trehalose lipids by rhodococcus erythroplis SD-74 grown on n-alkanes. *Agric. Biol. Chem.* 1989, 53, 765-769.

159. **Behler, A., Biermann, M., Hill, K., Raths, H., C., Saint Victor, M., E. and Uphues, G.** *Industrial surfactant synthesis.* New York , Marcel Dekker, 2001.

160. **Kosswig, K.** Aspekte der Tensidsynthese - heute. *Tenside Surf. Det.* 2001, 34, 417-422.

161. **Corkill, J., M., Goodman, J., F. and Ottewill, R., H.** Micellisation of homogenous nonionic detergents. *Trans. Faraday Soc.* 1961, 57, 1627-1636.

162. **Flory, P., J.** Molecular size distribution in ethylene oxide polymers. *J. Amer. Chem. Soc.* 1940, 62, 1561-1565.

163. **Santacesaria, E., Di Serio, M., Graffa, R. and Addino, G.** Kinetics and mechanism of fatty alcohol polyoxylation. 2. Narrow-range ethoxylation obtained with barium catalyst. *Ind. Eng. Chem. Res.* 1992, 31, 2419-2421.

164. **Santacesaria, E., Di Serio, M., Graffa, R. and Addino, G.** Kinetics and mechanism of fatty alkohol polyoxylation. 1. The reaction catalysed by potassium hydroxid. *Ind. Eng. Chem. Res.* 1992, 31, 2413-2418.

165. **Di Serio, M., Tesser, R. and Dimiccoli, A.** Kinetics of ethoxylation and propoxylation of ethylene gycol catalyzed by KOH. *Ind. Eng. Chem. Res.* 2002, 41, 5196-5206.

166. **Schubert, K.-V., Strey, R. and Kahlweit, M.** A new purification technique for alky polyglycol ethers and miscibility gaps for water-C_iE_j. *J. Colloid Interface Sci.* 1991, 141, 21-29.

167. **Lunkenheimer, K., Pergande, H.-J. and Krüger, H.** Apparatus for programmed high performance purification of surfactant solutions. *Rev. Sci. Instrum.* 1987, 58, 2313-2316.

168. **Corkill, J., M., Goodman, J., F. and Harrold, S., P.** Thermodynamics of micellisation of nonionic detergents. *Trans. Faraday Soc.* 1963, 60, 202-207.

169. **Rosen, M., J.** Purifications of surfactants for studies of their fundamental surface properties. *J. Colloid Interface Sci.* 1981, 79, 587-588.

170. **Meguro, K., Takasawa, Y., Kawahashi, N., Tabata, Y. and Ueno, M.** Micellar properties of a series of octaethyleneglycol-n-alkyl ethers with homogenous ethylene oxide chain and their temperature dependence. *J. Colloid Interface Sci.* 1981, 83, 50-56.

171. **Stubenrauch, C., Schlarmann, J., Sottmann, T. and Strey, R.** Purification of nonionic alkyl polyglycolether C_iE_j surfactants: The inverse 3PHEX technique. *J. Colloide Interface Sci.* 2001, 244, 447-449.

172. **Fujimatsu, H., Takagi, K., Matsuda, H. and Kuroiwa, S.** Temperature dependences of micellar molecular weight and radius of nonionic surface active agent in aqueous solution. *J. Colloid Interface Sci.* 1983, 94, 237-242.

173. **Carrol, B., J.** Purification of surfactants by solid adsorbens. *J. Colloid Interface Sci.* 1982, 86, 586.

174. **Carroll, B., J. and Haydon, D., A.** Electrokinetic and surface potential at liquid interface. *J. Chem. Soc., Faraday Trans. I.* 1975, 71, 361-377.

175. **Sigma Aldrich.** *Cetrificate of analysis.* Quality control. 2011, 1, Certificate of analysis.

176. **Morawetz, H.** Catalysis and inhibition in solutions of synthetic polymers and in micellar solutions. *Adv. Catalys.* 1969, 20, 341-371.

177. **Casalnuovo, A., L. and Calabrese, J., C.** Palladium-catalyzed alkylations in aqueous media. *J. Am. Chem. Soc.* 1990, 112, 4324-4330.

178. **Holmberg, K.** Organic reactions in mcroemulsions. *Eur. J. Org. Chem.* 2007, 2007, 731-742.

179. **Van Vyve, F. and Renken, A.** Hydroformylation in reverse micellar systems. *Catal. Today.* 1999, 48, 237-243.

180. **Tselikovsky, D. and Blum, J.** three phase microemulsion/sol-gel system for aqueous C-C coupling of hydrophobic substrates. *Eur. J. Org. Chem.* 2008, 2008, 2417-2422.

181. **Kuo, P.-L., Turro, N.; J., Tseng, C.-M., El-Asser, M., S. and Vanderhoff, J., W.** Photoinitiated polymerisation of styrene in microemulsions. *Macromolecules* 1987, 20, 1216-1221.

182. **Schomäcker, R.** Mikroemulsionen als Medium für chemische Reaktionen. *Nachr. Chem. Tech. Lab.* 1992, 40, 1377-1352.

183. **Pospech, J., Fleischer, I., Franke, R., Buchholz, S. and Beller, M.** Alternative metals for homogeneous catalyzed hydroformylation reactions. *Angew. Chem. Int. Ed.* 2012, 52, 2852-2872.

184. **Smith, D., F., Hawk, C., O. and Golden, P., L.** The mechanism of the formation of higher hydrocarbons from water gas. *J. Am. Chem. Soc.* 1930, 52, 3221-3232.

185. **Roelen, O.** The discovery of the synthesis of aldehydes from olefines, carbon monoxide and hydrogen - a contribution to the psychology of scientific research. *ChED Chem: Exp. Didakt.* 1977, 3, 119-124.

186. **Roelen, O.** Pat.Nr. *849548,* Deutschland, 1938.

187. **Beller, M., Cornils, B., Frohning, C., D. and Kohlpaintner, C., W.** Progress in hydroformylation and carbonylation. *J. Mol. Catal. A.* 1995, 104, 17-85.

188. **Heck, R., F. and Breslow, D., S.** The reaction of co-tetracarbonyl with olefines. *J. Am. Chem. Soc.* 1961, 83, 4023-4027.

189. **Brunsch, Y. and Behr, A.** Temperaturgesteuertes Katalysatorrecycling in der homogenen Übergangsmetallkatalyse: Minimierung des Katalysatorleachings. *Angew. Chem.* 2013, 125, 1627-1631.

190. **Li, C., Guo, L. and Garland, M.** Homogeneous hydroformylation of ethylene catalyzed by $Rh_4(CO)_{12}$. The application of BTEM to identify a new class of Rh carbonyl spectra: $RhCORh(CO)_3$(pi-C_2H_4). *Organometallics* 2004, 23, 2201-2204.

191. **Tricas, H., Diebolt, O. and van Leeuwen, P., W., N., M.** Bulky monophosphite ligands for ethene hydroformylation. *J. Catalys.* 2013, 298, 198-205.

192. **Tucci, E., R.** Hydroformylating terminal olefines. *Ind. Eng. Chem. Prod. Res. Develop.* 1970, 9, 516-521.

193. **Cornils, B. and Förster, I.** Vorgänge bei der Umsetzung von Kobaltcarbnoly oder kobalthydrocarbonyal mit Wasser. *Chem. Ztg.* 1973, 7, 374-377.

194. **Tucci, E., R.** Oxo product composition from bimetallic chromium cobalt catalysts. *Ind. Eng. Chem. Prod. Res. Dev.* 1986, 25, 27-30.

195. **Markert, J., Brunsch, Y., Munkelt, T., Kiedorf, G., Behr, A., Hamel, C. and Seidel-Morgenstern, A.** Analysis of the reaction network for the Rh-catalyzed hydroformylation of 1-dodecene in a thermomorphic multicomponent system. *Appl. Catalys. A* 2013, 462-463, 287-295.

196. **Mitsudo, T. and Konodo, T.** Ruthenium-catalyzed reactions with CO and CO_2. *Ruthenium in organic synthesis.* Wiley and Sons, New York, 2005, 277-305.

197. **Boymans, E., Janssen, M., Müller, C., Lutz, M. and Vogt, D.** Rh-catalyzed linear hydroformylation of styrene. *Dalton Trans.* 2013, 42, 137-142.

198. **Nelsen, E., R. and Landis, C., R.** Interception and characterisation of alkyl and acyl complexes in Rh-catalyzed hydroformylation of styrene. *J. Am. Chem. Soc.* 2013, 135, 9636-9639.

199. **Zheng, C., Mo, M., Liang, H., Zheng, X., Fu, H., Yuan, M., Li, R. and Chen, H.** Rhodium /bisphosphite catalytic system for hydroformylation of styrene and its derivatives. *Appl. Organomet. Chem.* 2013, 27, 474-478.

200. **Agbossou, F., Carpentier, J., F. and Mortreux, A.** Asymmetric hydroformylation. *Chem. Rev.* 1995, 95, 2485-2506.

201. **van Leeuwen, P., W., N., M., Kamer, P., C., Claver, C., Pamies, O. and Dieguez, M.** Phosphite-containing ligands for asymmetric catalysis. *Chem. Rev.* 2011, 111, 2077-2118.

202. **MacDougall, J., K. and Cole-Hamilton, D., J.** Direct formation of alcohols in homogenous hydroformylation catalysed by Rh complexes. *J. Chem. Soc, Chem. Commun.* 1990, 1990, 165-167.

203. **Ichihara, T., Nakano, K., Katayama, M. and Nozaki, K.** Tandem hydroformylation-hydrogenation of 1-dodecene catalyzed by Rh-bidentate bis(trialkylphosphine)s. *Chem. Asian J.* 2008, 3, 1722-1728.

204. **Pergola, R., D., Cinquantini, A., Diana, E., Garlaschelli, L., Laschi, F., Luzzini, P., Manassero, M., Repossi, A., Sansoni, M., Stanghellini, P., L. and Zanello, P.** Iron-Rhodium and Iron-Iridium mixed-metal Nitrido-Carbonyl clusters. Synthesis,characterization, redox properties, and solid-state structure of the octahedral clusters $[Fe_5RhN(CO)_{15}]^{2-}$, $[Fe_5IrN(CO)_{15}]^{2-}$, and $[Fe_4Rh_2N(CO)_{15}]^{-}$. *Inorg. Chem.* 1997, 36, 3761-3771.

205. **Horvath, I., T., Garland, M., Bor, G. and Pino, P.** Low temperature activation of molecular hydrogen in CO/H_2 mixtures in the presence of $CoRh(CO)_7$. *J. Organomet. Chem.* 1988, 358, C17-C22.

206. **Dümbgen, G. and Neubauer, D.** Großtechnische Herstellung von Oxo-Alkoholen bei der BASF. *Chem. Ing. Tech.* 1969, 41, 974-980.

207. **Evans, D., Osborn, J., A. and Wilkinson, G.** Hydroformylation of alkenes by use of rhodium complex catalysts. *J. Chem. Soc. A* 1968, 1968, 3133-3142.

208. **Cornils, B. and Kuntz, E., G.** Introducing TPPTS and realted ligands for industrial biphasic processes. *J. Organomet. Chem.* 1995, 502, 177-186.

209. **Cornils, B.** Industrial aqueous biphasic catalytsis: Status and directions. *Org. Process Res. Dev.* 1998, 2, 121-127.

210. **Behr, A., Brunsch, Y. and Lux, A.** Rhodium nanoparticles as catalysts in the hydroformylation of 1-dodecene and their recycling in termomorphic solvent systems. *Tetrahedron Lett.* 2012, 53, 2680-2683.

211. **Schäfer, E.; Brunsch, Y.; Sadowski, G.; Behr, A.** Hydroformylation of 1-dodecene in the thermomorphic solvent system dimethylformamide/decane. Phase behavior-reaction performance-catalyst recycling. *Ind. Eng. Chem. Res.* 2013, 51, 10296-10306.

212. **Andreetta, A., Barberis, G. and Gregorio, G.** Recovery and recycle of rhodium and cobalt complexes containing ligands with both phosphorus and nitrogen atoms. *Chim. Ind. Milano* 1978, 60, 887-892.

213. **Wiebus, E. and Cornils, B.** Die großtechnische Oxosynthese mit immobilisiertem Katalysator. *Chem. Ing. Tech.* 1994, 66, 916-923.

214. **Kohlpaintner, C., W., Fischer, R., W. and Cornils, B.** Aqueous biphasic catalysis: Ruhrchemie/Rhone-pulenc oxo process. *Appl. Catalys. A* 2001, 221, 219-225.

215. **Nowothnik, H., Rost, A., Hamerla, T., Schomäcker, R., Müller, C. and Vogt, D.** Comparison of phase transfer agents in the aqueous biphasic hydroformylation of higher alkenes. *Catal. Sci. Technol.* 2013, 3, 600-605.

216. **Hamerla, T., Rost, A., Kasaka, Y. and Schomäcker, R.** Hydroformylation of 1-dodecene with water soluble rhodium catalysts with bidentate ligands in multiphase systems. *ChemCatChem.* 2013, 5, 1854-1862.

217. **Casey, C., P., Paulsen, E., L., Beuttenmueller, E., W., Proft, B., R., Matter, B., A. and Powell, D., R.** Electronically dissymmetric DIPHOS derivatives give higher n:i regioselectivity in rhodium-catalyzed hydroformylation than either of their symmetric counterparts. *J. Am. Chem. Soc.* 1999, 121, 63-70.

218. **Piras, I., Jennerjahn, R., Jackstell, R., Spannenberg, A., Franke, R. and Beller, M.** A general and efficient iridium-catalyzed hydroformylation of olefines. *Angew. Chem.* 2011, 123, 294-298.

219. **Evans, D., Osborn, J., A., Jardine, A. and Wilkinson, G.** Homogeneous hydrogenation and hydroformylation using ruthenium complexes. *Nature* 1965, 208, 1203-1204.

220. **Schulz, H., F. and Bellestedt, F.** Hydroformylation of propene with Ruthenium catalysts. *Ind. Eng. Chem. Prod. Res. Dev.* 1973, 3, 176-183.

221. **Drent, E. and Budelzaar, P., H., M.** The oxo-synthesis catalyzed by cationic palladium complexes, selectivity control by neutral ligand and anion. *J. Organomet. Chem.* 2000, 593-594, 211-225.

222. **Slaugh, L., H. and Mullineaux, R., D.** *Hydroformylation of Olefines. 3239571,* USA, 1966.

223. **Wilkinson, G.** *Katalytische Verfahren. 1518236,* Deutschland, 1966.

224. **Protzmann, G. and Wiese, K.-D.** Status and future aspects of industrial hydroformylation. *Erdöl, Erdgas, Kohle* 2001, 117, 235-240.

225. **Cornils, B., Herrmann, A. and Rasch, M.** Otto Roelen, pioneer in industrial homogeneous catalysis. *Angew. Chem. Int. Ed.* 1994, 33, 2144-2163.

226. **Hamerla, T., Paul, N., Kraume, M. and Schomäcker, R.** Aufklärung der Stofftransportwege in mizellaren Merphasenreaktoren am Beispiel der Hydroformylierung. *Chem. Ing. Tech.* 2013, 85, 1-11.

227. **Wachsen, O., Himmler, K. and Cornils, B.** Aqueous biphasic catalysis: Where the reaction takes place. *Catal. Today.* 1998, 42, 373-379.

228. **Obrecht, L., Kamer, P, L. and Wouter, L.** Alternative approaches for aqueous-organic-biphasic hydroformylation of higher alkenes. *Catal. Sci. Technol.* 2013, 3, 541-551.

229. **Behr, A., Turkowski, B., Roll, R., Schöbel, R. and Henze, G.** Multiphase catalysis in temperature-dependent multi component solvent (TMS) systems. *Top. Organomet. Chem.* 2008, 23, 19-52.

230. **Baiker, A.** Supercritical fluids in heterogeneous catalysis. *Chem. Rev.* 1999, 99, 453-473.

231. **Schneider, M., J., Lijewski, M., Woelfel, R., Haumann, M. and Wasserscheid, P.** Continuous gas-phase hydroaminomethylation using supported ionic liquid phase catalysts. *Angew. Chem. Int. Ed.* 2013, 52, 6996-6999.

232. **Menger, F., M., Donohue, J., A. and Williams, R., F.** Catalysis in water pools. *J. Am. Chem. Soc.* 1973, 95, 286-288.

233. **Martin, C., A., Golich, T., G. and Jaeger, D., A.** Design of microemulsions based on "destructible" surfactants for use in organic sysnthesis. *J. Coll. Interf. Sci.* 1983, 99, 561-567.

234. **Fell, B., Schobben, C. and Papagodianakis, G.** Hydroformylierung homologer Alkencarbonsäureester mit wasserlöslichen Rhodiumcarbonyl/tert. Phosphankomplexkatalysatoren. *J. Mol. Catalys. A* 1995, 101, 179-186.

235. **Schwuger, M., J., Stickdorn, K. and Schomäcker, R.** Microemulsions in technical processes. *Chem. Rev.* 1995, 95, 849-864.

236. **Garcia-Rio, L., Leis, J., R., Mejuto, J., C. and Perez-Lorenzo, M.** Microemulsions as microreactors in physical organic chemistry. *Pure Appl. Chem.* 2007, 79, 1111-1123.

237. **van Vyve, F. and Renken, A.** Hydroformylation in reverse micallar systems. *Catalys. Today.* 1999, 48, 237-243.

238. **Tjandra, D., Lade, M., Wagner, O. and Schomäcker, R.** The kinetics of an interfacial reaction in a microemulsion. *Chem. Eng. Technol.* 1998, 21, 666-670.

239. **Behr, A. and Toslu, N.** Einphasige und zweiphasige Reaktionsführung in der Hydrolysierungsreaktion. *Chem. Ing. Tech.* 1999, 71, 490-493.

240. **Behr, A. and Fängewisch, C.** Rhodium-catalysed synthesis of branched fatty compounds in temperature-dependent solvent systems. *J. Mol. Catal. A* 2003, 197, 115-126.

241. **Behr, A,; Henze, G., Johnen, L. and Awungacha, C.** Advances in thermomorphic liquid/liquid recycling of homogeneous transition metal catalysts. *J. Mol. Catal. A* 2008, 285, 2028.

242. **Behr, A., Henze, G. and Schomäcker, R.** Thermoregulated liquid/liquid catalyst separation and recycling. *Adv. Synth. Catal.* 2006, 348, 1485-1495.

243. **Behr, A., Turkowski, B., Roll, R., Schöbel, R. and Henze, G.** Multiphase catalysis in temperature-dependent multi-component solvent systems. *Top. Organomet. Chem.* 2008, 23, 19-52.

244. **Behr, A., Vorholt, A., J. and Rentmeister, N.** Recyclable homogeneous catalyst for the hydroesterification of methyl oleate in thermomorphic solvent systems. *Chem. Eng. Sci.* 2013, 99, 38-43.

245. **Kiedorf, G., Hoang, D., M., Müller, A., Jörke, A., Markert, J., Arellano-Garcia, H., Seidel-Morgenstern, A. and Hamel, C.** Kinetics of 1-dodecene hydroformylation in a thermomorphic solvent

system using a rhodium-biphephos catalyst. *Chem. Eng. Sci.* 2013, in press, DOI: 10.1016/j.ces.2013.06.027.

246. **Riisager, A., Wasserscheid, P., van Hal, R. and Fehrmann, R.** Continous fixed-bed gas-phase hydroformylation using supported ionic liquid-phase (SILP) Rh catalysts. *J. Catalys.* 2003, 219, 452-455.

247. **Riisager, A., Fehrmann, R., Haumann, M., Gorle, B., S., K. and Wasserscheid, P.** Stability and kinetic studies of supported ionic liquid phase catalysts for hydroformylation of propene. *Ind. Eng. Chem. Res.* 2005, 44, 9853-9859.

248. **Haumann, M., Dentler, K., Joni, J., Riisager, A. and Wasserscheid, P.** Contious gas-phase hydroformylation of 1-butene using supported ionic liquid phase (SILP) catalysts. *Adv. Synth. Catal.* 2007, 349, 425-431.

249. **Haumann, M., Jakuttis, M., Werner, S. and Wasserscheid, P.** Supported ionic liquid phase (SILP) catalyzed hydroformylation of 1-butene in a gradient-free loop reactor. *J. Catalys.* 2009, 263, 321-327.

250. **Haumann, M., Jakuttis, M., Franke, R., Schönweiz, A. and Wasserscheid, P.** Contious gas-phase hydroformylation of a higly diluted technical C_4 feed using supported ionic liquid phase catalysts. *ChemCatChem.* 2011, 3, 1822-1827.

251. **Jakuttis, M., Schönweiz, A., Werner, S., Franke, R., Wiese, K.-D, Haumann, M. and Wasserscheid, P.** Rhodium-phosphite SILP catalysis for the highly selective hydroformylation of mixed C_4 feedstocks. *Angew. Chem. Int. Ed.* 2011, 50, 4492-4495.

252. **Sellin, M., F., Webb, P., B. and Cole-Hamilton, D., J.** Continous flow homogenous catalysis: hydroformylation of alkenes in supercritical fluid-ionic liquid biphasic mixtures. *Chem. Comm.* 2001, 2001, 781-782.

253. **Webb, P., B., Kunene, T., E. and Cole-Hamilton, D., J.** Continous flow hydroformylation of alkenes in supercritical fluid-ionic liquid biphasic systems. *J. Am. Chem. Soc.* 2003, 125, 15577-15588.

254. **Webb, P., B., Kunene, T., E. and Cole-Hamilton, D., J.** Continous flow homogeneous hydroformylation of alkenes using supercritical fluids. *Green Chem.* 2005, 7, 373-379.

255. **Desset, S., L., Hintermair, U., Gong, Z., Santini, C., C. and Cole-Hamilton, D., J.** Biphasic and flow systems involving water or supercritical fluids. *Top. Catal.* 2010, 53, 963-968.

256. **Kunene, T., E., Webb, P., B. and Cole-Hamilton, D., J.** Highly selective hydroformylation of long chain alkenes in a supercritical fluid ionic liquid biphasic system. *Green Chem.* 2011, 13, 1476-1481.

257. **Blanchard, L., A. and Brennecke, J., F.** Recovery of organic products from ionic liquids using supercritical carbon dioxide. *Ind. Eng. Chem. Res.* 2001, 40, 287-292.

258. **Schreuder-Goedheijt, M., Kamer, P., C., J. and van Leeuwen, P., W., N., M.** A water-soluble diphosphine ligand with a large "natural" bite angel for two-phase hydroformylation of alkenes. *J. Mol .Catal. A.* 1998, 134, 243-249.

259. **Grob, K.** Organic substances in portable water and it's precursor. *J. Chromatogr.* 1973, 84, 255-273.

260. **Colenutt, B., A. and Thorburn, S.** Optimization of a gas stripping cocncentration technique for trace organic water pollutants. *Internat. J. Environ. Anal. Chem.* 1980, 7, 231-244.

261. **Fischer, K.** Neues verfahren zur maßanalytischen Bestimmung des Wassergehaltes von Flüssigkeiten und festen Körpern. *Angew. Chem.* 1935, 48, 394–396.

262. **Kahlweit, M., Strey, R. and Firman, P.** Search for tricritical points in ternary systems: Water-oil-nonionic amphiphile. *J. Phys. Chem.* 1986, 90, 671-677.

263. **Ryan, L., D. and Kaler, E., W.** Microstructure properties of alkyl polyglucoside microemulsions. *Langmuir* 1999, 15, 92-101.

264. **Queste, S., Salager, J., L., Strey, R. and Aubry, J., M.** The EACN scale for oil classification revisited thanks to fish diagrams. *J. Coll. Interf. Sci.* 2007, 312, 98-107.

265. **Shinoda, K.** Thermodynamic aspects of nonionic surfactant - water systems. *J. Coll. Interf. Sci.* 1970, 34, 278-282.

266. **Degiorgio, V., Piazza, R., Corti, M. and Minero, C.** Critical properties of noionic micellar solutions. *J. Chem. Phys.* 1985, 82, 1025-1031.

267. **Sosa Ferrera, Z., Pardon Sanz, C., Mahugo Santana, C. and Santana Rodriguez, J., J.** The use of micellar systems in the extraction of organic pollutants in envirmontal samples. *Trends Anal. Chem.* 2004, 23, 479-488.

268. **Shi, Z., Zhu, X. and Zhang, H.** Micelle mediated extraction and cloud point preconcentration of aesculin and aesculitin in cortex fraxini by HPLC. *J. Pharm. Biomed. Anal.* 2007, 44, 867-873.

269. **Schulman, J., H. and Riley, D., P.** X-ray investigation of the structure of transparent oil-water disperse systems I. *J. Colloid Sci.* 1948, 3, 383-405.

270. **Dorn, U., Schrader, P. and Enders, S.** Aggregation and phase behavior of nonionic surfactants (C_iE_j) in aqueous solution. *Vestnik St. Petersburg University.* 2013, 4, 97-113.

List of own Publications:

Zeiner, T., Schrader, P., Enders, S. and Browarzik, D. Phase- and interfacial behavior of hyperbranched polymer solutions, *Fluid Phase Equilib.* 2011, 302, 321-330.

Schrader P., Dorn, U., Kulaguin – Chicaroux, A. and Enders, S. Phase equilibria of surfactant containing systems, In *Process Engineering and Chemical Plant Design*, (Eds.: Wozny, G.; Hady, L.), Universitätsverlag der TU Berlin 2011. ISBN 978-3-7983-2361-2.

Enders, S., Langenbach, K., Schrader, P., and Zeiner T., Phase diagrams for systems containing hyperbranched polymers, *Polymers* 2012, 4, 72-115.

Zeiner, T., Puyan, M., J., Schrader, P., Browarzik, C. and Enders, S. Phase behavior of hyperbranched polymer in demixed solvents, *Molecular Physics* 2012, 110, 1359-1373.

Dorn, U., Schrader, P. and Enders, S. Aggregation and phase behavior of nonionic surfactants (C_iE_j) in aqueous solution. *Vestnik St. Petersburg University* 2013, 4, 97-113.

Schrader, P. and Enders, S. Analytik für die Phasengleichgewichtsmessung im System nichtionisches Tensid + Wasser + Olefin, *Chem. Ing. Tech.* 2013, 85, 1523-1529.

Schrader, P., Culaguin-Chicaroux, A. and Enders, S., Phase behavior of the water+nonionic surfactant ($C_{12}E_8$) +1- dodecene ternary system across a wide temperature range, *Chem. Eng. Sci.* 2013, 93, 131-139.

Paul, N., Schrader, P., Enders, S. and Kraume, M., Effects of phase behaviour on mass transfer in micellar liquid/liquid systems, *Chem. Eng. Sci*. 2013, in print, DOI: 10.1016/j.ces.2013.02.018.

Schrader, P., Paasche, C. and Enders S., Phase behavior of systems containing Genapol X080 + technical 1-dodecene + water compared with the phase behavior of pure $C_{12}E_8$ + pure 1-dodecene + water, *Chem. Eng. Sci.* 2013, in print, DOI: 10.1016/j.ces.2013.04.030.

Althans, D., Schrader, P. and Enders, S., Solubilisation of quercetin: Hyperbranched polymers and hydrogels a comparison, in preparation.

Schrader, P., and Enders, S. Influence of the product formation and the catalyst on the phase beahvior of microemulsion forming systems used for hydroformylation, in preparation.